Environmental
Studies
Revolving
Funds

044

Motion and Impact of Icebergs

Canada

August 1986

The Environmental Studies Revolving Funds are financed from special levies on the oil and gas industry and administered by the Canada Oil and Gas Lands Administration for the Minister of Energy, Mines and Resources, and by the Northern Affairs Program for the Minister of Indian Affairs and Northern Development.

ENVIRONMENTAL STUDIES REVOLVING FUNDS

Report No. 044

August, 1986

MOTION AND IMPACT OF ICEBERGS

DEVELOPMENT OF A MODEL TO PREDICT ICE MASS MOTIONS IN THE VICINITY OF AN OFFSHORE STRUCTURE

HAY AND COMPANY CONSULTANTS INC.

Vancouver, B.C.

Scientific Advisor: F.J. Dello Stritto

The correct citation for this report is:

Hay and Company Consultants Inc. 1986. Motion and Impact of Icebergs. Environmental Studies Revolving Funds Report 044. Ottawa. 136 p.

Published under the auspices
of the Environmental Studies
Revolving Funds
ISBN 0-920783-43-0

TABLE OF CONTENTS

TABLE OF CONTENTS

continued

LIST OF TABLES

LIST OF FIGURES

MOUVEMENTS ET IMPACT DES ICEBERGS

REALISATION D'UN MODELE POUR LA PREVISION DES MOUVEMENTS DES MASSES GLACIAIARES A PROXIMITE D'UNE STRUCTURE OFFSHORE

1. RESUME

La firme Hay and Company Consultants Ltée a été retenue par le Fonds Renouvelable pour l'etude de l'Environnement en vue d'étudier les mouvements des masses glaciaires à proximité d'une structure offshore. L'ensemble de l'étude a été divisé en les points suivants:

1. tour des documents existants touchant à la question;
2. revue générale des modèles informatiques existants utiles pour l'étude du problème;
3. réalisation et essai d'un modèle informatique adapté à l'étude des interactions hydrodynamiques de deux corps soumis à l'action des vagues et des courants;
4. revue générale des installations équipées de bassins et pouvant conduire des essais sur le comportement des masses glaciaires à proximité immédiate d'une structure.

Le tour des documents informatiques existants n'a permis de receuillir que très peu d'information directement utilisable en vue d'une étude générale de la question. Un nombre considérable de recherches ont été menées sur les problèmes connexes et composants: dérive des masses glaciaires en eaux libres et mouvements, provoqués par les vagues, d'un corps flottant librement en eaux libres. Les documents relatifs à ces problèmes connexes sont analysés dans le présent rapport.

La revue générale des modèles informatiques existants a prouvé que la plupart des modèles appropriés partent due principe de la diffraction d'ondes. Le modèle qui a été retenu dans la présente

étude en vue d'une réalisation plus poussée est celui de M.M. Isaacson, qui était l'un des chercheurs principaux chargés de cette étude.

Il a été réalisé un modèle permettant de prévoir les mouvements des masses glaciaires sous l'effet des vagues et des courants à proximité d'une forte structure fixe située au large. La méthode utilisée repose sur la superposition du mouvement oscillatoire provoqué par des vagues et obtenu par la théorie de la diffraction d'ondes linéaires, d'une part, et des mouvements de dérive calculés au moyen d'une procédure séquentielle, d'autre part. Cette méthode est appliquée à deux corps voisins de forme tri-dimensionnelle arbitraire, dont l'un est fixe (la structure) et l'autre libre et flottant, avec six degrés de liberté (la masse glaciaire). Les effets d'interaction hydrodynamique produits entre les deux corps sont inclus dans la procédure, et ceux d'amortissement visqueux sont pris en compte grâce à l'inclusion de coefficients d'amortissement empiriques. Pour le calcul des mouvements de dérive, on considère que la masse glaciaire est affectée de deux degrés de liberté (déplacements vertical et latéral). Les équations du mouvement comprennent l'addition de masses de fréquence zéro, les forces de dérive (vagues) et de traînée (courants), tous facteurs qui peuvent varier en fonction de l'emplacement de la masse glaciaire eu égard à la proximité de la structure.

Une analyse partielle paramétrique et de sensibilité a été conduite en vue de démontrer les possibilités de ce modèle. Dans les passages d'essais, la structure est représentée par un gros cylindre circulaire vertical et qui touche au fond, et trois sortes de masses glaciaires sont considérées qui correspondent toutes à des cylindres circulaires en flottaison. Les essais comportent des variations des facteurs suivants: volume de la masse glaciaire, direction des vagues, emplacement initial de la masse glaciaire, profondeur de l'eau et force du courant, et ils permettent d'étudier l'influence des forces de dérive (vagues).

Les résultats sont présentés de façon à illustrer la trajectoire de la masse glaciaire et à montrer les variations de sa vélocité ainsi que les coefficients hydrodynamiques particuliers à chaque test. Ils révèlent que, pour les profils géométriques considérés, l'addition de masses de fréquence zéro est tout à fait insensible à la proximité de la masse glaciaire et de la structure, sauf dans les cas de proximité immédiate, et que la force de dérive (vagues) influe de façon plus sensible sur la trajectoire de la dérive des masses glaciaires de faible volume.

La revue générale des installations disposant de bassins a permis l'évaluation de seize laboratoires équipés d'installations où peuvent se conduire des études dans le domaine en question. Les détails touchant aux dimensions respectives de ces installations et à leur capacité de générer vagues et courants ont été classifiés. Les laboratoires sont évalués et de plus des idées sont proposées sur la façon de conduire les essais.

MOTION AND IMPACT OF ICEBERGS

DEVELOPMENT OF A MODEL PREDICTING ICE MASS MOTIONS IN THE VICINITY OF AN OFFSHORE STRUCTURE

1. SUMMARY

Hay and Company Consultants Inc. have been engaged by the Environmental Studies Revolving Funds to investigate ice mass motions in the vicinity of an offshore structure. The scope of the work was divided into the following tasks:

1. a review of available literature pertaining to the problem;
2. a survey of existing computer models useful in investigating the problem;
3. development and testing of a computer model appropriate for the hydrodynamic interactions of two bodies in waves and currents;
4. a survey of model tank facilities capable of performing tests of the behaviour of ice masses in close proximity to a structure.

The literature review identified very little information directly applicable to the overall study problem. A considerable number of studies have been carried out on the related and component problems dealing with ice mass drift in open water and with wave-induced motions of a freely floating body in open water. The literature on these related problems is discussed in this report.

The survey of existing computer models determined that the most appropriate models are those based on wave diffraction. The model utilized in this study for further development was that of

Dr. M. Isaacson, a principal investigator for this study.

A numerical model was developed for predicting ice mass motions due to waves and currents in close proximity to a large fixed offshore structure. The method is based on superposing the wave-induced oscillatory motion obtained by linear wave diffraction theory on the drift motions computed through a time-stepping procedure. The method pertains to two neighbouring bodies of arbitrary three dimensional shape. One body is fixed (the structure) and the other is freely floating with six degrees of freedom (the ice mass). Hydrodynamic interaction effects between the two bodies are included in the procedure. Viscous damping effects are taken into account by the inclusion of empirical damping coefficients. In the computation of drift motions, the ice mass is considered to have two degrees of freedom (surge and sway). The equations of motion include zero frequency added masses, wave drift forces and current drag forces, all of which may vary with ice mass location owing to the proximity of the structure.

A limited parametric and sensitivity analysis was carried out to demonstrate the model's capabilities. In the test runs, the structure is represented as a large, vertical, circular cylinder extending to the seabed. Three different ice masses are modelled, all corresponding to floating circular cylinders. The tests include variations in ice mass size, wave direction, initial ice mass location,water depth and current magnitude and examine the influence of wave drift forces.

Results are presented showing the trajectory of the ice mass, and the variations of ice mass velocity and selected hydrodynamic coefficients for each test. These results indicate that, for the geometries considered, the zero frequency added mass is quite insensitive to the proximity of the ice mass to the structure, except when it is very close to the structure, and that the wave drift force has a significant influence on the drift trajectory

of smaller ice masses.

The survey of model tank facilities assessed sixteen laboratories with facilities capable of studies in the problem area. The particulars of these facilities relative to their size, wave generating capabilities and current generating capabilities have been tabulated. The laboratories are rated and suggestions made regarding testing methods.

2. CONCLUSIONS AND RECOMMENDATIONS

2.1 Prior to this study, very little information was available regarding the drift motions of an ice mass due to waves and currents in close proximity to a large fixed offshore structure.

2.2 It was determined that existing computer models possessing a wave diffraction program would be suitable as a starting point for developing a model predicting drift in the near vicinity of an offshore structure. A model developed by Dr. M. Isaacson was utilized in this study.

2.3 A computer model has been developed for predicting ice mass motions in the near vicinity of an offshore structure. The model has been demonstrated to perform satisfactorily for a range of input conditions. These have been chosen to reflect variations in water depth; ice mass size; wave direction; current magnitude and direction; initial location and velocity of the ice mass; and degree of discretization of the ice mass and structure.

2.4 Small ice masses experience a negative drift force for certain ranges in the distance from the structure. This is consistent with previous results carried out for two body systems. A significant consequence of this variation in wave drift force is that the drift motion reverses.

2.5 The zero frequency added masses change significantly only when the gap between the ice mass and structure is very small. Further improvements to the routine used to calculate the Green's function for the zero frequency added mass determination are recommended.

2.6 The case of reduced depth, with a gap of 10 m between the ice mass and seabed, showed no significant effect on the ice

mass motions, bearing in mind that the wave length was altered in this study due to reducing the water depth to attain the 10 m gap.

2.7 Only a limited parametric and sensitivity analysis was undertaken in conjunction with the model development. A more comprehensive series of numerical tests should be carried out in order that additional parameters are varied and the influence of these examined.

2.8 The computer model may readily be extended to random waves although further numerical improvements in the diffraction calculation would be required to make it computationally efficient.

2.9 By incorporating the relevant ice properties, the computer model may ultimately be extended to predict ice mass motions after impact and the resulting forces on a structure.

2.10 A series of physical model tests should be carried out and used as a basis for verifying and calibrating the computer model developed in this study.

2.11 The combined use of physical and computer models would reduce testing costs in a laboratory study and would be particularly useful in determining cause effect relationships in observed model behavior.

2.12 Consideration should be given to towing the fixed structure as a means of creating a uniform current distribution. Careful attention would have to be taken in minimizing the distortion of waves.

2.13 On technical considerations, SSPD Maritime Research and Consulting in Sweden ranked highest in the tank survey. The David Taylor Naval Ship Research and Development Center in

the USA and Marintek A/S in Norway ranked a very close second while Hydraulic Research Ltd. and British Maritime Technology in England and Maritime Research Institute in Holland ranked a very close third. Any of the above facilities should be actively considered in a laboratory study.

3. INTRODUCTION

Hay and Company Consultants Inc. have been engaged by the Environmental Studies Revolving Funds of the Government of Canada to undertake a study of the motion and impact of ice masses in the vicinity of large, fixed offshore structures. In the last several years, exploration drilling has been carried out on a large scale off Canada's east coast. Iceberg encroachment in the Labrador Sea, the Flemish Pass and on the Grand Bank poses a unique problem for drilling rigs and for future production facilities. Presently, collisions are avoided by a variety of means including long range surveillance and moving threatened rigs. As production facilities under consideration include bottom founded structures, impacts with icebergs must be considered in their design.

The general problem involving impact from floating ice masses on a large fixed offshore structure covers a wide range of possible parameters. Typical ice masses range in diameter from under 10 m to more than 200 m, and in mass up to about 10^7 tonnes. East Coast offshore activity generally extends to water depths up to about 100 m but may extend to about 300 m. Structures of approximately 100 m diameter have been proposed for the area.

The original Request for Proposal involved a two component study:

(1) investigation of methods to estimate the drift and instantaneous velocities induced in an iceberg of known size and shape under known environmental conditions.

(2) investigation of methods to estimate the behaviour of icebergs in close proximity to a large, fixed offshore structure.

As a basis for a terms of reference, these components are rather broad, and could encompass both the drift of an iceberg in the

open ocean over long periods of time, and the drift of an iceberg in the near vicinity of an offshore structure. While these two problems are related, each requires a different computer model to properly address the phenomena involved.

At the initial meeting with the ESRF scientific advisor, it was decided to concentrate on the ice motions (including both drift and oscillatory components) in the near vicinity of an offshore structure.

Iceberg/structure impact is a complex phenomemon, and aspects of it have been the subjects of intensive investigation. An impact event may be divided into three separate phases or regions:

1. Far-Field Phase:
   The ice mass is sufficiently distant from the structure to be unaffected by it. Therefore, the ice mass motion is purely in response to the environmental driving forces.

2. Near-Field Phase:
   The ice mass and structure are in close proximity, and the far field motions are altered in response to the structure's presence.

3. Contact Phase:
   The ice mass and the structure are in physical contact. The impact is governed by the material and mechanical properties of both, the initial impact conditions, the hydrodynamic interactions and the environmental forces.

Considerable effort has been expended addressing aspects of Phases 1 (quantifying environmental driving forces, iceberg drift, iceberg occurrence and mass distributions), and 3 (quantifying ice material and mechanical properties, iceberg geometries, structure-foundation response). Little has been done

directly in addressing Phase 2.

Two aspects of the near field phase have immediate application in assessing impact loads. First, the effective kinetic energy that the ice mass brings to the physical impact may be appreciably altered from its far-field value. The change in energy may result from changes induced by the presence of the structure in the velocity and added mass. Secondly, the presence of the structure may alter the eccentricity of the impact, as the iceberg trajectory changes in response to the near-field flow. A change in eccentricity modifies not only the magnitude of the impact, but also the torsional load and the overall frequency of impacts occurring.

The near-field phase itself may be divided into two regions:

2a. Inertial Region:
The ice mass and structure are in close proximity, but are sufficiently separated so that the ice mass is only influenced by changes to the far-field flow induced by the structure. Such changes include diffraction and reflection of the wave field and distortion of the current.

2b. Viscous (or Very Near-Field) Region:
As the distance between the ice mass and structure decreases, the fluid viscosity becomes an increasingly important, and perhaps dominant, factor. The very near-field is that range of separations in which fluid friction cannot be ignored.

The main thrust of this study is directed to Region 2a, the inertially-dominated, near-field phase. To a lesser degree, far-field topics are addressed in that the response of ice masses in open water to waves and currents is of interest. Detailed investigation of the ice mass behaviour in Region 2b, and the

inclusion of hydrodynamic influences during Phase 3 are beyond the scope of the present study.

The specific tasks performed under this study are:

(a) Conduct a literature and data review and include not only information directly applicable to the problem under investigation but also general drift of floating bodies in the vicinity of a structure (Section 4).

(b) Identify available analytical models and evaluate the applicability of these models to the investigation (Section 5).

(c) Starting with one of the models identified in (b) above, develop a model capable of predicting drift of an iceberg in the vicinity of an offshore structure (Sections 6 and 7).

(d) Undertake a survey of available model tank facilities suitable for studies of iceberg motions in the vicinity of an offshore structure (Section 8).

4. LITERATURE AND DATA REVIEW

4.1 General

Estimation of ice mass motions, particularly in the vicinity of a fixed structure, has received only limited attention. Aspects of related, more thoroughly investigated, topics are applicable to the problem. These topics include wave loads on fixed structures, response of floating bodies to waves, interference effects between floating bodies and nonlinearities in wave excitation and structure response. Due to obvious practical applications, literature on floating bodies is particularly voluminous. Therefore, the literature and data review, which logically began with the limited information on iceberg response to waves and with the more substantial work on iceberg drift in open water, expanded to include these diverse topics. This section summarizes the pertinent work in each area. Under each topic, various avenues have been developed, and most do not directly relate to the method developed in Section 6. The diverse approaches are included in the summary both to document the scope of the available information, and to list alternatives which may be considered for future use.

The motions of an ice mass are governed primarily (1) by currents and winds, (2) by waves, and (3) by the hydrodynamic characteristics of the ice mass itself. The presence of a structure can affect all these factors. The ice-structure interaction after the initial instant of impact, depends also on the material properties of the ice mass but is not treated in this study. A brief but general review of this overall problem is given by Isaacson (1985).

The present study requires an understanding of the following related or component problems:

1. ice mass drift in open water and in the vicinity of a

large offshore structure,

2. wave-induced motions of a freely floating body (ice mass) in open water and in the vicinity of a large offshore structure.

The literature and data search has included a computer data base search using the following data bases: Compendex, NTIS, Oceanic Abstracts, Geoarchive, Engineering Meetings, and Fluidex. Keywords which were used in the searches have included added mass, hydrodynamic mass, hydrodynamic coefficients, iceberg, ice mass, floating body, barge, motion, drift, and wave. In addition, contact was made with several oil companies including Chevron, Mobil and Petro Canada; however, the review generally excludes reference to commercial projects which have not been reported in the open literature.

4.2 Ice Mass Drift

4.2.1 Drift In Open Water

Ice mass drift in open water is a relatively complex motion as indicated by iceberg trajectories observed in the field. While typical motions are predominantly rectilinear, frequently observed circular and cusp-like trajectories are indicative of the complex and variable set of forces acting on the ice mass. Models proposed to describe this motion can broadly be classified as kinematic, dynamic, or statistical in nature depending on the approach to the problem. Kinematic models utilize a correlation between ice mass velocities and known wind and current velocities. Dynamic models predict trajectories by estimating the forces on the ice mass and integrating the equation of motion. Statistical methods base predictions on the past trajectory of the iceberg.

Kinematic models were amongst the earliest proposed. Their methodology ignores the actual forces on the ice mass and concentrates on the physical phenomena which give rise to the forces. Invariably, a linear relationship is assumed between the ice mass velocity and the velocities of the environmental factors in the form:

$$V_i = \sum k_n V_n \qquad (4.1)$$

where V_i is the ice mass velocity, the V_n's are the velocities of the environmental factors, usually winds and currents, and the k_n's are the relative influence of each environmental factor. Dempster (1974) used a two term expression, one term representing a constant translational velocity and the second term representing a rotating tidal current. Cheema and Ahuja (1978) also used a two term representation; however in this case, ocean currents and winds were the environmental factors.

Dynamic models are more firmly based in the physical phenomena acting on the ice mass. The equation of motion can be written:

$$Ma = F^{(d)} + F^{(a)} + F^{(c)} + F^{(w)} \qquad (4.2)$$

where M is the iceberg mass combined with its added mass and is usually expressed in the form:

$$M = (1 + C_M)M_i \qquad (4.3)$$

with M_i the iceberg mass; and C_M its added mass coefficient; a is acceleration; and $F^{(d)}$, $F^{(a)}$, $F^{(c)}$ and $F^{(w)}$ are the forces of current drag, wind drag, Coriolis effect and waves respectively. The various dynamic models proposed differ mainly in the forces included and the value of the various coefficients required.

The current drag and the wind drag are computed from a quadratic relationship in the relative velocity as:

$$F^{(d)} \text{ or } F^{(a)} = 1/2\rho A C_d V_r |V_r| \qquad (4.4)$$

where ρ is the density of the fluid medium, A is the aerial or submerged cross sectional area normal to the relative velocity, C_d is the drag coefficient, and V_r is the velocity of the ice mass relative to the wind or current. Wind is generally recognized as being of lesser importance and is often omitted from the model (Sodhi and Dempster (1975); Russel, Riggs, and Robe (1977)). Currents are a principal driving force and have been treated with various levels of sophistication. Smith and Banke (1981, 1982) utilized a uniform current while Sodhi and El-Tehan (1980) and Mountain (1980) utilized multi-layered models to separate surface, wind driven currents from mean currents.

Forces due to the Corolis effect result from the motion of the ice mass and the sloping sea surface which arises from the geostrophic current. These are combined into a single expression in the form:

$$F^{(c)} = M_i (f \times V_r) \qquad (4.5)$$

where V_r is the velocity of the ice mass relative to the current and f is the component of the earth's angular velocity at latitude θ directed normal to the earth's surface with magnitude $2\Omega\sin\theta$ in which Ω is the earth's angular speed.

Wave forces are included in a model proposed by Hsiung and Aboul-Azm (1982). Only horizontal forces associated with long term drift were derived utilizing diffraction wave theory, ignoring oscillatory motions.

Various degrees of success have been claimed by the authors of these models. In general, the models predict trajectories which are predominantly rectilinear better than trajectories with a significant number of loops and cusps. A number of different

drift models are regularly used in preparing iceberg position forecasts for East Coast offshore operations and are widely recognized as not sufficiently accurate for that application. The major limitation in drift prediction accuracy is the inaccuracies on the model input (wind, current, and wave data; iceberg shape and mass parameters; and drag and added mass coefficients).

Statistical models are designed to overcome the sensitivity of deterministic models to uncertainties and errors in the input data. Garrett (1984) has proposed a statistical scheme using iceberg position and velocity data up to a given point in time to derive optimum linear estimators for future positions and velocities. Through the use of the Gauss-Markov Theorem, coefficients leading to the lowest mean square deviation from actual values are found. The iceberg's course is then projected into the future with a fading memory on the estimators. The further the berg travels from its last recorded position, the greater the uncertainty in the estimates. The statistical model shows promise for predicting short term drift, up to 12 hours from the last data.

A hybrid model, developed by Gaskill and Rochester (1984), employs a dynamic analysis similar to that described above but estimates the input data from the previous history of a berg's drift.

4.2.2 Drift Near A Structure

Little work has been done on the two body problem in which an ice mass drifts within a few diameters of a structure. Obviously, the disturbances in the flow field caused by the ice mass and the structure lead to some interactions which will influence the drift. Isaacson (1985) has suggested an approach to the problem using boundary elements, a methodology often employed in diffraction wave theory and thus is amenable to superposition of

wave and currents effects on iceberg motions near a structure. The method involves expressing the velocity potential as a sum of components representing a uniform current and the disturbance created by the ice mass and structure. The potential for the uniform current is:

$$\phi_c = U(x\cos\beta + y\sin\beta) \qquad (4.6)$$

where U is the current velocity and β is its angle with the x axis of the co-ordinate system. The disturbance potential can then be derived using methods described in Section 4.3.

4.2.3 Data Input To Drift Models

The accuracy of trajectory projections depended on the quality of the input data. Three categories of inputs are required in most models:

a. current, wind and wave conditions as functions of both space and time

b. appropriate force coefficients

c. iceberg parameters such as aerial and submerged shape, mass, orientation, and added mass.

Ball, Gaskill, and Lopez (1981) have assessed the problem by analyzing 250 iceberg trajectories observed in the field. Laboratory experimentation is also being utilized to refine drag coefficients (Shirasawa, Riggs, and Muggeridge (1984)).

A recent study, Arctic Sciences (1984), investigated the sensitivity of iceberg trajectory predictions to uncertainties in the inputs. The investigators found that the largest source of

uncertainty is associated with the water current information and the water drag force coefficient. They conclude that improvements required to obtain reliable predictions over large areas of the ocean are not likely in the near future.

Recognition that accurate long term drift predictions will not soon be available has focussed attention on short term drift in the vicinity of offshore structures. Lever (1984) and Arctec (1984), have performed laboratory investigations of wave and current induced drift which ultimately will be helpful in the development of a short term drift model.

4.3 Wave-Induced Motions Of Floating Bodies

4.3.1 Flow Regimes

Wave-structure interaction problems generally encompass two distinct flow regimes, one associated with small bodies, for which behaviour is governed by flow separation, (drag-dominated), and the other with large bodies, which diffract the incident waves (inertia-dominated). For small diameter fixed structure, flow separation occurs and influences the loading on the structure, and the waves propagate essentially unaffected. A large diameter structure diffracts the incident wave field and the resulting pressure field determines the load on the structure.

In the case of a freely floating body such as an ice mass, there are three distinct regimes. Sufficiently small ice masses essentially behave as fluid particles and follow the orbital motion of the fluid. For larger ice masses wave diffraction is the predominant factor in determining the motions of the body. Typically, diffraction becomes a significant influence when (diameter/wave length) exceeds about 0.2. For extremely large ice masses: (typically $D/L > 2.0$) the body still diffracts the

waves but its oscillatory motions are negligible. The presence of a large structure in the vicinity of the ice mass modifies the wave field and produces a reflected wave field immediately upstream of the structure.

4.3.2 General Calculation Method

Reviews of wave loading and structural response problems involving fixed and/or floating structures have been given in several texts and general reviews (e.g. Wehausen (1971), Hogben (1974), Hogben et al. (1977), Newman (1977), Garrison (1978), Mei (1978, 1983), Isaacson (1979), Sarpkaya and Isaacson (1981), Yeung (1982), Hooft (1983), etc.). Most computer models of motion response in waves are based on linear wave theory in which the body oscillates sinusoidally in a regular wave train of small amplitude. The body may oscillate with six degrees of freedom corresponding to surge, sway, heave, roll, pitch, and yaw, denoted by ζ_j, $j=1,\ldots,6$. In a linear analysis, the fluid force acting on the structure may be separated into components proportional to the acceleration and velocity components of the body motion, expressed as added-mass and damping coefficients respectively, and to a remaining component which involves the incident waves, termed the exciting force component. The equations of motion of the body may therefore be expressed as:

$$\{-\omega^2([M] + [A]) - i\omega[B] + [C]\}(\zeta) = (F_e) \qquad (4.7)$$

Here [M] is the mass matrix of the body, [C] is the stiffness matrix of the body associated with hydrostatic stiffness components, [A] is the added mass matrix, [B] is the damping coefficient matrix, and (F_e) is the exciting force vector. In general, [M] and [C] can be estimated from the configuration of the ice mass. The matricies [A] and [B] and the vector (F_e) may be obtained by a hydrodynamic analysis. For a small structure, or one composed of slender structural elements, this involves the

use of the Morison equation, with a suitable linearization of the drag force. For a large structure, this involves a solution to the related diffraction and radiation problems. Once [A], [B] and (F_e) are all known, Eq. 4.7 may be solved to obtain the motions (ζ).

The analysis for motions in regular waves may be extended to the case of irregular waves by means of the superposition principle of linear theory. The method involves solving Eq. 4.7 to determine the response amplitude operators, RAO's, for a series of regular incident waves of unit amplitude and spanning a range of frequencies. If required, the RAO's can then be applied to obtain time histories of the body response to a specified irregular wave record. More commonly, they can be used in conjunction with a specified wave spectrum $S_\eta(f)$ to obtain the corresponding spectra $S_\zeta(f)$ of the component motions:

$$S_\zeta(f) = \{RAO(f)\}^2 S_\eta(f) \qquad (4.8)$$

These response spectra can then be integrated to provide the root-mean-square motions and in turn the maximum expected motions in a sea state of specified duration. If required, a simple extension to this analysis provides the accelerations at various specified points on the body.

4.3.3 Small Floating Bodies

The analysis procedure for a floating body which is small relative to the wave length (or one which is composed of small diameter structural members) is treated in several reviews, including the texts of Sarpkaya and Isaacson (1981) and Hooft (1983). In such a case the Morison equation is used to express the force on a segment of each member in terms of the incident flow and velocities and accelerations of the structure. In order to develop the equations of motion into the form of Eq. 4.7, the

nonlinear drag term must be approximated by a linear term.

If the body consists of a single member (corresponding to an ice mass which is small relative to the incident wave length) then it generally follows the water particle motions providing no resonance occurs. A body with acceleration $\dot{u}_b$ immersed in a fluid which itself has an acceleration $\dot{u}_f$ experiences a force F equal to (ignoring resonance):

$$F = \rho V(1 + k)\dot{u}_f - \rho Vk\dot{u}_b \qquad (4.9)$$

where k is an added-mass coefficient, is the fluid density and V is the immersed body volume. The equation of motion of the body whose mass is ρV is $F = V\dot{u}_b$ and thus $\dot{u}_b = \dot{u}_f$. Since the relative velocity $\dot{u}_b - \dot{u}_f$ is small, the drag force is insignificant and the body follows the fluid motion.

4.3.4 Large Floating Bodies

For a large body which diffracts the incident waves, diffraction theory may be used to calculate the wave-structure interaction. This topic has been reviewed by a number of authors including Hogben (1974), Garrison (1978), Mei (1978, 1983), Isaacson (1979a), Sarpkaya and Isaacson (1981) and Yeung (1982). A number of theoretical and numerical methods are available for treating such problems. Some treat general three-dimensional bodies of arbitrary shape, others treat bodies with a two-dimensional irregularity and others are restricted to specific reference configurations.

(a) General Three-dimensional Bodies

The general case of three-dimensional structures of arbitrary shape may be treated numerically by either source distribution methods or finite element methods. In the former methods the surface of the submerged structure is discretized into a number

of surface elements or facets, [Garrison and Chow (1972), Faltinsen and Michelsen (1974), Hogben and Standing (1974), Loken and Olsen (1976), etc.] In the finite element methods the fluid domain (within a suitable exterior boundary) is discretized into three-dimensional elements [Mei (1978), Zienkiewicz, Bettess and Kelly (1978), etc.].

For ship-like structures which have a well-defined longitudinal axis, methods based on strip theory may also be used. The structure is divided into a series of parallel vertical planes and thereby extending two-dimensional methods to three-dimensional structures. This extension has been summarized by Newman (1977).

(b) Two-dimensional Configurations

Many structural configurations possess a two-dimensional rather than a three-dimensional irregularity, and only a discretization of the structure's profile (for boundary element methods) or of the two-dimensional fluid domain (for finite element methods) is needed. Three fundamental configurations possessing such a two-dimensional irregularity are:

a. vertical axisymmetric bodies,
b. horizontal cylinders of arbitrary section, and
c. vertical cylinders of arbitrary section.

The wave force on a fixed vertical axisymmetric body has been considered by several authors, including Fenton (1978). The extension to floating axisymmetric bodies, which includes the numerical calculation of hydrodynamic coefficients and response amplitude operators, has been treated by Isaacson (1982c). A boundary element method is used, with the body's axisymmetry utilized to reduce considerably the computational effort required from that for bodies of arbitrary shape.

The second case above corresponds to a two-dimensional problem in the vertical plane and a two-dimensional boundary element method employing a suitable Green's function or the finite element method may be employed to treat this. Corresponding programs for floating bodies have been described by a number of authors, including Adee and Martin (1974) and Maeda (1974) using the boundary element method and Bai and Yeung (1974) and Isaacson and Fraser (1979) using the finite element method. The extension to treat ship shapes by strip theory is outlined by Newman (1977).

The third case has been treated by Isaacson (1978a) for fixed structures, but this has not been extended to floating structures.

(c) Reference Configurations

A variety of specific solutions have been obtained for particular reference configurations. For example, various kinds of vertical circular cylindrical bodies that have been analyzed include a single surface-piercing cylinder, MacCamy and Fuchs (1954), two or more neighbouring surface-piercing cylinders, Spring and Monkmeyer (1974), Chakrabarti (1978), McIver and Evans (1984), a truncated cylinder at the free surface, Black, Mei and Bray (1971), Garrett (1971), a truncated cylinder resting on the seabed, Black, Mei and Bray (1971), an axisymmetric compound cylinder with components of unequal radii, Isaacson (1979b) and so on. These different solutions are usually very specific so as not to be directly applicable to the study problem.

4.3.5 Nonlinear Wave Effects

The full Morison equation with appropriate force coefficients is required with a suitable nonlinear wave theory. However, the extension to force spectra associated with irregular waves is more difficult and the problem is usually analyzed in the time

domain.

The extension for the case of large bodies is much more involved. Two separate approaches have been developed to treat the problem. One is based on a perturbation procedure, in which linear diffraction theory is extended to a second order on the basis of the Stokes expansion procedure. The fundamental case of a surface-piercing fixed vertical circular cylinder has received particular attention (e.g. Rahman (1984) and a number of others papers referred to therein). The more general case of a structure of arbitrary shape has been treated by Lighthill (1979) who describes the general formulation of the problem (for a fixed structure) but does not obtain any results, and also by Garrison (1984). The second order solution involves a numerical integration over the free surface in the vicinity of the structure, thus increasing the degree of computational effort in relation to the first order problem.

A second approach has been to solve the complete nonlinear equations numerically, which requires a time stepping procedure since the surface boundary conditions must be applied at the instantaneous free surface which is continuously changing. The methods which have been developed are all essentially boundary integral methods, in which a boundary integral equation is solved at each time step to provide the required variables over the fluid boundary.

Faltinsen (1977) treated the two-dimensional vertical plane case of an oscillating cylinder in deep water. More recently, Vinje and Brevig (1981) and Vinje, Xie and Brevig (1982) have used a similar procedure to describe the development of wave breaking and wave interaction with a fixed or oscillating cylinder, again for the two-dimensional vertical plane case. Stansby and Slaouti (1984) have treated the vertical plane problem using a vortex sheet approach.

A numerical treatment of the complete three-dimensional nonlinear diffraction problem involving a floating structure has been given by Isaacson (1982a, b). For example, the heave and surge response of a floating circular cylinder subjected to a specified incident wave condition are presented and the extent of the nonlinear effect is demonstrated.

4.3.6 Interference Effects

The interference effect between large neighbouring structures in waves has application to the behaviour of an ice mass in the vicinity of a large offshore structure. This topic has been studied in the past to assess the interference effects for such situations as neighbouring offshore storage tanks, neighbouring columns of a gravity platform, neighbouring hulls of a vessel, etc.

The interference effect between fixed vertical circular cylinders has been studied by several authors including Ohkusu (1974), Spring and Monkmeyer (1974), Chakrabarti (1978), Isaacson (1978b) and McIver and Evans (1984). Generally, the interference is most severe when the cylinders are aligned with the wave direction and is associated with the upstream cylinder lying in the reflected wave system of the other. Isaacson (1978) reports that even for cylinders which are ten radii centre to centre apart, the in-line force on one cylinder may be increased by as much as 25%. When cylinders are aligned with the incident wave crests the interference effect is relatively small. Matsui and Tamaki (1981) studied an extension to this problem dealing with the interference effect between groups of vertical axisymmetric bodies in waves and presented results for a pair of circular cylinders of finite draft.

Van Oortmerseen (1979, 1981) considered the interference effect between neighbouring floating cylinders, with one cylinder circu-

lar and the other almost square and both with the same draft. In general he found that the presence of a neighbouring structure results in added mass and damping coefficients versus frequency curves that oscillate around the corresponding curves for an isolated structure, and that the interference effect on these diminish as the frequency tends to zero. A structure is also subject to forces resulting from motions of the neighbour and results of these interaction coefficients were present over the entire frequency range. Loken (1981) subsequently carried out a similar study and compared his results with those of van Oortmerseen (1979).

The case of neighbouring horizontal cylinders has also been considered by several authors, mainly in the context of interference effects between neighbouring hulls of a vessel, and corresponding to a two-dimensional vertical plane problem. This has been treated by several authors including Wang and Wahab (1971) and Ohkusu (1974), who have considered pairs of semi-immersed cylinders of various sectional shapes and have presented results on exciting forces, added-mass and damping coefficients and response amplitude operators.

The interference between neighbouring bodies immersed in a uniformly accelerating flow of an infinite fluid has been considered by Yamamoto (1976). He provides expressions and results for the hydrodynamic forces on an arbitrary number of cylinders in arbitrary motion based on potential theory and considers several special cases. The force exerted on a moving cylinder in the presence of a fixed neighbour and an otherwise stationary fluid is of interest here and is given as:

$$F = - \pi \rho a^2 C_1 \dot{u}_b + \rho a C_3 | u_b |^2 \qquad (4.10)$$

where a is the cylinder radius and the coefficient C_1 is the added mass coefficient. (C_1 = 1 for an isolated cylinder). C_3 is a convective force coefficient which arises from the velocity

squared terms in the Bernoulli equation for pressure. (C_3 = 0 for an isolated cylinder). As an example of the results obtained, for two cylinders of equal radii, C_1 increases by about 10% when the gap width e = a, and by about 25% when e = 0.2a. The other coefficient C is about 0.1 when e = a and increases to about 1.0 when e = 0.2a. This force always acts in a direction so as to attract the two bodies, and thus opposes the drag force when one cylinder is approaching the other.

4.3.7 Viscous Damping of Large Bodies

Additional damping associated with viscous effects may have a significant influence on resonant oscillations of a large floating body. This may arise from shear stresses associated with the boundary layer on a smooth structure surface such as a ship's hull, or from vortex shedding off the sharp edges of a body. The latter case is important in the prediction of roll damping and resonant roll amplitudes for rectangular-section barges or other sharp-edged floating vessels. Graham (1980) has carried out a fundamental investigation into the forces associated with vortex shedding off a sharp edge in oscillatory flow and provides estimates of the forces which arise.

For roll motions of a vessel, the viscous damping force is nonlinear and dependent on the roll amplitude, so that the complete solution for roll response requires a time integration method. Alternatively, it may be convenient to adopt a method of equivalent linearization, with the equivalent linear damping taken as a function of the roll response. These procedures have been reviewed by Kaplan (1983).

4.3.8 Low Frequency Hydrodynamic Coefficients

A significant number of studies deal with the added mass and damping coefficients of floating bodies in waves. The low frequency limit is of particular interest to the study problem since this affects the drifting motion of an ice mass, and this topic has received some attention in the context of low frequency drifting oscillations of moored vessels. The damping coefficients (due to wave damping only) approach zero in the limit of zero frequency, but the added-mass coefficients do not.

As examples of experimental and numerical studies, Wichers and van Suijj (1979) provided data on damping coefficients associated with low frequency motions of tankers, and subsequently Wichers (1982) discussed the low frequency damping coefficients associated with radiation and viscous damping for tankers and compared measured and computed damping coefficients and drift motions for model tankers. Chakrabarti (1984) reported on experimental measurements of added-mass and damping coefficients for several structures which included a barge, tanker, semisubmersible and a floating vertical cylinder. The dependence of these on wave frequency was presented.

4.3.9 Response of Ice Masses

Relatively few studies address wave effects on ice masses themselves. Wave effects on larger icebergs and ice floes have been studied mainly in the context of iceberg motions and breakup due to wave-induced flexural failure. Schwerdtfeger (1980) carried out a simple linear analysis to determine the heave and pitch resonance frequencies of a berg, but did not predict its motion amplitudes in waves. Orheim et al.(1982) reported on measurements of surface strain and heave motions of large tabular icebergs in waves. Squire (1981) and Kristensen and Squire

(1983) reported on a field study and theoretical analysis of the strains and motions of large ice in waves. Wadhams, Kristensen and Orheim (1983) measured the heave and roll motions and strains for three Antarctic icebergs and correlated these to wave measurements.

With regard to smaller ice masses, Lever et al. (1984) describes a laboratory study of the wave-induced motions of small ice masses corresponding to prototype masses in the range 10 to 10^5 tonnes. They concluded that for D/L less than 1/13, where D is the ice mass diameter, the ice masses essentially act as fluid particles and follow the wave flow. When heave resonance occurs, however, amplification factors up to 3.6 were measured. For D/L greater than about 1/10 the ice mass motion differed from the particle motion, due to viscous and/or diffraction effects.

5. SURVEY OF AVAILABLE COMPUTER MODELS

Due to the wide range of environmental conditions and possible ice mass and structure sizes and shapes, a prime objective of this study is the acquisition and/or development of an appropriate computer model.

During the past 15 years, considerable model development has been undertaken in support of offshore oil activities. Models predicting the response of floating bodies to waves and wave forces on structures have been developed and are available commercially from many sources. In order not to duplicate previous work, computer models which might provide a starting point for the study objectives here were investigated.

Oil drilling activity off Canada's East Coast has also led to the development of computer models predicting the drift of icebergs in the open sea. As described in Section 4.2, these models compute the forces on an iceberg due to wind, currents, and waves, and include forces that are important in long term drift predictions such as the Coriolis force. None of these models, however, has the option of including a second, fixed body. Since many of their features are superfluous to ice motions near a structure and since their formulations do not permit modifications to include a structure, these models were not considered for evaluation.

The unique demand of the present study, relative to the general capabilities of available models, is the inclusion of the second, fixed body. Models whose principal component is a three dimensional diffraction and radiation analysis (Section 4.3) hold the best hope for significant capabilities in the general area of interest. Numerous such computer models developed by companies undertaking research and development or design in support of shipbuilding or offshore oil drilling were identified. Many are proprietary to the companies which developed them and some are

available for purchase under limiting licensing arrangements.

Most of the models were originally developed for specific applications, and cannot be readily adapted to different types of problems. For example, one candidate program computes current-induced drift, but cannot accommodate distortions to the current field caused by a fixed or floating body. A number of programs were identified which address multi-body problems. Many of these, however, assume a complete de-coupling of the body interactions from the wave and current fields. Such simplifications are acceptable for the originally intended applications, but not for the present study. To allow a solution to the two-body problem, de-coupling assumptions are also introduced (Section 6.1.3) in this study. These assumptions, however, are far less restrictive than those used in past work, and retain the key features of the interactions.

Major practical restrictions, which could not be addressed within the resources of this study, precluded the use of most commercially-available models, requiring modifications for the study problem. These limitations include:

(1) some of the models are modules of larger suites of programs, and are not designed to be easily extracted and developed separately;

(2) under licensing agreements, some of the models can not be modified by anyone other than the vendor and thus do not meet the terms of reference for the study;

(3) even within licensing arrangements, the task of becoming familiar with the logic and programming of the model would take more time than was available to the study;

(4) the cost of purchasing the models was well beyond the

means of the study.

One model which did not suffer from the above constraints is that developed by Prof. M. Isaacson who is a principal investigator in this study. His model was developed as a research tool and included a single-body diffraction and radiation program. Currents were not included in the model and, therefore, it was not as advanced in that sense as some of the commercially available models. Owing to the problems faced by the commercial models though, the Isaacson model was adopted as a starting point.

6.0 THEORETICAL AND NUMERICAL DEVELOPMENT OF THE MODEL

6.1 Background

This section describes the theoretical and numerical development of computer programs for treating motions of an ice mass due to waves and currents in close proximity to a large fixed offshore structure. The general situation is indicated in Figure 1. The fundamental approach superposes the wave-induced oscillatory motions of the ice mass on the drift motion due to the current field, so that two component problems are treated. The wave-induced motions, obtained by a diffraction calculation, depend on the ice mass proximity to the structure. The motions therefore must be recalculated at a series of points along the drift trajectory. Furthermore, the drift may be influenced by wave drift forces and by the zero frequency added mass components of the ice. Both of these terms also vary with the location of the ice mass and may be obtained by the wave diffraction calculation. Thus the two component problems, current drift and wave-induced motions, are coupled.

The development below is similar in many respects to those for well-established single-body problems. Though formulations of the single-body problem are available in standard references (e.g. Sarpkaya and Isaacson, (1981) a complete, self-contained development is provided here for two reasons. First, a working computer model can be prepared using this section as a basis; and secondly, existing single-body models can be extended to two-body models, also using this section. As part of this study, a two-body computer model was developed from a single-body program. As the original program (Section 5) is proprietary, a significant portion of the coding of the final program is also. Therefore, inclusion of the full theoretical and numerical developments circumvents the difficulties of proprietary coding.

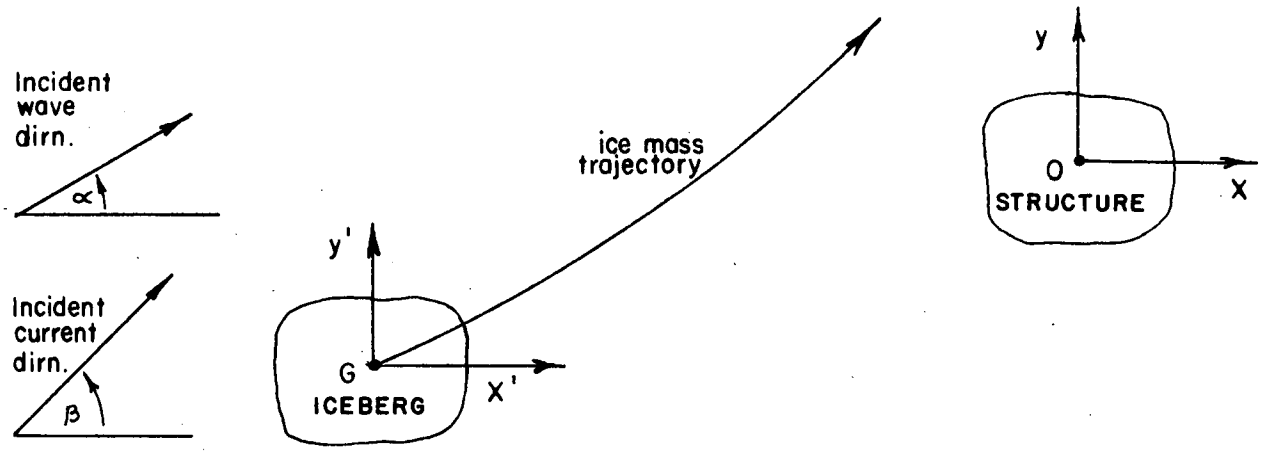

(a) PLAN

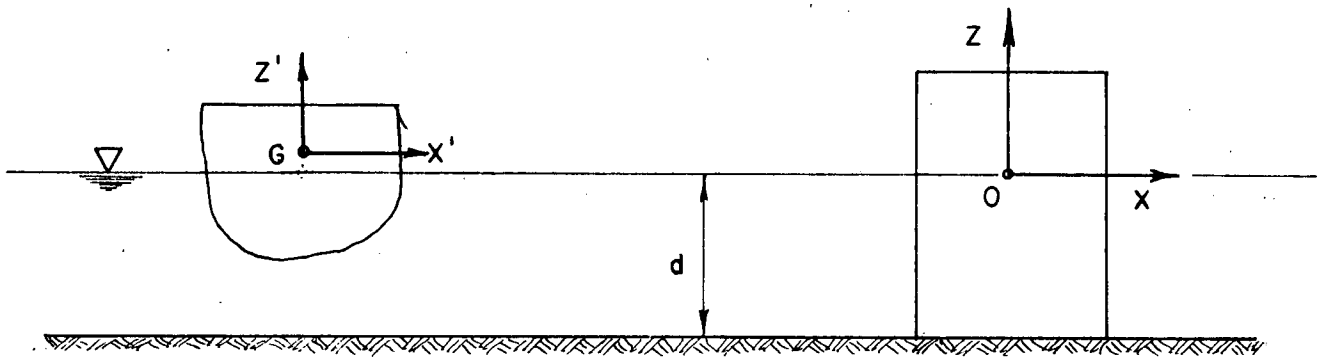

(b) ELEVATION

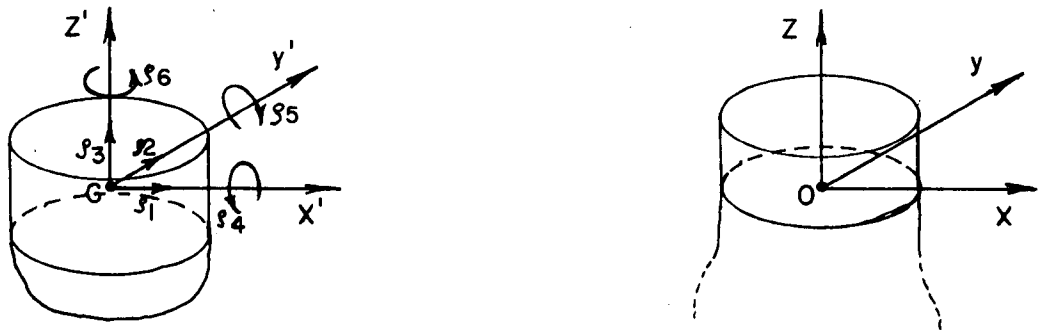

(c) COMPONENT MOTIONS

HAY & COMPANY CONSULTANTS INC.

ENVIRONMENTAL STUDIES
REVOLVING FUNDS
MOTION & IMPACT OF ICEBERGS

DEFINITION SKETCH

FIG. 1

6.1.1 Wave-Induced Motions

Three distinct flow regimes are associated with the wave-induced motions. For ice masses of a diameter to wave length D_i/L between approximately 0.2 and 2, the oscillatory motions of the ice mass are not negligible. Wave diffraction and radiation by the ice mass as well as wave diffraction by the structure are significant and must be considered in the ice mass motions. These are obtained by solving the two body linear wave diffraction problem in which one body (the structure) is fixed and the other (the ice mass) is freely floating. For very large ice masses, corresponding to D_i/L greater than about 2, both the ice mass and the structure diffract the waves but the ice mass oscillatory motions are negligible. The wave drift force, however, is required for the drift motion computation so that a diffraction computation is necessary. For smaller ice masses corresponding to D_i/L less than about 0.2, wave diffraction from the ice mass is negligible. The ice mass then essentially behaves as a fluid particle and follows the orbital motion of the fluid. In this case, only a single, fixed body diffraction computation is required to obtain the orbital velocities at the ice mass location. For certain ranges of parameters, however, the oscillating motions may be increased by resonance effects in heave, pitch and roll. The calculation of these effects requires calculations of the added masses and damping characteristics of the ice mass which are obtained from the two body diffraction solution.

Overall, a two body diffraction calculation is usually necessary over the full range of ice mass sizes, although a single fixed body diffraction calculation may sometimes be adequate.

In the calculation of wave-induced motions, the ice mass is considered to possess all six degrees of freedom, corresponding to surge, sway, heave, roll, pitch and yaw.

6.1.2 Drift Motion

Different flow regimes also apply for drift motions. When the ice mass diameter to structure diameter D_i/D is sufficiently small, the ice mass may be considered to be located in the nonuniform current field as influenced by the structure. The trajectory of the ice mass then obtained by a time-stepping procedure applied to this constant current field. If D_i/D is sufficiently large, the extent of the disturbed flow field around the structure is on the same order as the size of the ice mass and, therefore, has a smaller influence on the ice mass. In this case, a uniform current field may be assumed and the presence of the structure on the current field ignored.

With respect to drift motions, the ice mass possesses two degrees of freedom - surge and sway.

The drift motions may depend also on the wave drift forces and zero frequency added masses. The relative importance of wave drift forces may be assessed with reference to the ratio of wave drift force $F^{(w)}$ to current drag force $F^{(d)}$, for a floating truncated circular cylinder. This is given approximately as:

$$\frac{F^{(w)}}{F^{(d)}} = 0\left[\frac{0.1gH^2}{U_r^2 h}\right] \qquad (6.1)$$

where g is the gravitational constant, H is the wave height, U_r is the current magnitude relative to the drift velocity of the ice mass and h is the draft of the ice mass. Thus for any specified situation, this ratio may be used to assess the need to include wave drift forces in the drift computation.

The zero frequency added masses also appear in the drift

equations of motion and depend on the proximity of the ice mass to the structure. They are obtained by solving the two body diffraction problem at a very low wave frequency. Certain simplifications may be applicable in this calculation, particularly in the Green's function used and in the absence of any incident flow.

6.1.3 Underlying Assumptions

A complete modelling of the full physical problem including the numerous nonlinear and secondary influences, is not at present possible. Assumptions, valid over a practical range of physical conditions and parameters, are introduced to render the problem solvable. The chief implicit assumptions are:

1) The current is sufficiently slow so that free surface effects associated with the current field in the absence of waves can be neglected.

2) Nonlinear interaction terms are sufficiently small so that the wave and current fields are each treated separately.

3) In the wave diffraction calculations, the ice mass is assumed to have a fixed equilibrium position (i.e., the oscillatory motions and wave radiation are not influenced by the superposed mean drift). This quasi-steady assumption is valid for relatively slow drift velocities. Typically, the fluid particle velocities due to waves are an order of magnitude greater than those due to currents.

4) Likewise, the drift forces are calculated using the mean, rather than the total (mean plus oscillatory) ice mass velocities. As the wave-induced motions are zero-

mean and as the wave drift is calculated separately, the assumption is appropriate. Assumptions 1 through 4 describe the de-coupling of wave and current interactions introduction by the proposed solution.

5) As is commonly adopted in diffraction analyses, the wave height is assumed small relative to the wave-length.

6) The fluid is incompressible and inviscid. The flow is assumed irrotational to allow a solution in terms of velocity potential. Flow separation is therefore initially neglected. Viscous damping effects on the ice motion are included through the use of empirical coefficients in the equations of motion.

7) Yaw motion in the drift is ignored. The assumption is independent in that it is a consequence of the treatment of the drift flow regimes described in Section 6.1.2.

8) In Section 6.1.2, the effect due to wind, Coriolis force and sea-surface slope are ignored.

6.1.4 Computer Procedure

A computer procedure, based on the above considerations, is described by the flow chart given in Figure 2. In essence, initial diffraction and current field calculations are first carried out, and then a time-stepping procedure is applied to the drift equations of motion in order to obtain successive values of the drift velocity and location of the ice mass. At each time step the current field at the ice mass location is recalculated, and, after a user-specified number of time steps, the diffraction calculation is repeated.

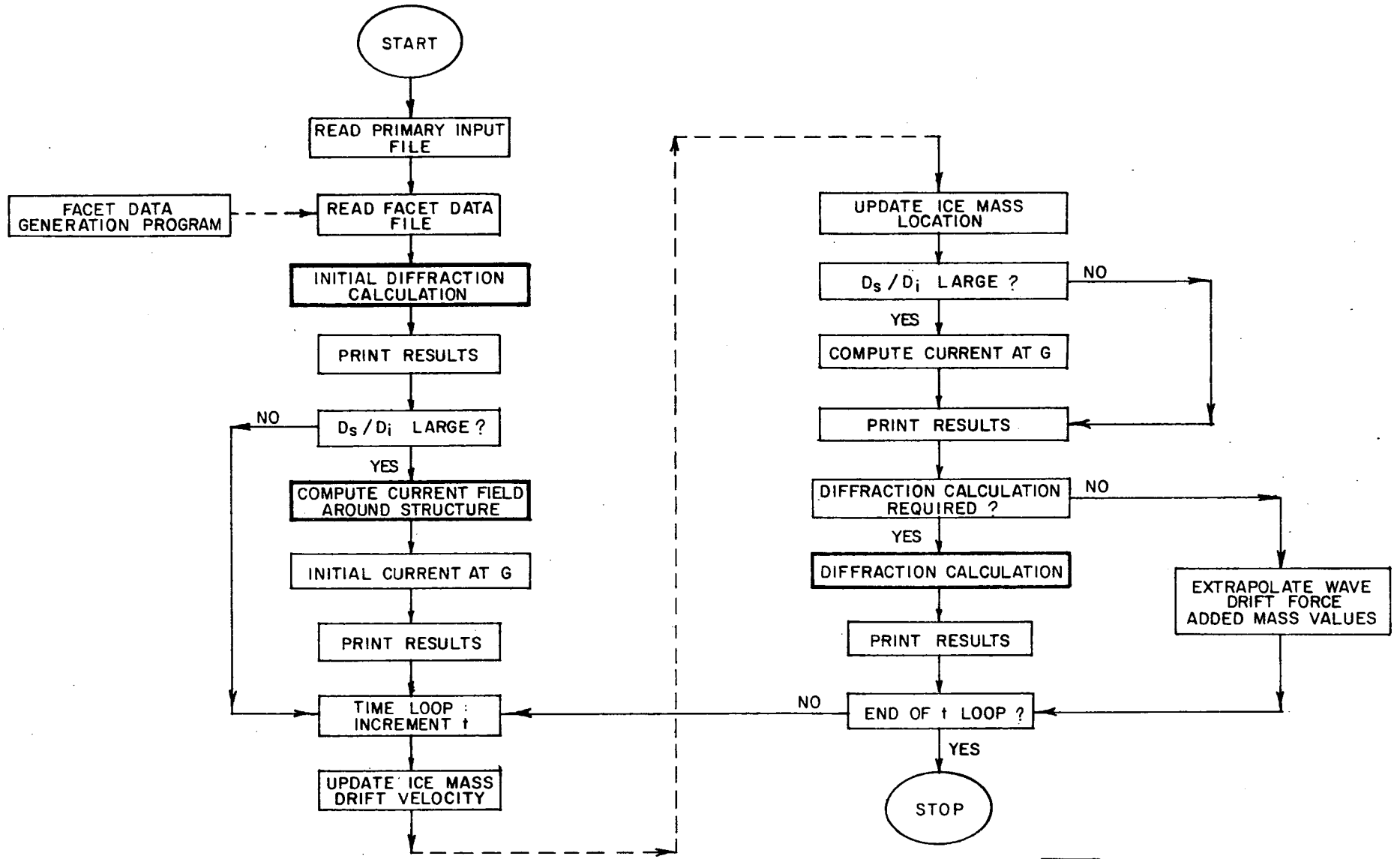

HAY & COMPANY CONSULTANTS INC.

ENVIRONMENTAL STUDIES REVOLVING FUNDS

MOTION & IMPACT OF ICEBERGS

FLOW CHART OF COMPUTER PROGRAM

FIG. 2

6.2 Wave Induced Motions

The method described below is based on a boundary element method utilizing a three-dimensional Green's function. It is applicable to a two-body problem, with one fixed and the other freely floating in regular waves. The notation and conventions are consistent with those used in common formulations of the single-body problem (Sarpkaya & Isaacson, (1981)). The extension to random waves is straightforward in principle and essentially requires a repetition of the diffraction calculation for a series of wave frequencies. The extension requires a large number of separate diffraction computations to be carried out because the calculation must also be performed for a series of ice mass locations. The computations would thus be extremely expensive and were not attempted in this study. A further extension to directional seas is possible in a similar way, but again would substantially increase the computational effort required.

6.2.1 Governing Equations

A regular small amplitude wave train propagates in water of constant depth d past a fixed offshore structure and a freely floating ice mass, both of arbitrary three-dimensional shape as depicted in Figure 1. Since the ice mass is drifting and its component motions are conveniently described with respect to axes fixed relative to its drifting location, it is appropriate to employ two coordinate systems as indicated on the figure. G is the centre of gravity of the ice mass and Gx'y'z' forms a right-handed Cartesian coordinate system relative to which the component motions of the ice mass are defined and with axis Gz' taken as vertical. Oxyz forms a second Cartesian coordinate system, fixed in space, with the origin 0 conveniently located at a reference point within the structure and at the still water level. The axis x is measured horizontally and parallel to the axis Gx' of the ice mass and the axis z measured upwards.

Although the ice mass is drifting, the wave-induced motions are treated by considering the ice mass to have a fixed equilibrium position so that for any one computation the Gx'y'z' coordinate system is considered fixed. Three parameters are then needed to determine the relationship between the two, parallel coordinate systems. This conveniently involves x_G, y_G, z_G, the x, y, z coordinates of G, and is simply:

$$x' = x - x_G$$

$$y' = y - y_G \qquad (6.2)$$

$$z' = z - z_G$$

The wave train has a height H and angular frequency ω and propagates in a direction α to the x axis. The fluid is assumed incompressible and inviscid, and the flow irrotational so that the fluid motion may be described by a velocity potential (defined here such that the fluid velocity vector $\underline{u} = \nabla\phi$) which satisfies the Laplace equation within the fluid region. The wave height is assumed sufficiently small for linear wave theory to apply so that ϕ is subject to the usual boundary conditions, linearized where appropriate, at the seabed; the ice mass and structure submerged surfaces; the free surface; and the far field.

In general, the ice mass oscillates with six degrees of freedom corresponding to surge, sway, heave, roll, pitch and yaw, denoted by the subscripts 1, ..., 6 respectively, and defined with respect to the Gx'y'z'system as indicated in Figure 1. Each mode of motion is harmonic and may be expressed in the form $\zeta_k \exp(-i\omega t)$, in which t is time and ζ_k is the complex amplitude of each component motion.

Since the drift motion over a few wave periods is small, the

linearized boundary condition on the ice mass surface is applied on its equilibrium surface S which is considered fixed. Thus this boundary condition on the submerged equilibrium surface of the ice mass S_i and on the submerged surface of the structure S_s is given as:

$$\frac{\partial \phi (\underline{x})}{\partial n} = \begin{cases} 0 & \underline{x} \text{ on } S_s \\ V_n(\underline{x}) & \underline{x} \text{ on } S_i \end{cases} \tag{6.3}$$

where $\underline{x}$ represents a point in the fluid, and n denotes distance in the direction of the unit vector $\underline{n}$ directed normally out of S. Also V_n is the velocity of the ice mass surface in the direction $\underline{n}$ and is itself given as:

$$V_n(\underline{x}) = \sum_{k=1}^{6} -i\omega\zeta_k n_k(\underline{x})\exp(-i\omega t) \tag{6.4}$$

in which

$$\begin{aligned} n_1 &= n_x \\ n_2 &= n_y \\ n_3 &= n_z \\ n_4 &= y'n_z - z'n_y \\ n_5 &= z'n_x - x'n_z \\ n_6 &= x'n_y - y'n_x \end{aligned} \tag{6.5}$$

where n_x, n_y, n_z are the direction cosines of $\underline{n}$ in the x,y,z (or x',y',z') direction respectively.

The flow potential is made up of components associated with the incident waves (subscript 0), the scattered waves due to both the

structure and ice mass (subscript 7) and forced waves due to each mode of motion (subscripts 1, ..., 6), each of the latter being proportional to the corresponding motion amplitude. Thus, it is convenient to express the total flow potential as:

$$\phi = \{-\frac{i\,H}{2}(\phi_0 + \phi_7) + \sum_{k=1}^{6} -i\omega\zeta_k\phi_k\}\exp(-i\omega t) \tag{6.6}$$

in which ϕ_k is generally complex.

Substituting Eqs. 6.4-6.6 into Eq. 6.3, and separating out terms corresponding to the diffraction problem (k = 0, 7) and to each component of the radiation problem (k = 1, ..., 6), the body surface boundary condition can be decomposed into the form:

$$\frac{\partial\phi}{\partial n}k(\underline{x}) = \tfrac{1}{2}b_k(\underline{x}) \tag{6.7}$$

where:

$$b_k(\underline{x}) = \begin{cases} 0 & k=1,\ldots,6 \text{ and } \underline{x} \text{ on } S_s \\ 2n_k(\underline{x}) & k=1,\ldots,6 \text{ and } \underline{x} \text{ on } S_i \\ -2\frac{\partial\phi_0}{\partial n}(\underline{x}) & k=7 \text{ and } \underline{x} \text{ on } S \end{cases} \tag{6.8}$$

and S represents the combined surfaces S_i and S_s.

The incident potential ϕ_0 is known and is given as:

$$\phi_0 = \frac{\cosh(k(z+d))}{k\sinh(kd)}\exp[ik(x\cos\alpha + y\sin\alpha)] \tag{6.9}$$

where k is the wave number.

6.2.2 Source Distribution Representation

The unknown potentials may each be represented by a distribution of point wave sources over the surface S. Thus the potential $\phi_k(\underline{x})$ at a general point $\underline{x}$ within the fluid is expressed as:

$$\phi_k(\underline{x}) = \frac{1}{4\pi} \int_S f_k(\underline{\xi}) G(\underline{x}, \underline{\xi}) dS \qquad k=1,\ldots,7 \tag{6.10}$$

where $f_k(\underline{\xi})$ represents a source strength distribution function, ξ is a point on the surface S over which the integration is performed, and $G(\underline{x},\underline{\xi})$ is a Green's function for the general point $\underline{x}$ due to a source of unit strength located at ξ. G is itself chosen to satisfy the Laplace equation, the seabed boundary condition, the linearized free surface condition and the radiation condition. Alternative expressions for G have been developed. (See, e.g. Hogben & Standing, 1974).

The source strength functions f_k may be determined by applying the body surface boundary condition. This condition, given by Eqs. 6.7 and 6.8, together with the representation for ϕ_k given by Eq. 6.10, gives rise to a set of surface integral equations for f_k:

$$-f_k(\underline{x}) + \frac{1}{2\pi} \int_S f_k(\underline{\xi}) \frac{\partial G}{\partial n}(\underline{x},\underline{\xi}) dS = b_k(\underline{x})$$

$$k = 1,\ldots,7 \tag{6.11}$$

where $\underline{x}$ now lies on the surface S at the point where the boundary condition is applied, n is measured from $\underline{x}$, and the integration is carried out over the points ξ.

6.2.3 Discretization Procedures

In a numerical solution to Eq. 6.11, the surface S is discretized into a number of small facets, with a total of N facets being made up of N_i and N_s facets on S_i and S_s respectively, and the functions f_k are taken as uniform over each facet. The integral equations are then applied at each facet centre in turn and so may be expressed as seven sets of linear algebraic equations:

$$\sum_{j=1}^{N} A_{ij} f_j^{(k)} = b_i^{(k)} \qquad i=1,\ldots,N \quad k=1,\ldots,7 \tag{6.12}$$

where $f_j^{(k)}$ and $b_i^{(k)}$ denote $f_k(\underline{x}_i)$ and $b_k(\underline{x}_i)$ respectively, and $\underline{x}_j$ is the value of x at the centre of the j-th facet. If the facet sizes are small relative to the wave length, an approximate expression for the coefficients A_{ij} may be developed as follows:

$$A_{ij} = \begin{cases} \frac{\Delta S_j}{2\pi} \frac{\partial G}{\partial n_i}(\underline{x}_i, \underline{\xi}_j) & i \neq j \\ -1 & i = j \end{cases} \tag{6.13}$$

where ΔS_j is the area of the j-th facet. Equations 6.11 may now be solved to determine the source strengths f_k. Once the source strengths are known, the potentials ϕ_k at the facet centres on the ice mass may themselves be obtained from a discretized form of Eq. 6.10:

$$\phi_i^{(k)} = \sum_{j=1}^{N} B_{ij} f_j^{(k)} \tag{6.14}$$

where $\phi_i^{(k)}$ denotes $\phi_k(\underline{x}_i)$. An approximate expression for the coefficients B_{ij} may be obtained in a similar way as for A_{ij} and is:

$$B_{ij} = \begin{cases} \frac{\Delta S_j}{4\pi} G(\underline{x}_i, \underline{\xi}_j) & i \neq j \\ \frac{\Delta S_i}{4\pi} \Gamma \quad \frac{\Delta S_i}{4\pi} G(\underline{x}_i, \underline{\xi}_i) & i = j \end{cases} \tag{6.15}$$

where

$$\Gamma = \frac{1}{\sqrt{\Delta S_i}} \int_{\Delta S_i} \frac{1}{R} \, dS \tag{6.16}$$

$R = |\underline{x} - \underline{\xi}|$ and $G(\underline{x}_i, \underline{\xi}_i)$ excludes the singular term $1/R$ which appears in the expression for G. The integral Γ may be obtained for any given facet shape as indicated by Hogben and Standing (1974).

6.2.4 Hydrodynamic Coefficients

The components of fluid force or moment acting on the ice mass are expressed as:

$$F_j = -i\omega \int_{S_i} \phi n_j \, dS \qquad j=1,\ldots,6 \tag{6.17}$$

Here F_1, F_2, F_3 denote the force components along the x', y', z' axes and F_4, F_5, F_6 denote the moment components about the x', y', z' axes as indicated for ζ_k in Figure 1. Each such component may be decomposed into an exciting force component $\underline{F}_j^{(e)}$ associated with $\phi_0 + \phi_7$, and components associated with the forced potentials $\phi_1, \ldots, \phi_6$. The latter may in turn be described in terms of added masses μ_{jk} and damping coefficients λ_{jk} (which are real) so that F_j is expressed as:

$$F_j = F_j^{(e)} + \sum_{k=1}^{6} (\omega^2 \mu_{jk} + i\omega\lambda_{jk})\zeta_k \exp(-i\omega t) \qquad (6.18)$$

Expressions for $\underline{F}^{(e)}$, μ_{jk} and λ_{jk} may be obtained by substituting Eqs. 6.6 and 6.18 into Eq. 6.17 and collecting corresponding terms. Using the discretization approximation already described, this gives:

$$F_j^{(e)} = -\tfrac{1}{2}\rho g H k \sum_{i=1}^{N_i} (\phi_i^{(0)} + \phi_i^{(7)}) n_{ij} \Delta S_i \qquad (6.19)$$

$$\mu_{jk} = -\rho \mathrm{Re}\{I_{jk}\} \qquad (6.20)$$

$$\lambda_{jk} = -\rho\omega \mathrm{Im}\{I_{jk}\} \qquad (6.21)$$

where

$$I_{jk} = \sum_{i=1}^{N_i} \phi_i^{(k)} n_{ji} \Delta S_i \qquad (6.22)$$

n_{ji} denotes $n_j(\underline{x}_i)$ and Re {} and Im {} denote the real and imaginary parts respectively.

6.2.5 Response Amplitude Operators

Once the various hydrodynamic coefficients described above have been obtained, it is relatively straightforward to solve the equations of motion of the ice mass in order to determine the six components of motion. The equations of motion may be written in the form:

$$\sum_{k=1}^{6} \{-\omega^2(m_{jk} + \underline{\mu}_{jk}) - i\omega(\lambda_{jk} + \lambda_{jk}^{(v)})\} = c_{jk}\,\zeta_k = F_j^{(e)} \qquad (6.23)$$

where m_{jk} is the mass matrix, c_{jk} is the hydrostatic stiffness matrix and $\lambda_{jk}^{(v)}$ are empirical viscous damping coefficients which are taken as zero except possibly for heave, roll and pitch motions.

The mass matrix components are given as:

$$m_{jk} = \begin{bmatrix} m & 0 & 0 & 0 & 0 & 0 \\ 0 & m & 0 & 0 & 0 & 0 \\ 0 & 0 & m & 0 & 0 & 0 \\ 0 & 0 & 0 & I_1 & -I_{12} & -I_{13} \\ 0 & 0 & 0 & -I_{12} & I_2 & I_{23} \\ 0 & 0 & 0 & -I_{13} & -I_{23} & I_3 \end{bmatrix} \qquad (6.24)$$

where m is the mass of the ice and I_1, I_2, I_3 are its moments of inertia about the x', y', z' axes respectively. Also, I_{12}, I_{13} and I_{23} are its products of inertia defined as:

$$\begin{aligned} I_{12} &= \int_V \rho_i x'y'dV \\ I_{13} &= \int_V \rho_i x'z'dV \\ I_{23} &= \int_V \rho_i y'z'dV \end{aligned} \qquad (6.25)$$

where ρ_i is the density of the ice and V is its volume. For an ice mass which is symmetrical about the Gx'z' plane, $I_{12} = I_{23} = 0$; and for an ice mass which is symmetrical about the Gy'z' plane, $I_{12} = I_{13} = 0$.

The hydrostatic stiffness matrix components are given as:

$$C_{jk} = \begin{bmatrix} 0 & 0 & 0 & 0 & 0 & 0 \\ 0 & 0 & 0 & 0 & 0 & 0 \\ 0 & 0 & C_{33} & C_{34} & C_{35} & 0 \\ 0 & 0 & C_{34} & C_{44} & 0 & 0 \\ 0 & 0 & C_{35} & 0 & C_{55} & 0 \\ 0 & 0 & 0 & 0 & 0 & 0 \end{bmatrix} \tag{6.26}$$

where:

$$\begin{aligned} C_{33} &= \rho g S_w \\ C_{34} &= -\rho g S_2 \\ C_{35} &= -\rho g S_1 \\ C_{44} &= \rho g S_{22} + mgz'_B \\ C_{55} &= \rho g S_{11} + mgz'_B \end{aligned} \tag{6.27}$$

in which z'_B is the z' coordinate of the centre of buoyancy. Also S_1, S_2, S_{11}, S_{22} and S_w are the waterplane area and moments defined as:

$$\begin{aligned} S_w &= \int dS \\ S_1 &= \int x' dS \\ S_2 &= \int y' dS \\ S_{11} &= \int x'^2 dS \\ S_{22} &= \int y'^2 dS \end{aligned} \tag{6.28}$$

where the above integrals are taken over the waterplane. For an ice mass which is symmetrical about the x-z and y-z planes we have $S_1 = S_2 = 0$.

The viscous damping coefficients $\lambda^{(v)}_{jk}$ may be generally taken as zero except for heave, roll and pitch motions, corresponding to $\lambda^{(v)}_{33}$, $\lambda^{(v)}_{44}$ and $\lambda^{(v)}_{55}$ and may be expressed in terms of empirical viscous damping ratios cj as:

$$\lambda^{(v)}_{jj} = 2c_j\sqrt{c_{jj}(m_{jj} + \mu_{jj})} \tag{6.29}$$

(Note that the definition of c_j used here is based on values of μ_{jj} at the oscillation frequency, whereas values based on the natural frequency are also used as an alternative.)

The solution to Eq. 6.23 can now be carried out to obtain the response amplitude operators which describe the ice mass responses for incident waves as required. With the values of ζ_k determined, the potential (Eq. 6.6) and thus the pressure field ($p=-\rho\partial\phi/\partial t$, from the linearized Bernoulli equation) are explicitly known.

6.2.6 Wave-Drift Forces

In the drift motion calculation described in Section 6.3.2, wave drift forces, important in certain circumstances, are obtained from the diffraction solution described here. In the calculation of drift motions, the ice mass is assumed to have two degrees of freedom (surge and sway) and thus only the corresponding drift force components are required. These are obtained from formulae provided by Faltinsen and Michelsen (1974) which involve the source strengths f_k and the oscillatory motion amplitudes ζ_k already determined.

6.2.7 Zero Frequency Added Masses

The drift motion calculation also depends on the zero frequency added masses of the ice with respect to surge and sway motions. These can be obtained from the diffraction calculation, now applied at a very low wave frequency. The Green's function need not be the same as that used in the wave diffraction calculation because a zero frequency limit is required. In this case, the simpler Green's function used in the current field computation may be employed (e.g. Garrison, 1978). However, the general procedure used to obtain the added masses exactly follows that outlined in this section.

6.2.8 Small Ice Masses

When the ice mass is relatively small (D_i/L less than about 1/10) it may be assumed not to affect the wave motion. This case is considerably simpler to treat since only the wave diffraction around the fixed structure need be considered in establishing the fluid flow. Furthermore, the computation need be carried out only once since it is now independent of the ice mass location.

The full theoretical development proceeds along the lines already discussed for a large ice mass, but various simplifications may be introduced. Only a single body, corresponding to the offshore structure is considered, so that $S = S_s$, and terms relating to S_i alone are absent. Secondly, since the structure is fixed, the forced potentials, corresponding to k = 1, ..., 6 are absent, and only the problem corresponding to k = 7 need be treated. Only the 0xyz coordinate system is required to solve the diffraction problem and the location of the ice mass only enters the problem in determining the velocity components at its location. Once the potential ϕ_k has been obtained, the equations of motion are not solved directly as before, but rather the fluid velocity at the

location G of the ice mass may be obtained.

To account for resonance effects, the added mass and damping coefficients of the ice mass must be included into the equations of motion. The coefficients are determined from the same two body diffraction calculation as applied to larger ice masses.

6.3 Drift Motions

When the ice mass diameter to structure diameter ratio D_i/D_s is sufficiently small, the ice mass is considered to be in the nonuniform current field produced by the structure. The current field around the structure need then be computed and the trajectory of the ice mass then obtained by a time-stepping procedure applied to this non-uniform current field. If D_i/D_s is sufficiently large the structure has little influence on the current field around the ice mass. In this case, a uniform current field may be assumed and the presence of the structure on the current field ignored.

With respect to drift motions, the ice mass possesses three degrees of freedom (surge, sway and yaw). As an appropriate simplification, the drift in yaw is neglected. The extension to include yaw would require a computation of the flow field around the entire ice mass surface and applying this to a semi-empirical expression for the resulting torque on the ice mass. Due to flow separation effects, considerable uncertainty would be attached to this procedure.

Section 6.3.1 below describes the calculation of the current field around the structure which is required for relatively small values of D_i/D_s. If D_i/D_s is large, then the calculation can proceed directly with the equations of motion as described in Section 6.3.2.

6.3.1 Current Field for Small D_i/D_s

Since an input is only affected by the flow around the upstream side of the structure and since the ice mass is assumed to be relatively small, flow separation around both the structure and the ice mass are neglected. Potential flow theory is used, and the description given below largely follows that in Section 6.2 for the wave diffraction calculation.

A freely floating ice mass is situated in a uniform current which flows past a fixed large offshore structure, as depicted in Figure 1. As before, Oxyz forms a right-handed Cartesian coordinate system with x measured horizontally and z measured upwards from the still water level. The fluid is assumed incompressible and inviscid, and the flow is assumed irrotational. The fluid motion is described by a velocity potential (defined such that the fluid velocity vector $\underline{u} = \nabla\phi$) which satisfies the Laplace equation within the fluid region. The potential ϕ is subject to boundary conditions on the free surface, the seabed, the structure submerged surface and the far field.

The velocity potential ϕ is expressed as:

$$\phi = \phi_c + \phi_d \tag{6.30}$$

where ϕ_c is the potential associated with the incident current flow alone and ϕ_d is the disturbance potential due to the presence of the structure. If the incident flow is represented as a uniform current of magnitude U flowing at an angle β to the x axis, then:

$$\phi_c = U(x\cos\beta + y\sin\beta) \tag{6.31}$$

The incident potential ϕ_c is thus known and ϕ_d is to be determined such that it also satisfies the Laplace equation and that the boundary conditions are satisfied.

The body surface boundary condition requires that there is no flow velocity normal to the submerged structure surface S and may be written as:

$$\frac{\partial \phi}{\partial n}(\underline{x}) = \tfrac{1}{2} b(\underline{x}) \qquad \underline{x} \text{ on } S$$
$$b_k(\underline{x}) = -2\frac{\partial \phi}{\partial n} c(\underline{x}) \tag{6.32}$$

and n denotes distance in the direction of the unit normal vector $\underline{n}$ directed normally out from S.

The disturbance potential ϕ_d may be represented as a distribution of point sources around the submerged structure surface S. Thus the potential $\phi_d(\underline{x})$ at a general point $\underline{x}$ within the fluid may be expressed as:

$$\phi_d(\underline{x}) = \frac{1}{4\pi} \int_S f(\underline{\xi}) G(\underline{x}, \underline{\xi}) dS \tag{6.33}$$

where $f(\underline{\xi})$ is a source strength distribution function, $\underline{\xi}$ is a point on the surface S over which the integration is performed, and $G(\underline{x},\underline{\xi})$ is a Green's function for the general point $\underline{x}$ due to a source of unit strength located at $\underline{\xi}$.

G is itself chosen to satisfy the Laplace equation and the various boundary conditions. The current is assumed to be sufficiently slow so that free surface effects can be neglected

and the free surface condition then corresponds simply to the requirement that the vertical velocity there is zero. The Green's function thus corresponds to that of a point source with reflection terms to account for the seabed and free surface conditions, and is known (e.g. Garrison, 1978).

The source strength function f is required and may be determined by applying the body surface boundary condition. This condition, Eq. 6.32, yields a surface integral equation for f:

$$-f(\underline{x}) + \frac{1}{2\pi}\int_S f(\underline{\xi})\frac{\partial G}{\partial n}(\underline{x}, \underline{\xi})dS - b(\underline{x}) \qquad (6.34)$$

where $\underline{x}$ now lies on S at the point where the boundary condition is applied, n is measured from $\underline{x}$ and the integration is carried out over the points $\underline{\xi}$.

In a numerical solution to Eq. 6.34 the surface is discretized into N small facets with the function f taken as uniform over each facet. The surface integral equation is then approximated as a set of linear algebraic equations for $F_j = f(\underline{x}_j)$:

$$\sum_{j=1}^{N} A_{ij}f_j = b_i \qquad i=1,\ldots,N \qquad (6.35)$$

where $b_i = b(\underline{x}_i)$ and $\underline{x}_i$ is the value of $\underline{x}$ at the centre of the i-th facet. The matrix coefficients may be approximated as:

$$A_{ij} = \begin{cases} \frac{\Delta S_j}{2\pi}\frac{\partial G}{\partial n}(\underline{x}_i, \underline{\xi}) & i \neq j \\ -1 & i=j \end{cases} \qquad (6.36)$$

where ΔS_j is the area of the j-th facet. With the source strengths f_j evaluated, the velocity potential is obtained by a

discretized form of Eq. 6.33. The velocity components obtained by differentiating Eq. 6.33 with respect to the corresponding directions and then applying a similar discretized procedure. The current velocity components $u_1^{(c)}$ and $u_2^{(c)}$ in the x and y directions respectively are given as:

$$u_i^{(c)} = \frac{\partial \phi}{\partial n_i}(\underline{x}) = \frac{\partial \phi c(\underline{x})}{\partial n_i} + \sum_{j=1}^{N} B_{ij} f_j \qquad i=1,2 \qquad (6.37)$$

where

$$B_{ij} = \frac{\Delta S_j}{4\pi} \frac{\partial G}{\partial n_i}(\underline{x}, \underline{\xi}_j) \qquad (6.38)$$

and n_i is here taken as the x and y directions in turn.

6.3.2 Equations of Motion

The forces acting on the ice mass are comprised of the current drag, the wave drift force, the wind drag and the combined force associated with the Coriolis force and the effect of sea surface slope. For short term motion predictions in the vicinity of a structure as required here, the current drag and possibly the wave drift force are expected to be the most significant and are included while the remainder are neglected.

The horizontal drag force vector $\underline{F}^{(d)}$ involves the local current velocity $\underline{u}^{(c)}$ and the ice mass velocity $\underline{u}$ and may be expressed as:

$$\underline{F}^{(d)} = \tfrac{1}{2}\rho A C_d \underline{u}^{(r)} |\underline{u}^{(r)}| \qquad (6.39)$$

where $\underline{u}^{(r)}$ is the current velocity vector relative to the ice mass and is given as $\underline{u}^{(r)} = \underline{u}^{(c)} - \underline{u}$, C_d is a drag coefficient and A is the projected area of the ice mass on to the plane perpendicular to $\underline{u}^{(r)}$. Equation 6.39 may be expressed in terms of the drag force components in the x and y directions as:

$$F_i^{(d)} = \tfrac{1}{2}\rho A C_d u_i^{(r)} |\underline{u}^{(r)}| \qquad i=1,2 \qquad (6.40)$$

where the subscripts 1 and 2 denote the components in the x and y directions respectively. The wave drift force $\underline{F}^{(w)}$ may be computed from the diffraction calculation as already described in Section 6.2.6.

The equations for surge and sway may now be expressed as:

$$(m + \mu_i)\dot{u}_i = F_i^{(d)} + F_i^{(w)} \qquad i=1,2 \qquad (6.41)$$

where μ_1, μ_2 are the zero frequency added masses in the x and y directions respectively and may be obtained as indicated in Section 6.2.7. The equations of motion are conveniently written as:

$$\dot{u}_i = a_i \qquad i=1,2 \qquad (6.42)$$

where

$$a_i = (F_i^{(d)} + F_i^{(w)})/(m + \mu_i) \qquad (6.43)$$

Equation 6.42 represents a pair of nonlinear equations for u_i and may be solved by a suitable time-stepping procedure. Many such methods are available, including the Runge-Kutta methods and others. As a relatively simple but reliable method the Adams-

Bashforth two-step formula may be used and gives the solution at an advanced time $t + \Delta t$ in terms of the solution at previous time steps t and $t - \Delta t$ as:

$$u_i(t+\Delta t) = u_i(t) + \tfrac{1}{2}\Delta t[3a_i(t) - a_i(t-\Delta t)] \qquad (6.44)$$

In applying Eq. 6.44, the right-hand sides contain quantities at times t and $t - \Delta t$ which are known from previous iterations so that the ice mass velocity u_i at the new time $t + \Delta t$ may be obtained.

Once the drift velocity has been found, the new location may also be determined by a time-stepping procedure applied in a similar way to obtain the new location of the ice mass, described by the coordinates x , y . Thus:

$$\begin{aligned} x_G(t+\Delta t) &= x_G(t) + \tfrac{1}{2}\Delta t[3u_1(t) - u_1(t-\Delta t)] \\ y_G(t+\Delta t) &= y_G(t) + \tfrac{1}{2}\Delta t[3u_2(t) - u_2(t-\Delta t)] \end{aligned} \qquad (6.45)$$

6.4 Computer Procedure

6.4.1 Computational Considerations

The accuracy of the diffraction calculation is strongly influenced by the discretization of the submerged ice mass and structure surfaces into a suitable number of facets. The usual representation of the surfaces is by plane polygonal facets. To ensure that the surfaces are divided up sufficiently finely, facet diameters should be less than about 1/8 of the incident wave length and also sufficiently small so as to represent the surface configuration realistically. One or two hundred facets are typically required.

The diffraction calculation is computationally rather expensive, with computer storage and cost considerations limiting the number of facets used. For a single diffraction calculation the computation involves the calculation of a corresponding set of matrix coefficients, which include lengthy expressions based on the Green's function, and a solution of the full matrix equation. Since the interaction between the ice mass and the structure is of paramount interest, the diffraction calculation has to be repeated for different ice mass locations along its trajectory, but it need not be repeated at every time step of the drift motion calculation. Rather it is repeated every several time steps and intermediate values of zero frequency added mass and wave drift force, required for the drift calculation, are obtained by a simple extrapolation procedure.

Numerical instabilities in the diffraction procedure are not generally expected since considerable experience has been gained in the context of motion response calculations for floating vessels, including interference effects between neighbouring bodies. Some numerical difficulties may arise when the facets on the ice mass and structure surfaces are less than about one facet diameter apart (Section 7). These can be avoided for particular situations by a judicious choice of facet size and number. Similarly, the time-stepping procedure applied to the drift equations of motion is of a general form which has been treated rather extensively in the past, and associated numerical instabilities are not expected.

6.4.2 Program Computations

The proposed computer procedure is indicated in the flow chart given in Figure 2. The facet data required for the diffraction and wave field solutions are prepared by a pre-processing program. The main procedure involves an initial diffraction

calculation to obtain initial values of the wave-induced motions, the wave drift forces and the zero frequency added masses. If the structure diameter to ice mass diameter ratio is sufficiently large the current field around the structure is then computed and the initial current velocity at the ice mass location is determined.

The program then enters a time loop with calculations performed at successive time steps to trace the trajectory of the ice mass. At each time step the equations of motion of the ice mass are used to obtain the updated drift velocity of the ice mass and its new location. The current velocity at this new location is then calculated if necessary (i.e. if D_i/D_s is sufficiently large). Every few time steps, the diffraction solution is also carried out to obtain the wave-induced motions, the wave drift force and the zero frequency added masses corresponding to this new location. The time loop is then repeated to provide an updated drift velocity and location of the ice mass.

A fairly small time step size is needed in order to reproduce a sufficiently accurate drift trajectory of the ice mass. The variation of oscillatory motions, wave drift forces and hydrodynamic coefficients along the trajectory is not expected to be required to the same level of precision. The major computational effort corresponds to the heavily bordered blocks in Figure 2. Of these, the diffraction calculation at successive time steps is the most lengthy, and may be calculated with a coarser time interval than that used for the drift equations of motion calculation. This refinement is indicated in the figure.

7.0 PARAMETRIC AND SENSITIVITY TESTS

Based on the theoretical and numerical considerations outlined in Section 6, a computer model was developed, and tests were undertaken to demonstrate the capabilities of the model. This section presents the results of the parametric and sensitivity tests.

7.1 Test Conditions

A series of numerical tests are described which assess the influences of variations in ice mass size, wave direction, initial ice mass location, current magnitude and water depth, and examines the influence of wave drift forces. A considerable number of parameters are required as input to the computer model and, due to time and budget restraints, many are held constant. The structure is represented as a fixed, surface-piercing, vertical, circular cylinder of diameter 100 m extending to the seabed. The three ice masses are represented as floating circular cylinders of diameters 100 m, 50 m and 10 m, all with drafts equal to the corresponding radii. The dimensions and dynamic properties of the three ice masses are summarized in Table 1.

Environmental parameters for the tests are:

Wave height:	10 m
Wave period:	15 s
Current direction:	0
Drag coefficient:	1.0
Viscous damping ratio:	0.05
Current magnitude:	1.0 m/s (except test 9, where U = 0.4 m/s)
Water depth:	100 m (except test 10, where d = 60 m)

TABLE 1. ICE MASS PROPERTIES

	Ice Mass A	Ice Mass B	Ice Mass C
D_i (m)	100	10	50
h (m)	50	5	25
ℓ (m)	5.9	0.6	2.9
m/ρ (m^3)	392700	392.7	49087
$I_1/m = I_2/m$ (m^2)	885.3	8.85	221.3
I_3/m (m^2)	1250	12.5	312.5
z_G (m)	- 22.06	- 2.21	- 11.03
z_B (m)	- 25	- 2.5	- 12.5
S (m^2)	7854	78.5	1963.5
$S_{11} = S_{22}$ (m^4)	4.91×10^6	491	307×10^3
T_n (sec)	18	6	12

TABLE 2. TEST CONDITIONS

TEST	ICE MASS	WAVE DIR $\alpha(°)$	INITIAL OFFSET y_G (m)	WAVE DRIFT FORCE	OTHER/COMMENT
1	A	0	0	Incl	Symmetrical
2	A	0	25	Incl	Initial offset
3	A	5	0	Incl	Oblique wave dir.
4	A	5	25	Incl	Initial offset and oblique wave dir.
5	B	0	0	Incl	Symmetrical
5A	B	0	0	Excl	
6	B	0	25	Incl	Initial offset
6A	B	0	25	Excl	
7	B	0	1	Incl	Very small initial offset
7A	B	0	1	Excl	
8	B	5	0	Incl	Oblique wave dir.
8A	B	5	0	Excl	
9	A	5	25	Incl	Current = 0.4 m/s
10	A	0	25	Incl	Depth = 60 m
11	C	0	25	Incl	Initial offset; Ice mass C
12	A	Specified locations close to structure			
13	B				

Table 2 lists the conditions for the seventeen test runs (numbered 1 through 13, and 5A through 8A. Tests 1-4 involve the large ice mass A with different combinations of initial offset y_G and wave direction α. A similar set of tests were also undertaken for ice mass B in tests 5-8. In the case of the small ice mass, however, the wave drift force has been found to be a critical factor in the drift motion and thus pairs of tests have been carried out so as to include (tests 5, 6, 7, 8) and exclude (tests 5A, 6A, 7A, 8A) the wave drift force. Tests 7 and 7A include a small initial offset y_G = 1 m to test the possibility of an instability in the drift motion. Test 9 corresponds to the same conditions as test 4 except that the current magnitude is reduced, U = 0.4 m/s rather than 1.0 m/s. Test 10 corresponds to the same conditions as test 2 except that the water depth is reduced, d = 60 m rather than 100 m. Test 11 treats an intermediate size ice mass C with initial offset y_G = 25 m and wave direction $\alpha = 0^o$. Finally, tests 12 and 13 have been carried out with the large and small ice masses relatively close to the structure to examine the possible variation of zero frequency added mass as the gap between the ice mass and structure is reduced.

The numbers of facets used to discretize the ice masses and structure are summarized in Table 3. In the table, N_c and N_d are respectively the number of circumferential and depth divisions used to carry out the discretization. The values given correspond to a maximum facet side length of about 25 m for most tests, except that this length is smaller in tests 12 and 13. The numerical results are unreliable when the gap between the ice mass and structure or seabed is less than the facet size.

The initial drift velocity of the ice mass is generally chosen to give it a zero or small initial x-ward drift acceleration so that the drag force counteracts the wave drift force. The ice mass undergoes a drift acceleration if it is initially drifting at the current velocity because the current drag is then zero and the

TABLE 3. DISCRETIZATION OF STRUCTURE AND ICE MASSES

TEST	ICE MASS	STRUCTURE			ICE MASS		
		N	N_c	N_d	N	N_c	N_d
1-4, 9	A	48	12	4	37	12	2
5-8, 5A-8A	B	48	12	4	25	8	2
10	A	48	12	4	65	16	3
11	C	48	12	4	37	12	2
12	A	108	18	6	73	18	3
13	B	120	20	6	25	8	2

TABLE 4. PERCENTAGE INCREASE IN ZERO FREQUENCY ADDED MASS WITH GAP SIZE FOR ICE MASS A

	GAP SIZE		
	15 m	10 m	5 m
Surge	4.3	9.4	-
Sway	1.8	3.3	-3.1

wave drift force is unbalanced. The initial x-ward locations of the ice masses were taken to correspond to x_G = -300 m for ice mass A and to x_G = -200 m for ice masses B and C.

7.2 Test Results

The computer model output provides (1) the specified input parameters; (2) parameters initially calculated, including various wave frequency parameters, and mass and stiffness matrices of the ice mass; and (3) at each time step, the ice mass velocity and location and the current velocity at the ice mass location. For those time steps at which the diffraction computations are carried out, the output also provides the exciting forces (magnitude and phase), added masses, damping coefficients, response amplitude operators (magnitude and phase), wave drift forces, and the zero frequency added mass (a sample output is shown in the Appendix).

Since a large number of parameters are generated for each test, only the major ones are presented to illustrate the fundamental features of the different motions predicted. The corresponding results of tests 1-11 are shown in Figures 3 - 18. The figures show the ice mass trajectory, the x-ward and y-ward drift velocity components u_1 and u_2, the zero frequency added masses μ_1 and μ_2, the radiation damping coefficients λ_{11}, λ_{22} and λ_{33}, and the motion amplitudes ζ_1, ζ_2, and ζ_3, all as functions of the x-ward location of the ice mass, x_G. (Note that y_G and x_G are plotted to different scales so that the trajectory shown is generally distorted.) In the figures, the following dimensionless forms of the hydrodynamic coefficients are used:

$$\mu_i' = \frac{\mu_i}{\rho D_i^3} \qquad (7.1)$$

$$\mu_{ii}' = \frac{\mu_{ii}}{\rho D_i^3}$$

$$\lambda'_{ii} = \frac{\lambda_{ii}}{\rho\omega D_i^3} \qquad (7.1)$$

cont'd.

$$\zeta'_i = \frac{\zeta_i}{H/2}$$

Here ρ is the water density, D_i is the ice mass diameter, H is the wave height, and $i = 1, 2, 3$ denote the surge, sway and heave components respectively. ζ_i corresponds to the response amplitude operators (RAO's) of the ice mass and is defined with respect to the still water level.

The zero frequency added mass in heave is theoretically infinite for the finite depth cases treated here and so these are absent from the figures.

The results of test 1 are shown in Figure 3. Since the test conditions are symmetrical, the ice mass does not deviate from its initial direction so that y_G remains at zero (Figure 3(a)). Figure 3(b) shows the x-ward drift velocity u_1 to vary only slightly because the ice mass is relatively large in size, and the y-ward component u_2 remains at zero. (The abrupt changes in drift velocity shown here and in subsequent results are associated with a relatively coarse time interval used in the diffraction calculations.) Figure 3(c) indicates that the zero frequency added masses increase only when the gap between the ice mass and structure is of order 0.1 of the ice mass diameter. Thus, only immediately prior to impact is the effect of proximity to the structure important relative to the zero frequency added masses. As stated in Section 6.4.2, at such separations, numerical limitations arise from the facet size. This effect is considered subsequently in tests 12 and 13. Finally, Figures 3(d)-(f) show the wave frequency added masses, damping coefficients and response amplitude operators all as functions of

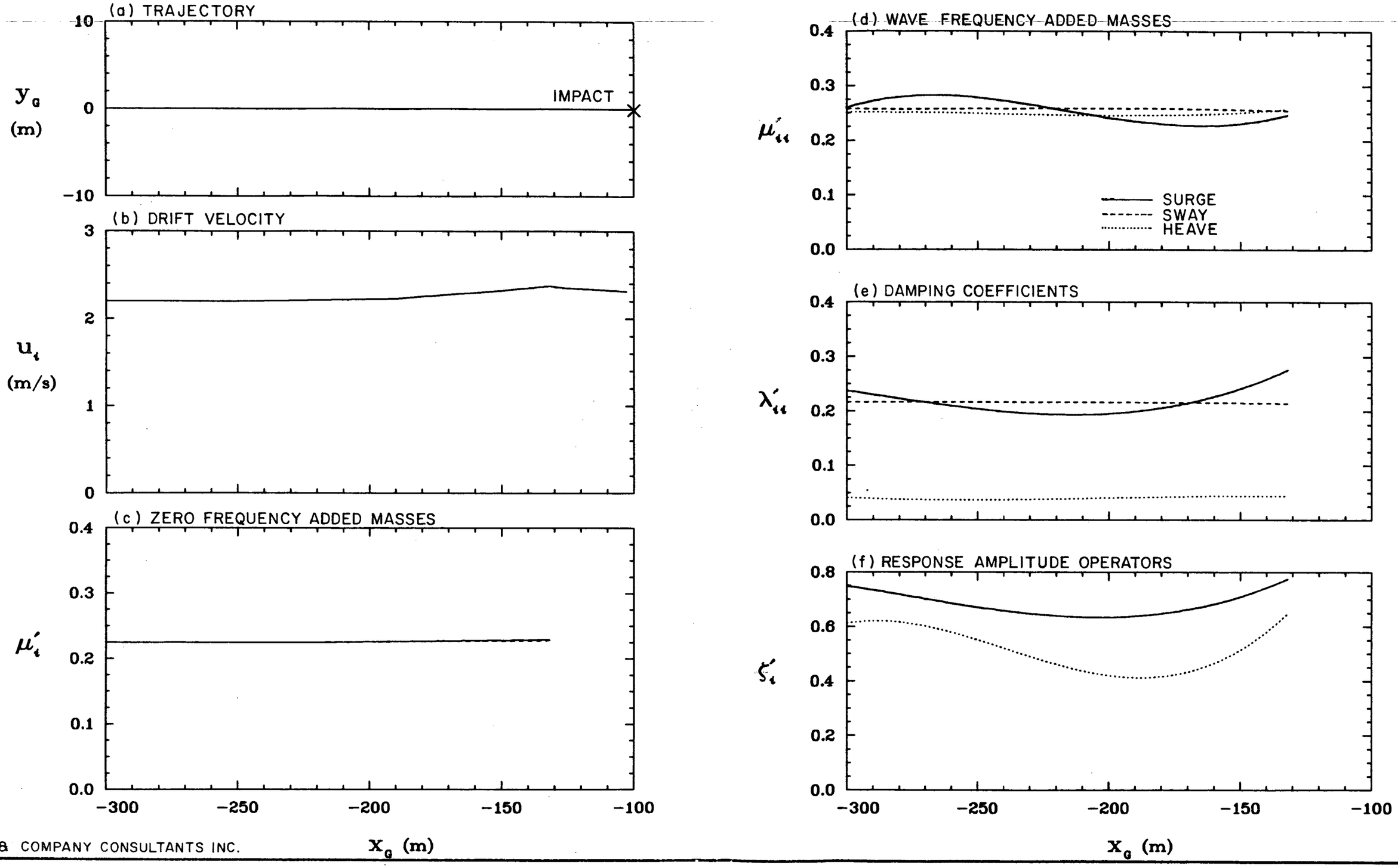

HAY & COMPANY CONSULTANTS INC.

ENVIRONMENTAL STUDIES REVOLVING FUNDS

MOTION & IMPACT OF ICEBERGS

SELECTED RESULTS OF TEST 1

FIG. 3

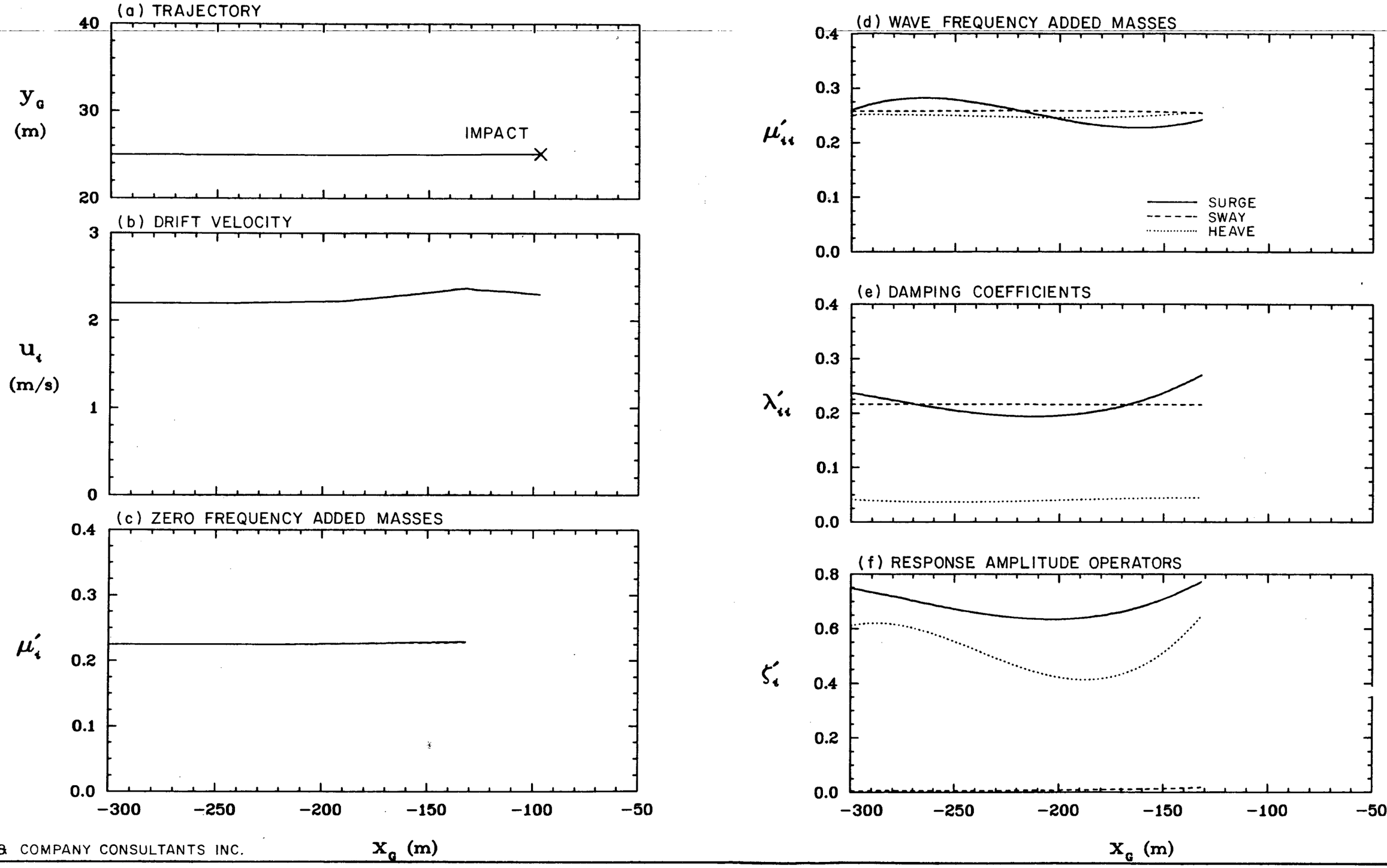

HAY & COMPANY CONSULTANTS INC.

ENVIRONMENTAL STUDIES REVOLVING FUNDS

MOTION & IMPACT OF ICEBERGS

SELECTED RESULTS OF TEST 2

FIG. 4

x_G. These all show cyclic variations with x_G, with a length scale corresponding to the incident wave length. This cyclic behaviour is associated with the interference effect of the structure on the wave field experienced by the ice mass. As with all the tests of zero initial offset and wave direction, the sway RAO is zero.

Test 2 (Figure 4) corresponds to an initial offset y_G = 25 m and a wave direction $\alpha = 0^o$. The results are very similar to those of test 1. Figure 4(a) indicates that because of the relatively large ice mass size, the ice mass continues drifting in its initial direction so that y_G remains at 25 m. The variation of hydrodynamic coefficients with x is virtually the same as in test 1, except that there is now a small sway component to the RAO caused by the asymmetrical interference effect of the structure.

Test 3 (Figure 5) corresponds to a zero initial offset and an oblique wave direction $\alpha = 5^o$. Because of the influence of wave drift forces, the trajectory is now slightly curved with a y_G value of about 2 m at impact, and a small y-ward component to the drift velocity developing. Again, results for the hydrodynamic coefficients are similar to those of test 1, but now the sway response amplitude operator (RAO) is more noticeable because of the oblique wave direction.

Test 4 (Figure 6) corresponds to an initial offset y_G = 25 m and an oblique wave direction $\alpha = 5^o$. There is a similar trend to the trajectory and drift velocity as in test 3, except that this is now with respect to the initial value of y_G. As expected, the hydrodynamic coefficients are very similar to those in the previous tests.

Test 5 (Figure 7) treats a small ice mass with symmetrical initial offset and wave conditions, y_G = 0 m and $\alpha = 0^o$. The trajectory remains along y_G = 0 m as required by symmetry.

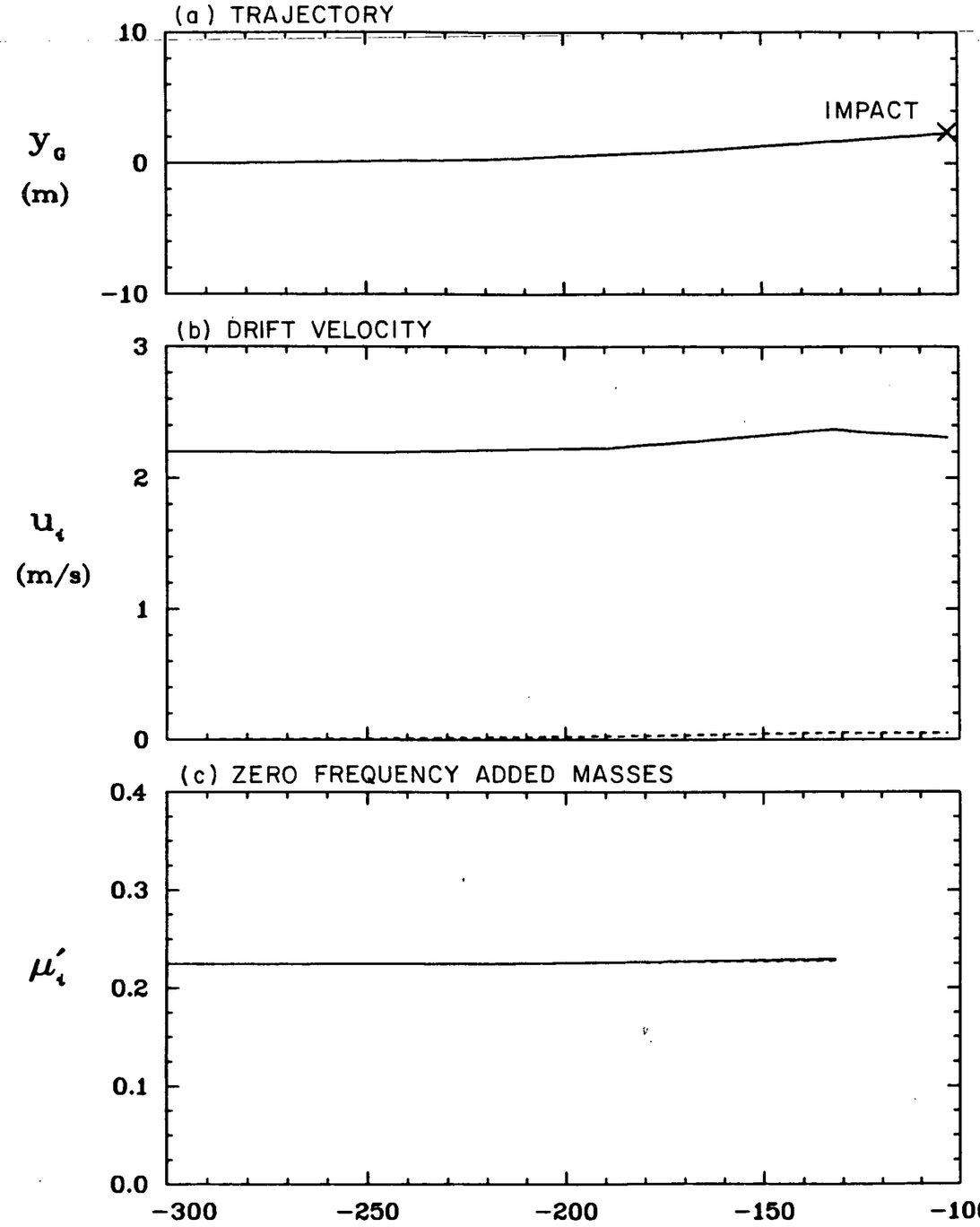

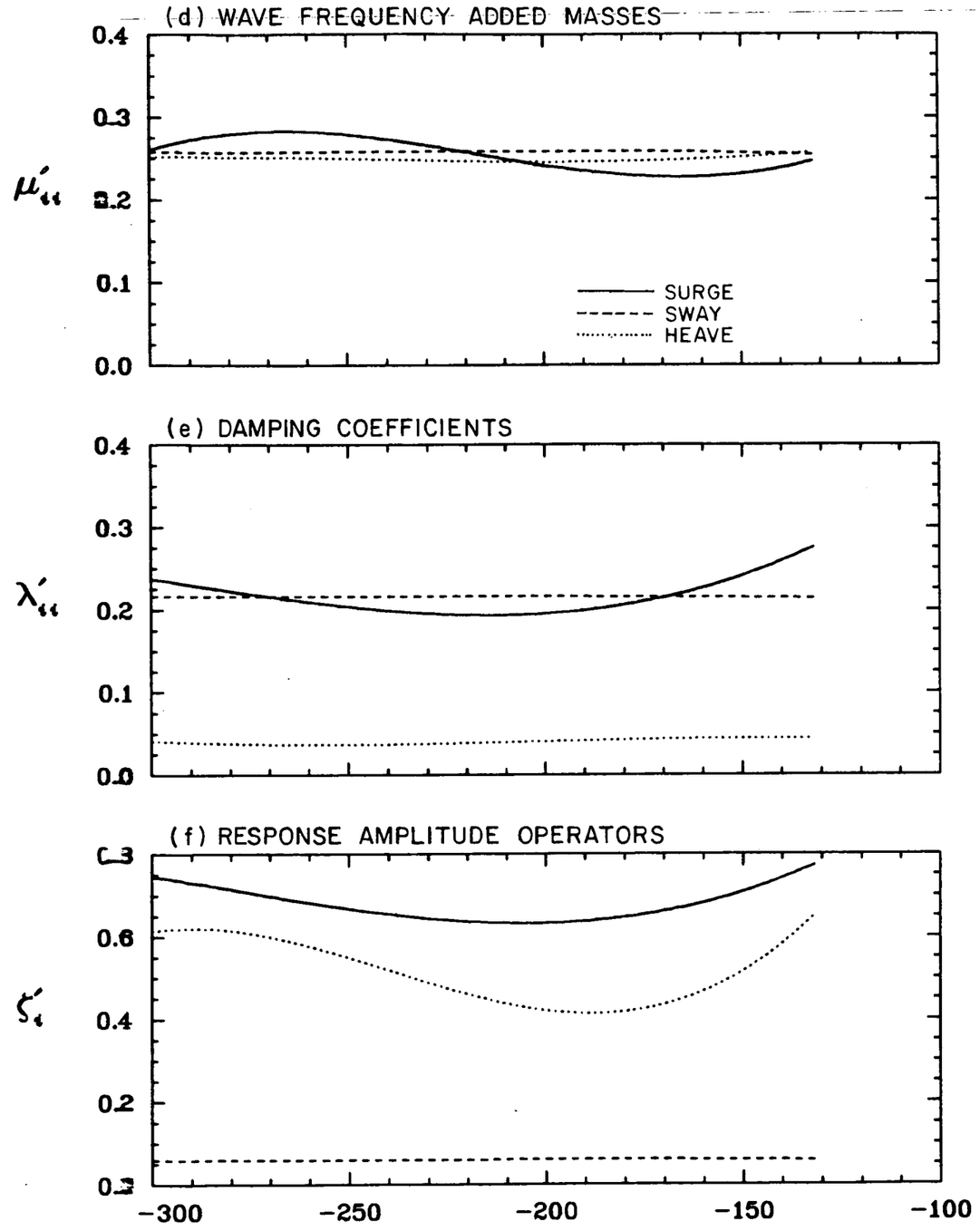

HAY & COMPANY CONSULTANTS INC.

ENVIRONMENTAL STUDIES REVOLVING FUNDS
MOTION & IMPACT OF ICEBERGS

SELECTED RESULTS
OF TEST 3

FIG. 5

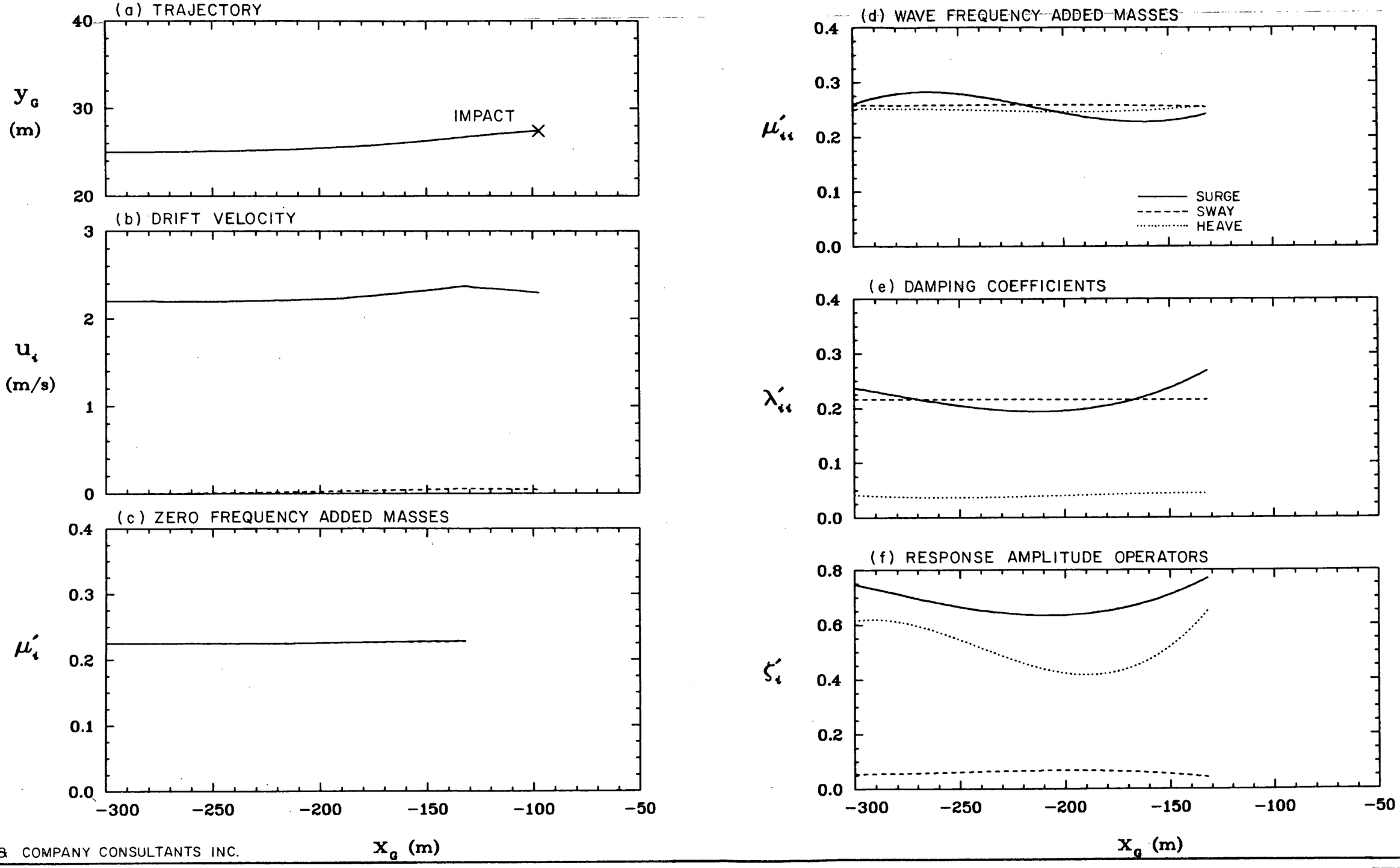

HAY & COMPANY CONSULTANTS INC.

ENVIRONMENTAL STUDIES REVOLVING FUNDS

MOTION & IMPACT OF ICEBERGS

SELECTED RESULTS OF TEST 4

FIG. 6

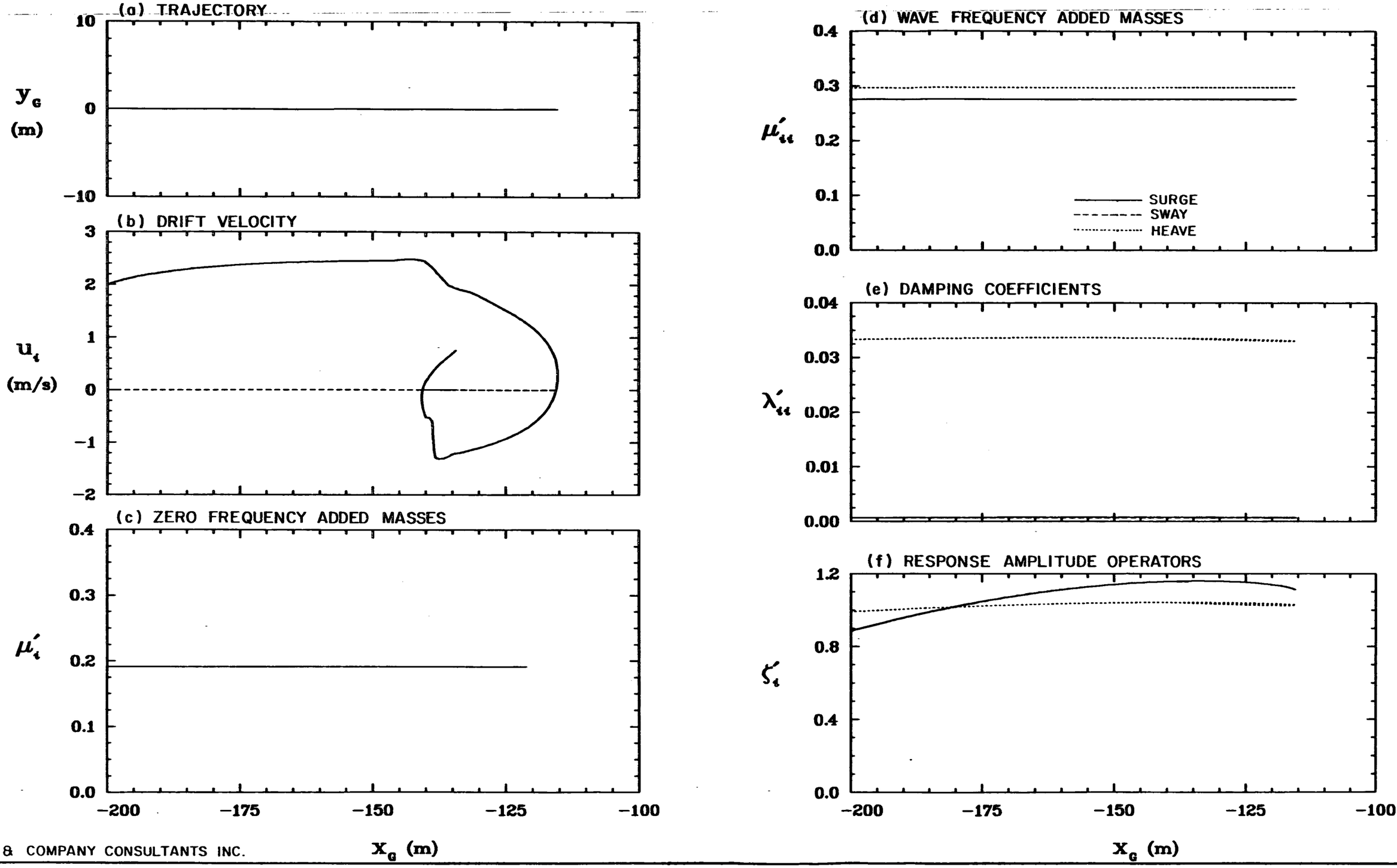

HAY & COMPANY CONSULTANTS INC.

ENVIRONMENTAL STUDIES REVOLVING FUNDS

MOTION & IMPACT OF ICEBERGS

SELECTED RESULTS OF TEST 5

FIG. 7

Figure 7(b) shows that the drift velocity first increases, then decreases and then increases again, such that ice mass reaches a maximum value of x_G, then reverses direction travelling away from the structure, and eventually undergoes decaying oscillations in its x-ward location.

This somewhat surprising result may be explained by examining the current drag and the wave drift force. The current drag opposes the relative motion between the ice mass and the current. For this ice mass the wave drift force varies cyclically with distance from the structure, such that it is negative over certain ranges of x and positive otherwise. The negative drift force (i.e. acting in an opposite direction to that of the wave propagation) is associated with the interference effect from the structure. Previous studies (e.g. Loken, 1981, van Oortmerssen, 1981) have indicated that cyclic variations in wave drift force with distance from a body (or with wave frequency) do occur and negative wave drift forces have been encountered. The effect is more pronounced here because of the relatively small ice mass.

The effect of this kind of drift force behaviour on the drift motion may be examined through a simple drift model in which the wave drift force varies cyclically with distance from the structure. The drift equation of motion may be simplified to the form:

$$\dot{u}_1 = A \cos(kx) + B (u_1 - U) |u_1 - U|$$

where A and B are parameters describing the relative magnitude of the wave drift and drag forces, k is a wave number and U is the (uniform) current velocity. The solution to this equation exhibits cyclic variations in u_1 and gives rise to negative values of u provided that the ratio A/B is sufficiently large. A sketch of a typical solution is shown in Figure 8. Figure 8(a) shows u and x as functions of time, and Figure 8(b) shows u_1 as a function of x. These results are of the same general form to

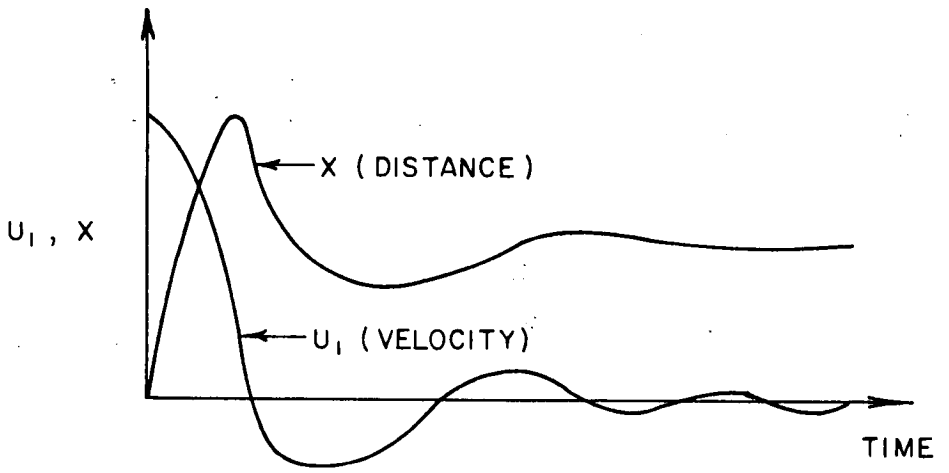

(a) DRIFT VELOCITY AND LOCATION VARIATION WITH TIME.

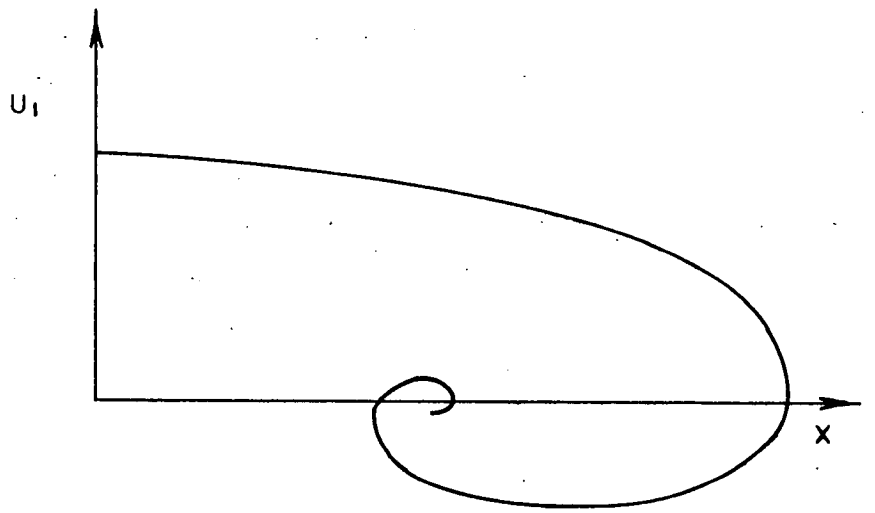

(b) DRIFT VELOCITY VARIATION WITH LOCATION.

HAY & COMPANY CONSULTANTS INC.

ENVIRONMENTAL STUDIES
REVOLVING FUNDS

MOTION & IMPACT OF ICEBERGS

RESULTS OF
DRIFT MODEL

FIG. 8

those in Figure 7b.

The hydrodynamic coefficients, Figures 7(c)-(e) do not show a noticeable variation with distance from the structure. The range of x_G shown is restricted because of the drift reversal. The surge exciting force, which is not shown, varies more strongly with x_G and thus the surge RAO shows a more noticeable variation with x_G. The sway RAO is zero because of symmetry.

To investigate further the influence of the wave drift force, test 5A (Figure 9) corresponds to the same conditions as test 5, except that the wave drift force is now excluded from the drift equations of motion and the initial drift velocity is modified to provide for no initial x-ward acceleration. In this case the reversal of the drift motion is no longer present and the ice mass continues along $y_G = 0$ with a slightly decreased drift velocity until impact occurs. The hydrodynamic coefficients do not change strongly with x_G, but as the ice mass approaches the structure more closely than in test 5, the cyclic variation in the surge RAO is now apparent.

Test 6 (Figure 10) corresponds to an initial offset $y_G = 25$ m, and shows the same behaviour in the x-ward component of drift velocity as in test 5. The continuous increase in y_G is due to the non-uniform current flow around the structure. This combines with the reversing x-ward drift to produce the trajectory shown in Figure 9(a). As in test 5, the hydrodynamic coefficients do not change strongly with location, except that the surge RAO does increase as the ice mass approaches the structure. A small sway RAO muses from the sway exciting force associated with the asymmetric interference effect of the structure.

Test 6A (Figure 11) shows the results for the same conditions as test 6, except that the wave drift force is omitted, and the initial drift velocity is correspondingly altered. As in test 5A, the trajectory and drift velocity now indicate no motion

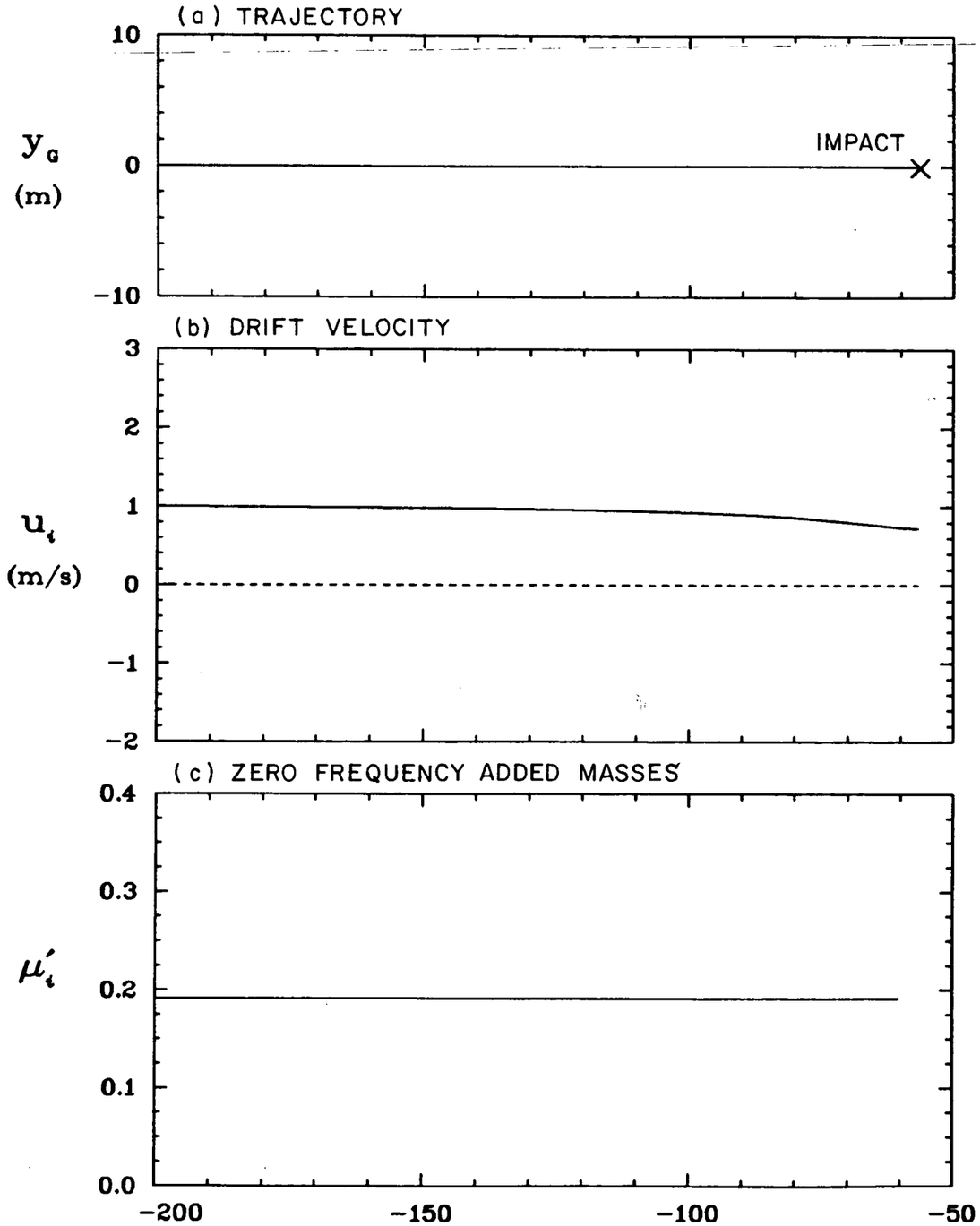

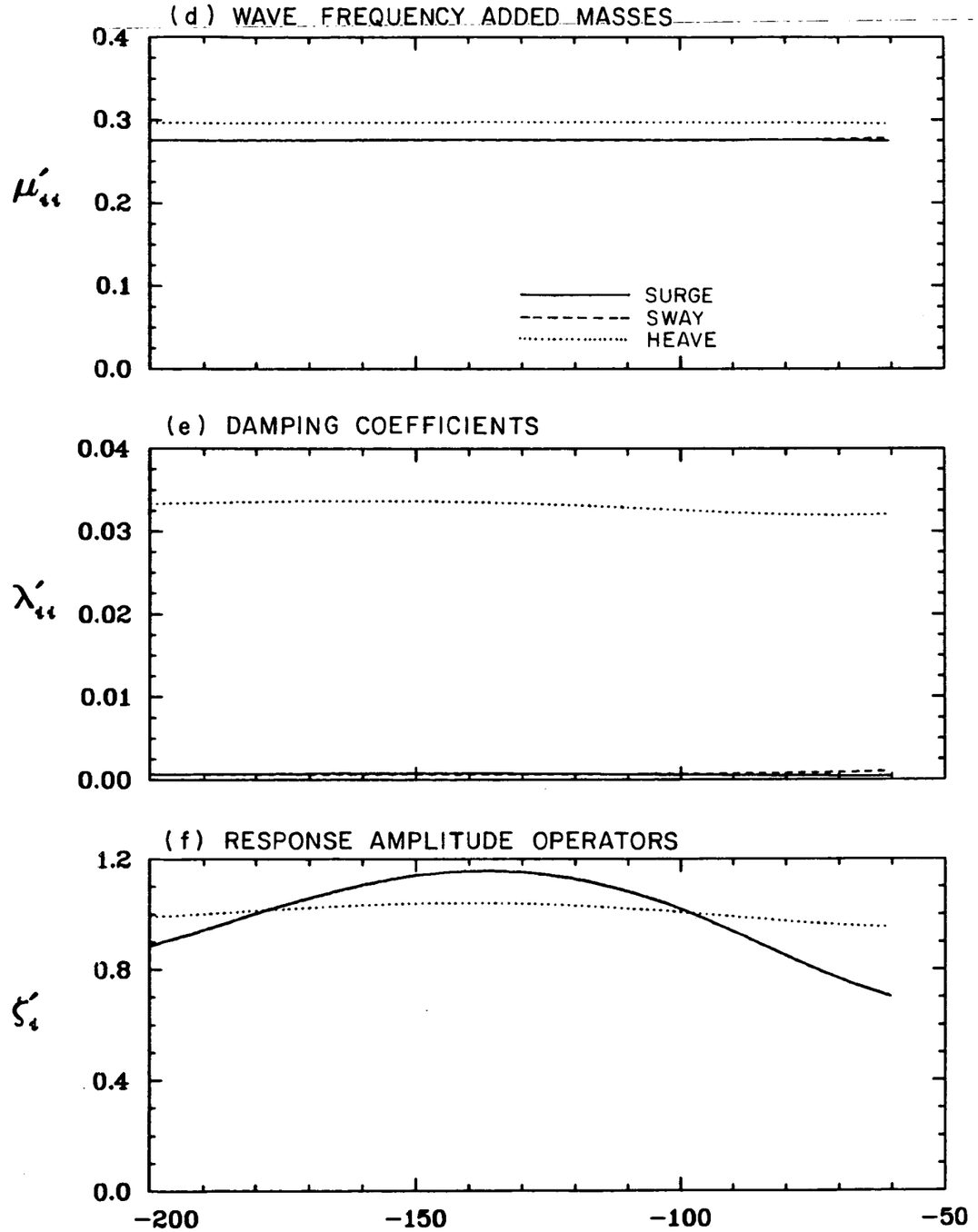

HAY & COMPANY CONSULTANTS INC.

ENVIRONMENTAL STUDIES REVOLVING FUNDS

MOTION & IMPACT OF ICEBERGS

SELECTED RESULTS OF TEST 5A

FIG. 9

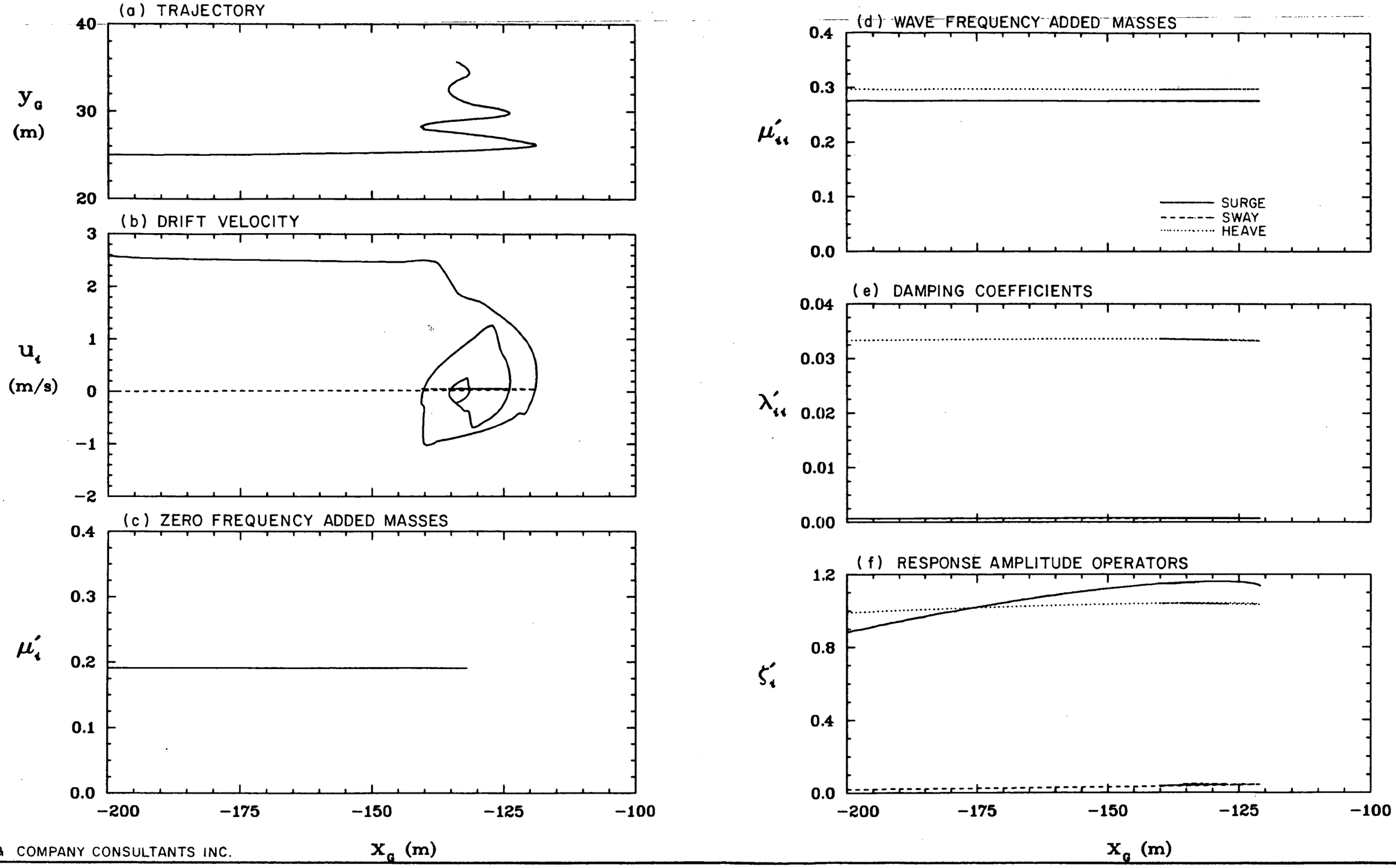

HAY & COMPANY CONSULTANTS INC.

ENVIRONMENTAL STUDIES REVOLVING FUNDS

MOTION & IMPACT OF ICEBERGS

SELECTED RESULTS
OF TEST 6

FIG. 10

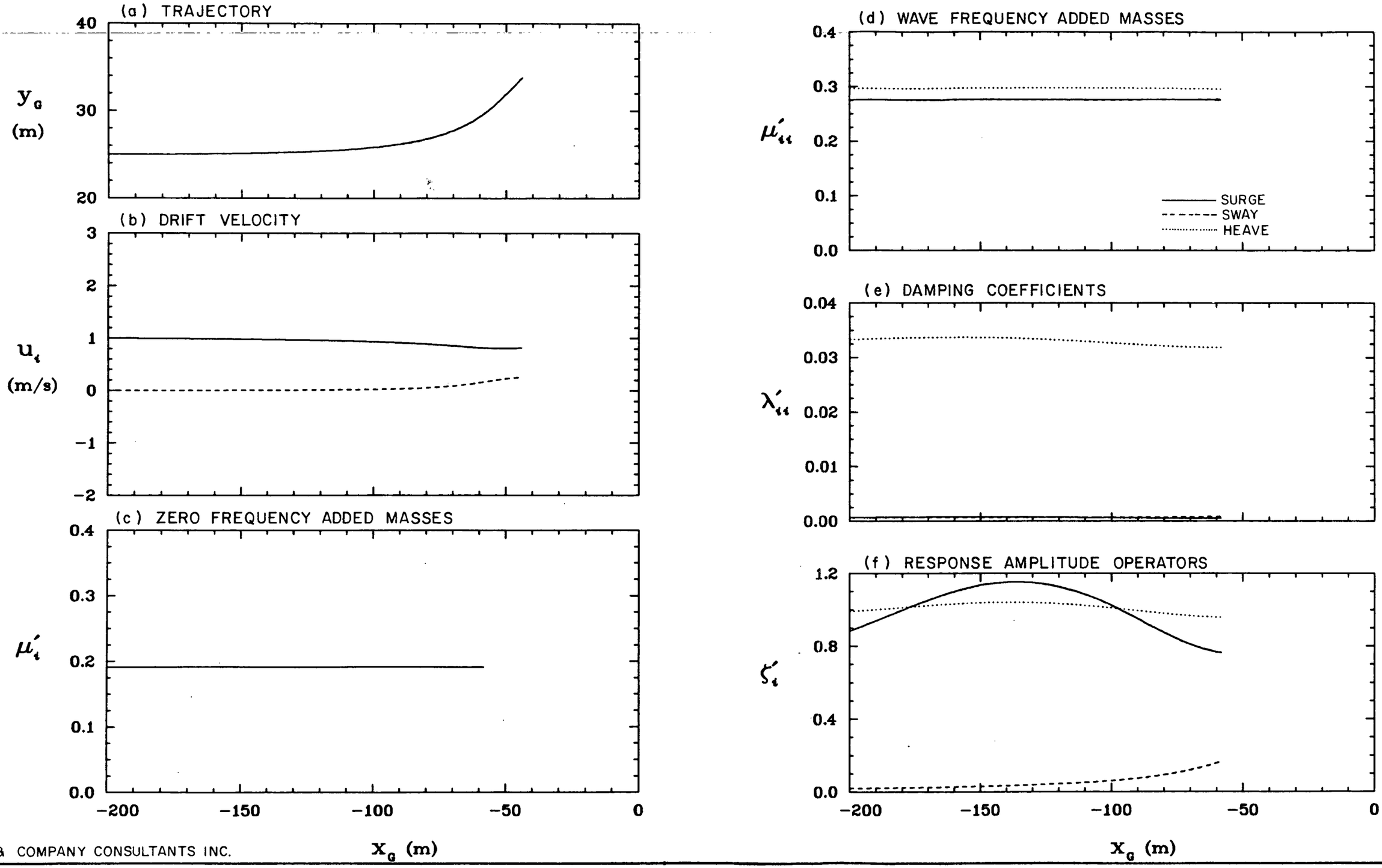

HAY & COMPANY CONSULTANTS INC.

ENVIRONMENTAL STUDIES REVOLVING FUNDS

MOTION & IMPACT OF ICEBERGS

SELECTED RESULTS
OF TEST 6A

FIG. 11

reversal. Similarly, as the ice mass approaches the structure more closely than in test 6, the variation in surge RAO with x_G is again apparent, and the sway RAO increases as the gap reduces.

Test 7 (Figure 12) corresponds to an initial offset y_G = 1 m instead of the 25 m value used in test 6. y_G does not increase significantly as the ice mass approaches the structure because the y-ward component of the current velocity is very small. Test 7A (Figure 13), with the wave drift force excluded, shows again that y_G hardly changes and that the x-ward component of drift velocity u_1 decreases slightly as the ice mass approaches the structure. The hydrodynamic coefficients behave in almost the same way as in test 6A, with a very small sway component now developing because of the slight asymmetry in the drift trajectory.

Test 8 (Figure 14) corresponds to a zero initial offset and an oblique wave direction $\alpha = 5^o$. Since the wave drift force acts primarily in the wave direction, y_G starts to increase from its initial zero value; when the wave drift force later becomes negative for certain ranges in x_G, y_G then decreases and hence the trajectory develops as shown in Figure 14(a). With the wave drift forces excluded from the drift equations of motion (test 8A, Figure 15), no y-ward excitation to the drift motion arises and hence y_G remains at zero. The x-ward drift velocity increases as in test 6. The surge RAO shows some cyclic variation with x_G as before, and there is a small sway RAO due to the wave direction.

Tests 5-8 described above all refer to the small ice mass B. Tests 9 and 10 refer to the large ice mass A again. Test 9 (Figure 16) corresponds to the same conditions as test 4, with initial offset y_G = 25 m and wave direction $\alpha = 5^o$, but now the current velocity is set at 0.4 m/s. In addition, the diffraction and zero frequency added mass calculations are carried out at more frequent intervals, and are performed for the ice mass

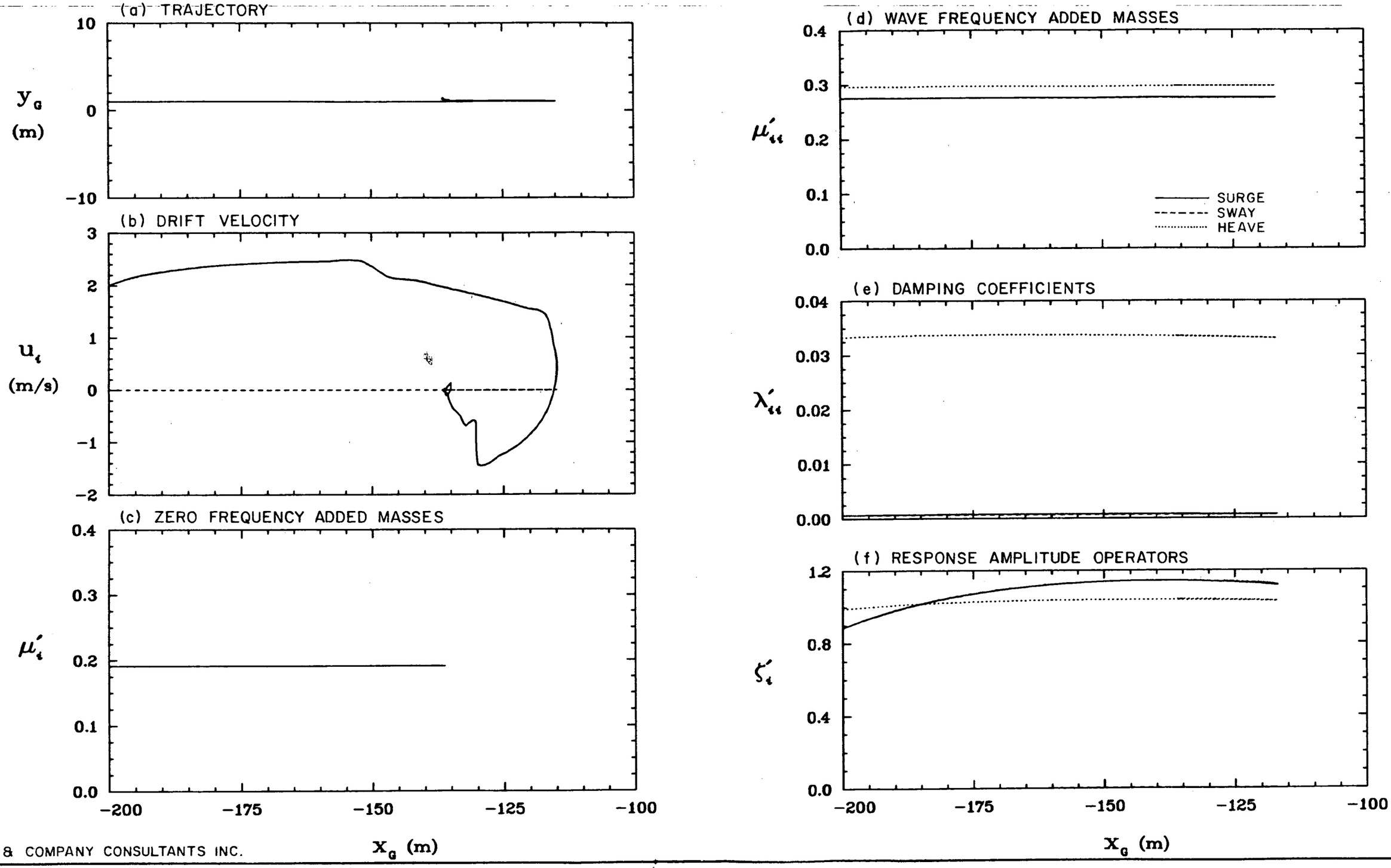

HAY & COMPANY CONSULTANTS INC.

ENVIRONMENTAL STUDIES REVOLVING FUNDS

MOTION & IMPACT OF ICEBERGS

SELECTED RESULTS
OF TEST 7

FIG. 12

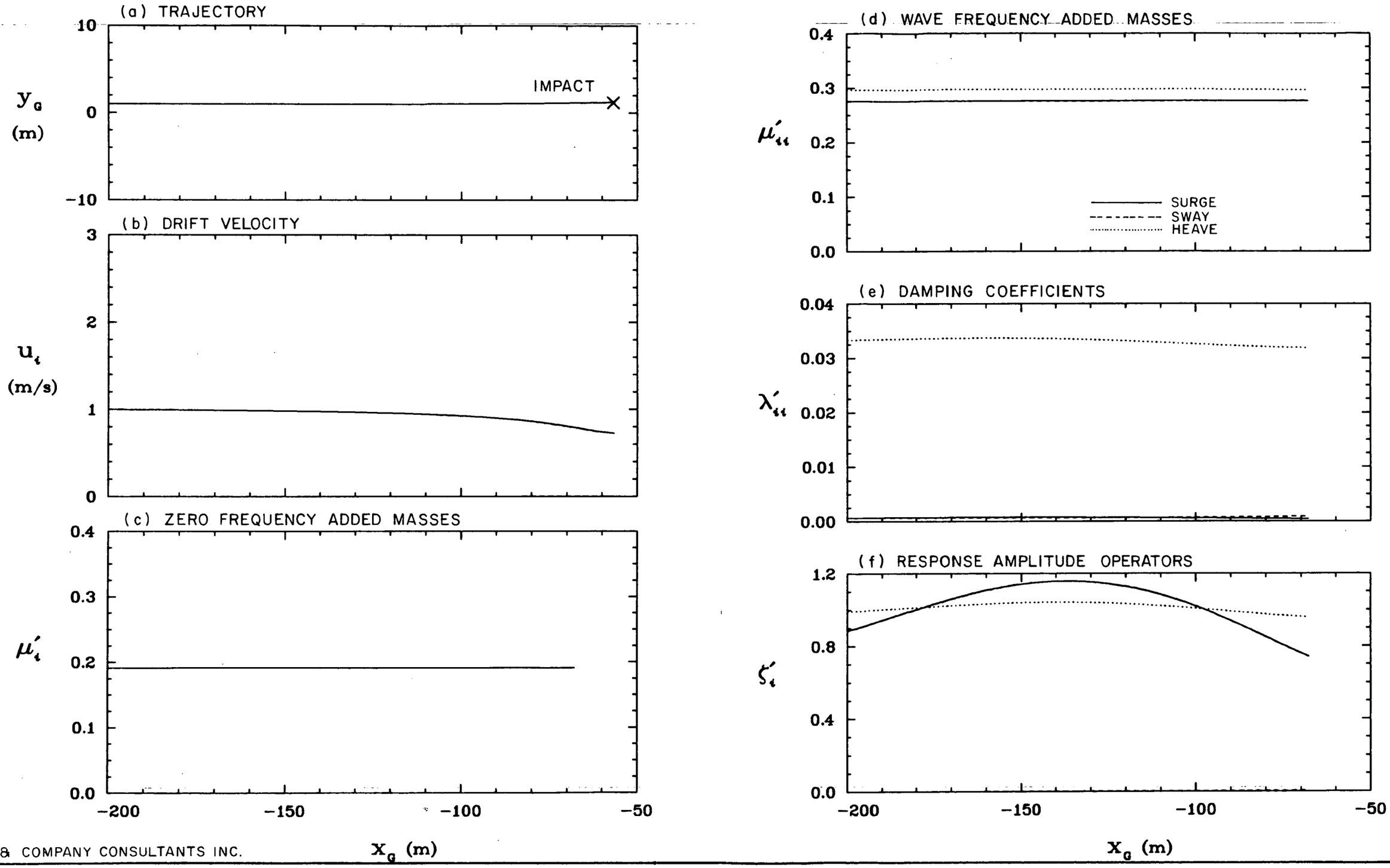

HAY & COMPANY CONSULTANTS INC.

ENVIRONMENTAL STUDIES REVOLVING FUNDS

MOTION & IMPACT OF ICEBERGS

SELECTED RESULTS
OF TEST 7A

FIG. 13

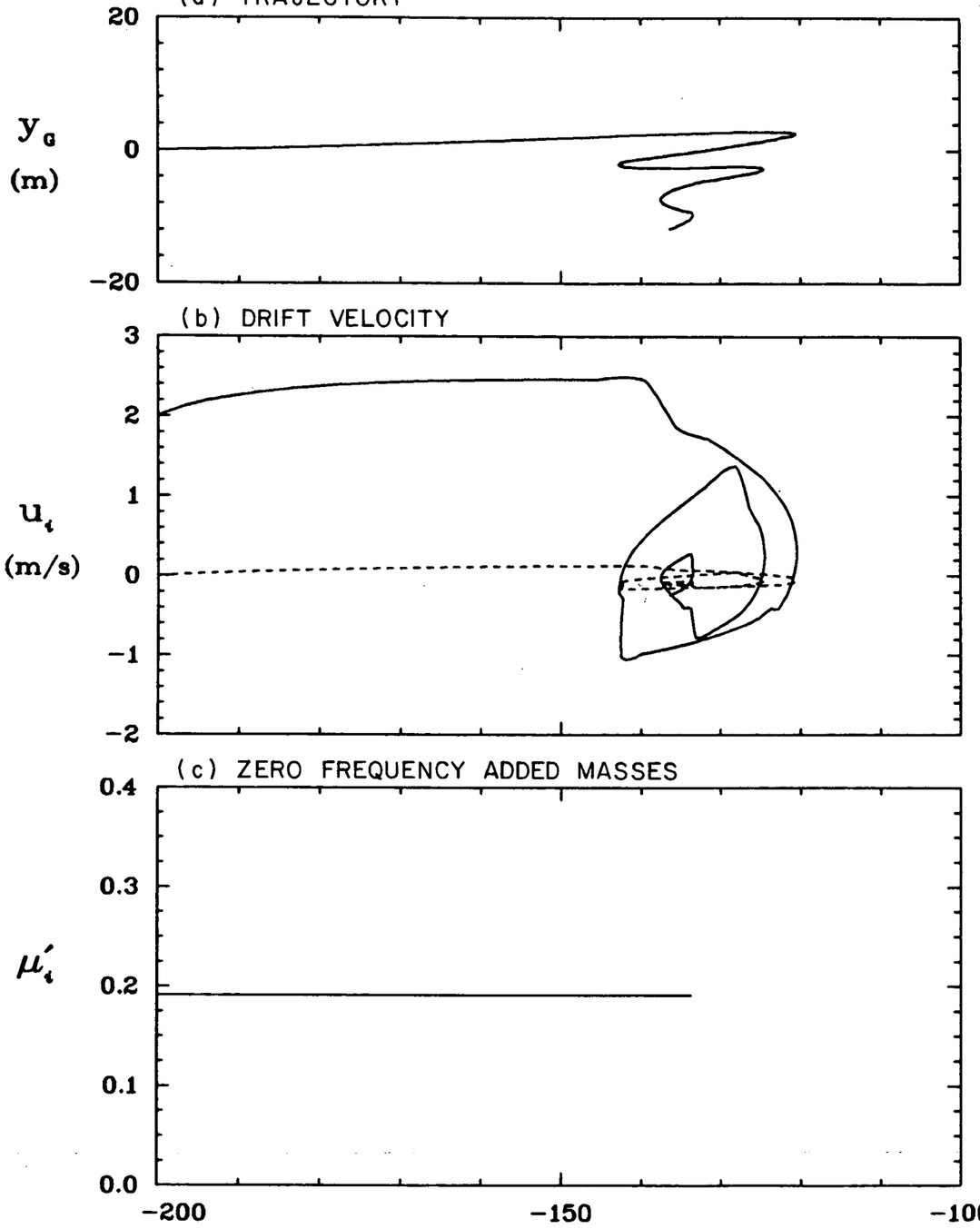

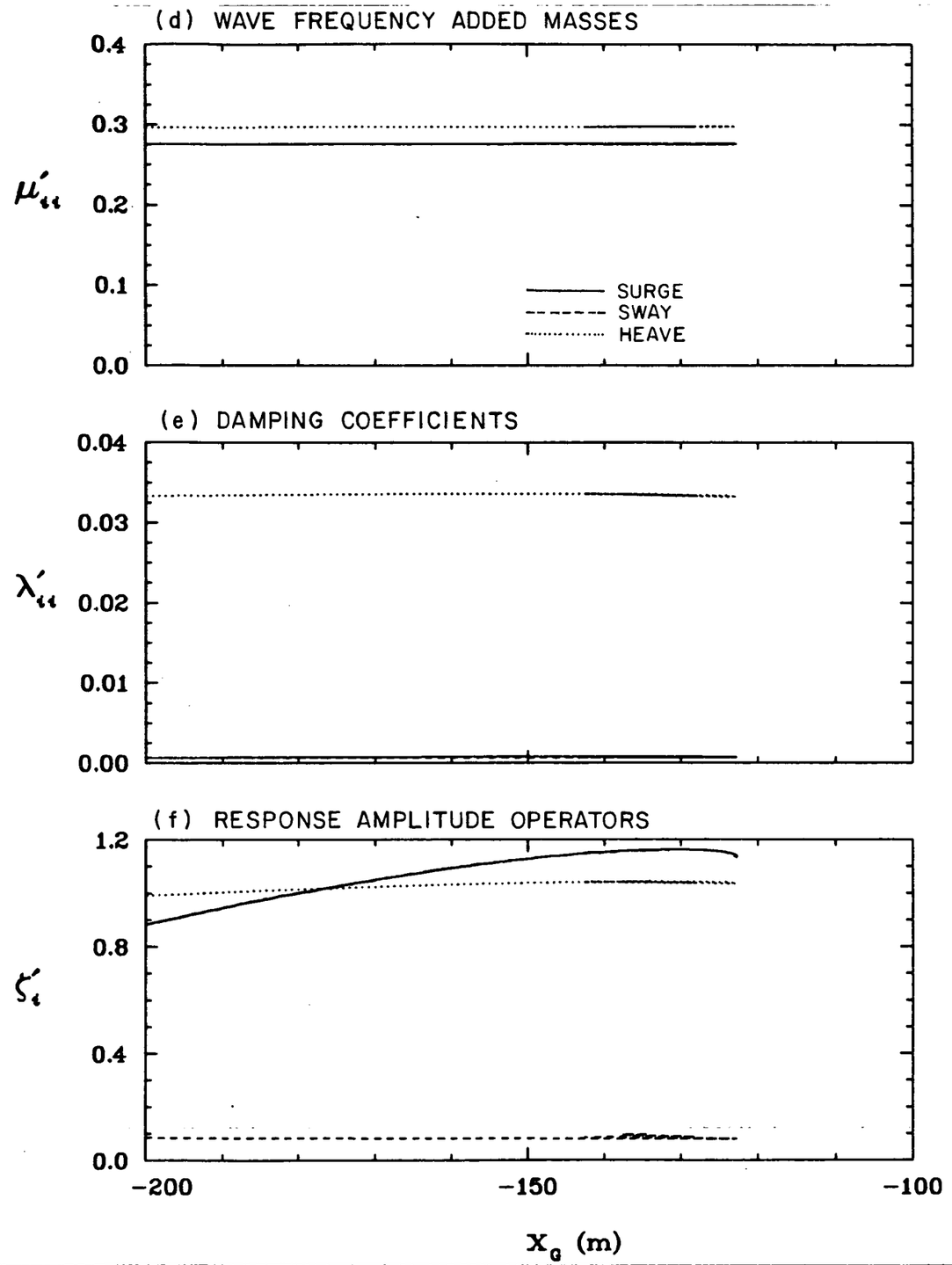

HAY & COMPANY CONSULTANTS INC.

ENVIRONMENTAL STUDIES REVOLVING FUNDS

MOTION & IMPACT OF ICEBERGS

SELECTED RESULTS
OF TEST 8

FIG. 14

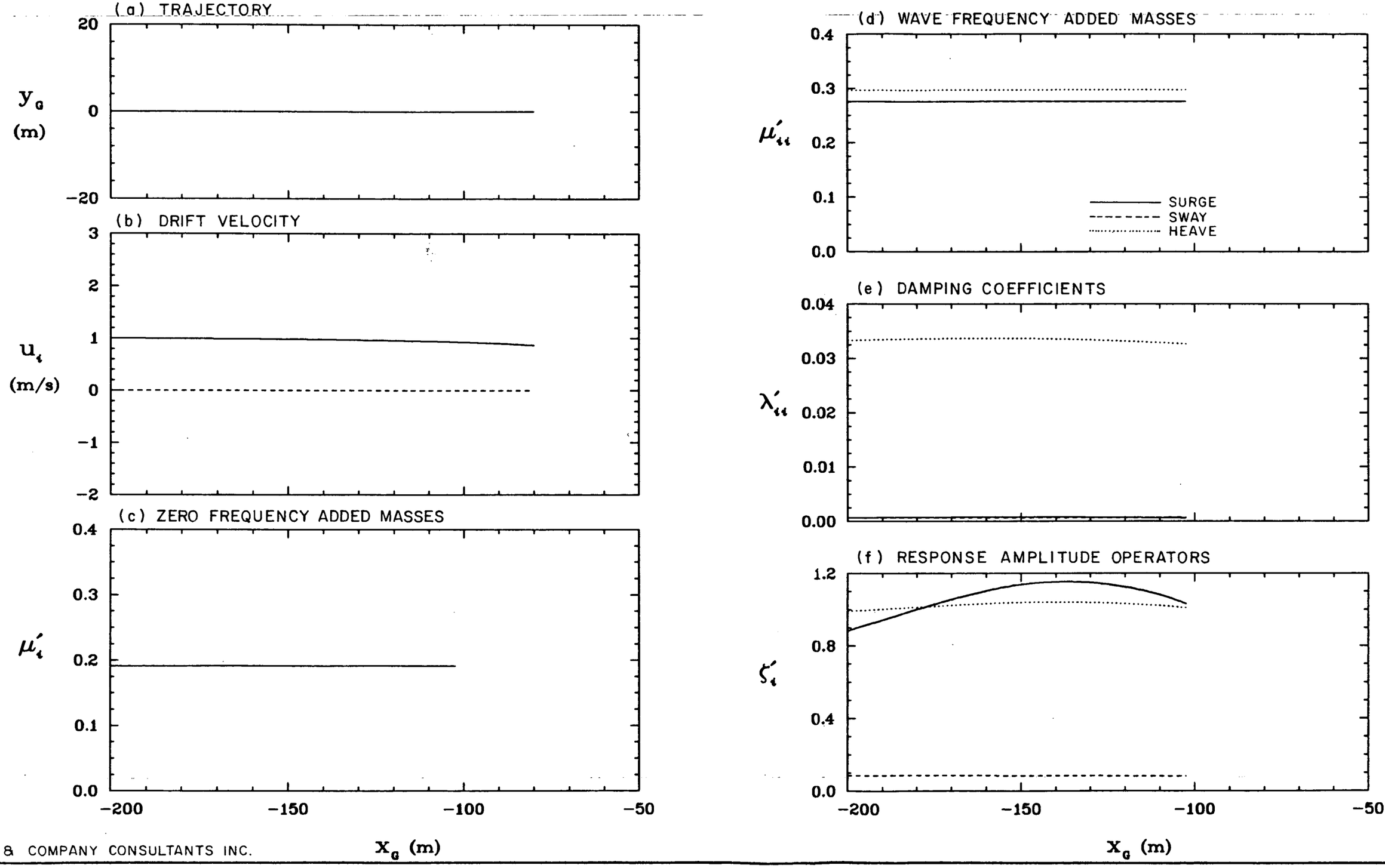

HAY & COMPANY CONSULTANTS INC.

ENVIRONMENTAL STUDIES REVOLVING FUNDS

MOTION & IMPACT OF ICEBERGS

SELECTED RESULTS OF TEST 8A

FIG. 15

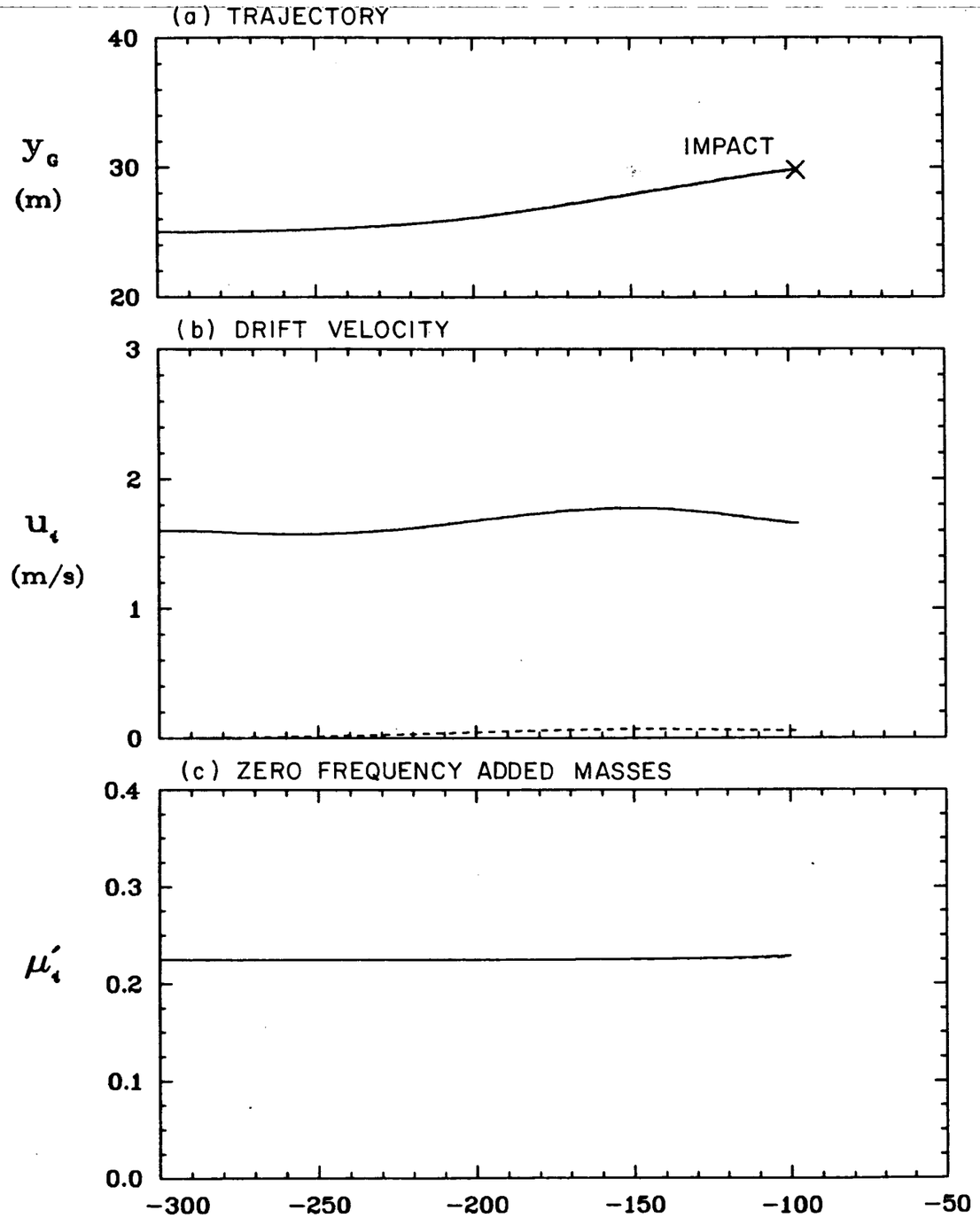

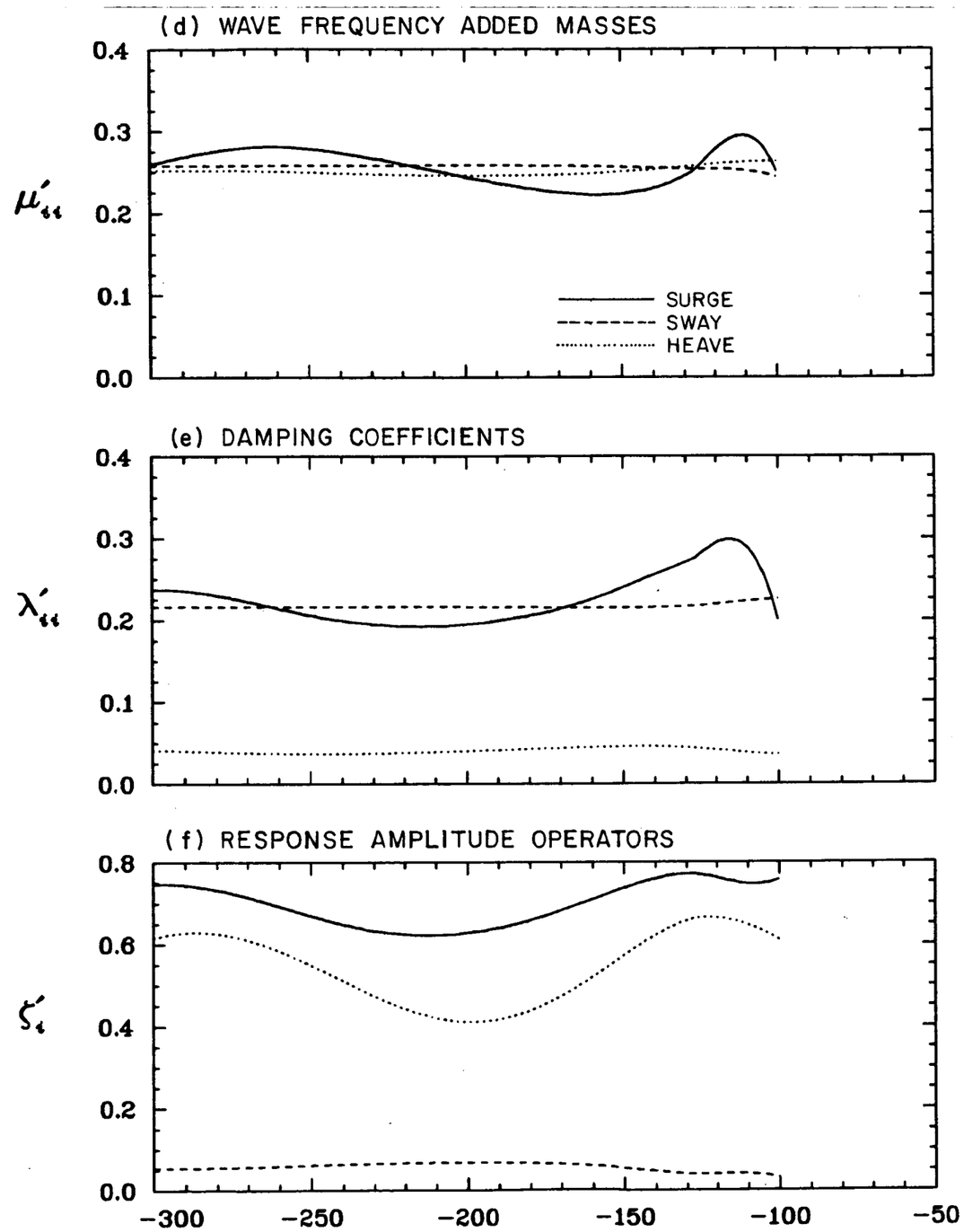

HAY & COMPANY CONSULTANTS INC.

ENVIRONMENTAL STUDIES REVOLVING FUNDS

MOTION & IMPACT OF ICEBERGS

SELECTED RESULTS
OF TEST 9

FIG. 16

closer to impact than in test 4. Consequently, the predicted drift velocity shows a much smoother variation than previously. Furthermore, the hydrodynamic coefficients now show relatively more change just before impact occurs. However, since the facet size is about 25 m, the numerical results obtained immediately prior to impact are unreliable.

Test 10 (Figure 17) corresponds to the same conditions as test 2, with initial offset y_G = 25 m and wave direction $\alpha = 0^o$, except that the water depth is now 60 m, corresponding to a 10 m gap between the bottom of the ice mass and the seabed. One consequence of this change in water depth is that the same wave period gives rise to a shorter wave length (300 m as opposed to 355 m for test 2). Overall, the results of test 10 are not significantly different to those of test 2.

Test 11 (Figure 18) corresponds to the third ice mass considered, ice mass C with a diameter of 50 m, and to an initial offset y_G = 25 m and wave direction $\alpha = 0^o$ as in test 2 with ice mass A and test 6 with ice mass B. In this case, the increase in zero frequency added mass prior to impact is quite noticeable. The wave frequency added mass in surge also shows such an increase. The wave drift force remains positive and no drift reversal occurs as in test 6 because ice mass C is significantly larger than ice mass B.

Finally, tests 12 and 13 were carried out with the ice masses A (large) and B (small) respectively, located at specified points far upstream of the structure and with gaps of 5, 10 and 15 m from the structure. The intention here is to use a finer discretization of the ice masses, as indicated in table 3, to investigate the effect of gap width on the zero frequency added masses. Since the degree of discretization alters slightly the numerical values of zero frequency added mass obtained, the results are presented in terms of percentage variations and are given in Table 4 for the large ice mass. The table shows some

increase as the gap is reduced and this eventually falls off for a gap of 5 m as the discretization becomes too coarse for a reliable result. For the small ice mass, the results are not shown since they remain virtually unchanged except that the added mass in sway increases by 1.5% for the 5 m gap. For this case, a relatively small gap is needed to detect an appreciable increase in added mass.

The calculation of the zero frequency added masses involves a Green's function which is calculated by a summation of terms corresponding to multiple reflections of a point source. In order to examine the effect of a small gap more efficiently, a more efficient routine should be developed for the Green's function. This is possible by applying algebraic manipulation to the infinite series expression for this function. A theoretical study of the zero frequency added mass immediately prior to and after impact would be appropriate in this context.

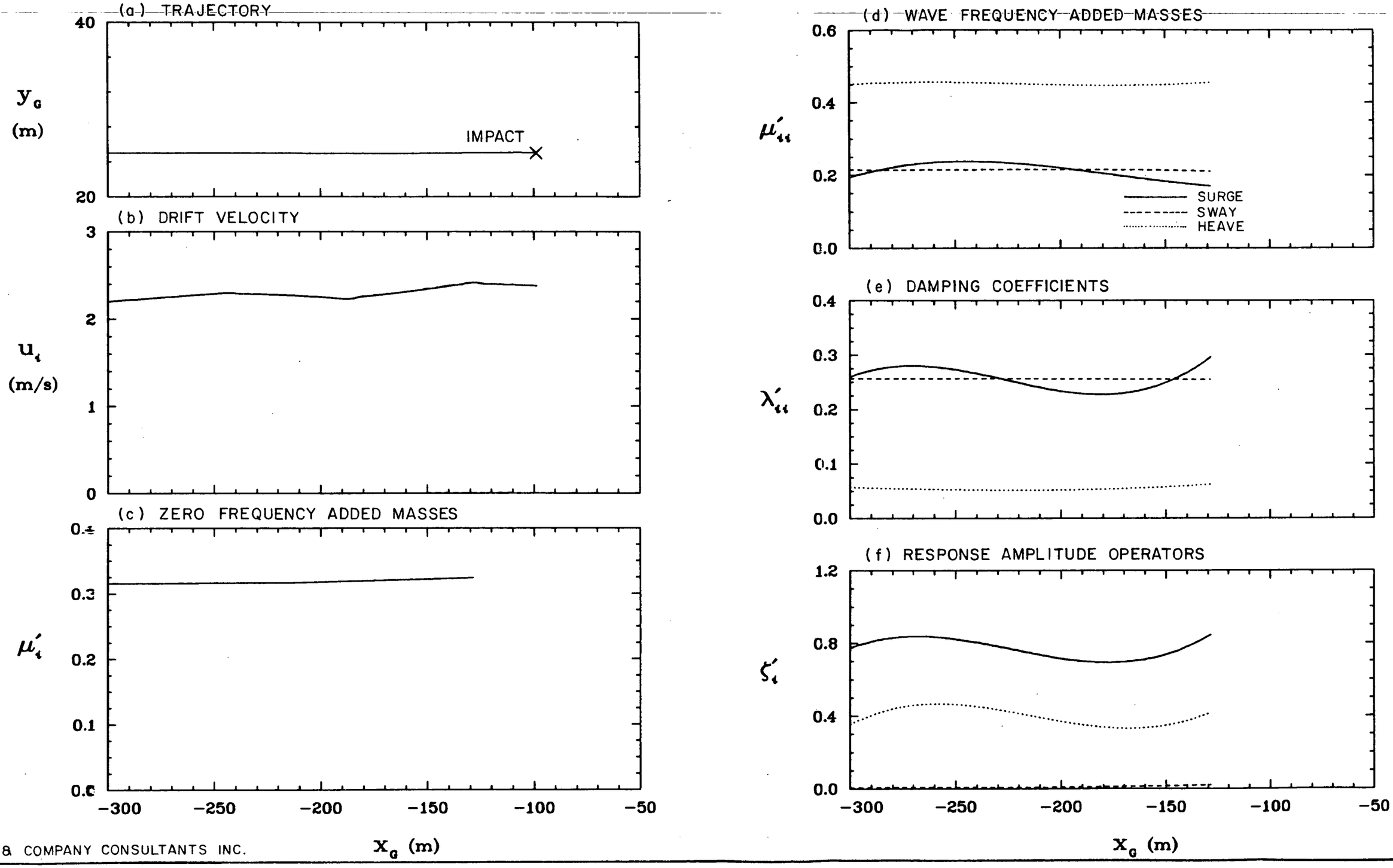

HAY & COMPANY CONSULTANTS INC.

ENVIRONMENTAL STUDIES REVOLVING FUNDS

MOTION & IMPACT OF ICEBERGS

SELECTED RESULTS
OF TEST 10

FIG. 17

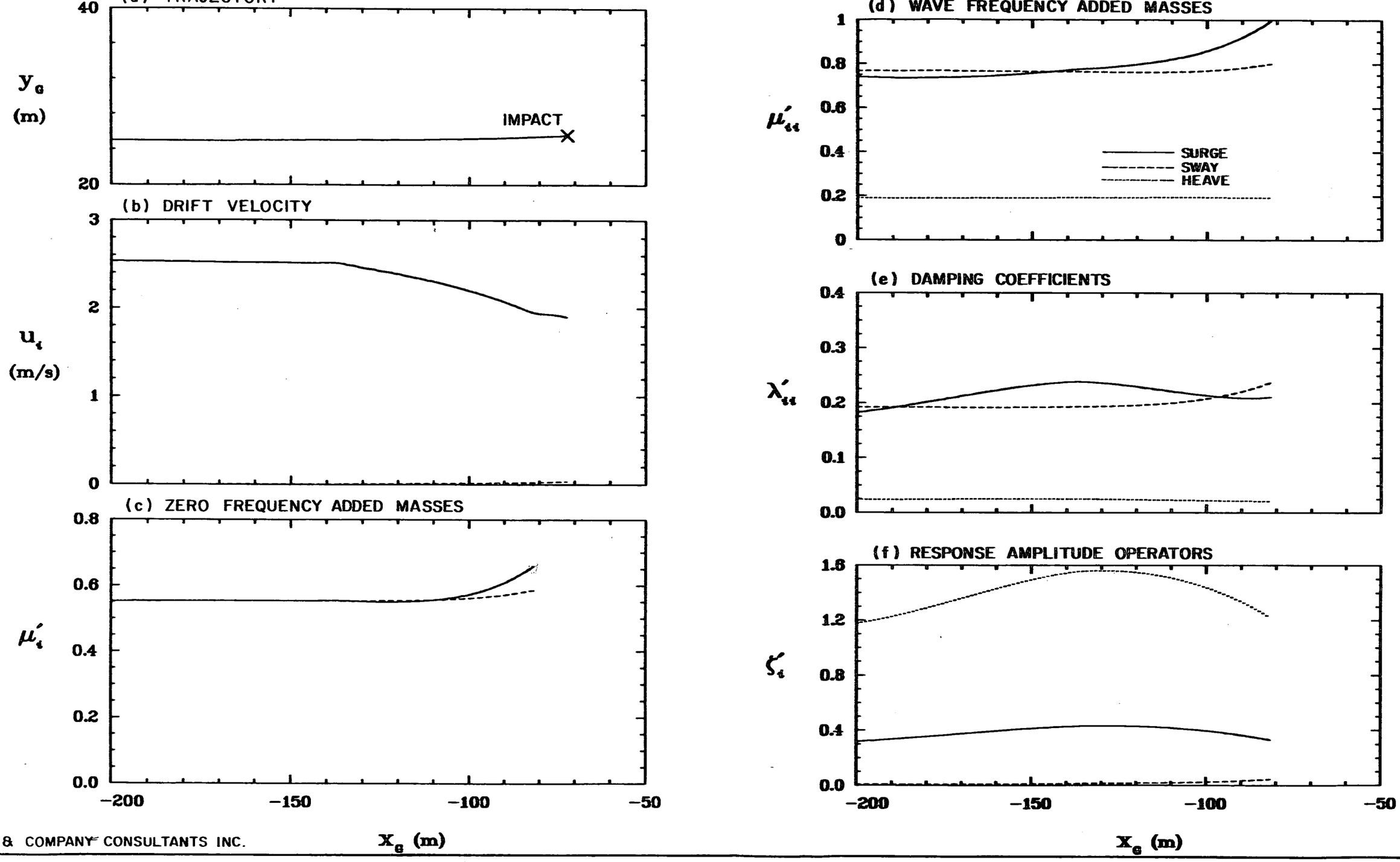

HAY & COMPANY CONSULTANTS INC.

ENVIRONMENTAL STUDIES REVOLVING FUNDS

MOTION & IMPACT OF ICEBERGS

SELECTED RESULTS OF TEST 11

FIG. 18

8.0 SURVEY OF MODEL TANK FACILITIES

Part of the terms of reference for this study is a survey of laboratory facilities capable of undertaking a model study of iceberg drift in the vicinity of an offshore structure. The survey was undertaken in two parts:

1. Identify facilities capable of undertaking studies and obtain data on those facilities

2. Evaluate the facilities and make recommendations as to a suitable test program.

While there are innumerable hydraulic laboratories in North America and Europe, the study of iceberg drift in the vicinity of an offshore structure under realistic sea conditions requires specialized facilities. The need for these specialized facilities narrows the number of potential candidate laboratories considerably. Queries were made to universities, government laboratories, and other institutes to identify candidate facilities. Questionnaires were then addressed to each of the laboratories identified while independent research in the open literature was also carried out.

This section of the report describes the results of the survey.

8.1 Description of Required Facilities

Ultimately, the purpose in laboratory testing iceberg drift in the vicinity of an offshore structure is to aid in determining the forces imparted by an iceberg during a collision with a structure. The magnitude of these forces depends on iceberg dimensions; current speed and direction; wave height, period and direction; and initial iceberg offset from the stagnation streamline of the structure. Simulating and controlling all

these variables in a manner which reflects actual open sea conditions requires very special facilities. In choosing the appropriate facilities, the following features should be considered.

A. Facility Size

Model scale effects can be minimized in a facility with large enough dimensions. Basically, there are two types of facilities which may be considered, wave flumes and wave tanks.

Wave flumes are long and narrow and are designed to represent a two dimensional slice of the ocean. Wave capabilities are generally uni-spectral and uni-directional owing to the flume geometry. Most flumes do not create currents by recirculating water but rather tow the model by means of a towing carriage (captive model). The advantages of wave flumes are that a large number of facilities are available and the tests tend to be simpler owing to the limited geometry. The disadvantages are that tests are limited to fit the two dimensional geometry (waves and currents in the same direction, etc.) and the size of the structures is limited if blockage effects are to be avoided.

Wave tanks vary in size but differ from flumes in that their horizontal dimensions are comparable. They are designed to test with the full three-dimensional aspects of the open sea. This includes multi-directional and multi-spectral wave capabilities plus currents created by recirculation or by towing. The advantage of wave tanks is the full range of testing possible under simulated ocean conditions while the disadvantage is the complexity of controlling all the test variables.

B. Wave Generating Capabilities

A single location in the open sea can receive waves generated from storm activity located thousands of kilometres away and from several different directions simultaneously. In addition, wave spectra from each direction can be different. To truly simulate open sea conditions, therefore, the facility must be capable of generating multi-directional, multi-spectral waves.

C. Current Generation

There are two possible ways to simulate currents, one is to recirculate the water in the tank and the other is to tow the model with a towing carriage. A uniform current is difficult to achieve by recirculating owing to the small distance available for flow development at the upstream end of the tank and the effect on the velocity profile of the tank boundaries. Towing a model creates a uniform velocity profile as seen by an observer moving with the speed of the carriage. The effect of currents on waves (wave steepening, etc.) is not simulated when towing is used, however, this effect is small for long period waves.

D. Special Considerations

Two other special considerations are wave reflections from tank or flume boundaries and wave induced currents which lead to non-uniform velocity profiles. In very large facilities, testing can be carried out for a considerable length of time before these effects become important. Irrespective of size, virtually all facilities utilize beaches to dissipate incident wave energy and these are very effective except for long wave lengths for which the beaches are too small. In addition, some wave generating systems correct for reflections so that the desired outgoing

spectrum is maintained. Wave induced currents are more of a problem in small facilities than in large facilities. While the problem is recognized, no corrective measures are taken in the facilities queried in this study beyond an initial mapping of the current field.

Other features which are also important include instrumentation, data aquisition system and, while not a part of the physical facilities, experience in testing floating structures.

8.2 Results of the Survey

The laboratories in the following list were determined to have facilities suitable for testing iceberg drift:

(1) Maritime Research Institute
The Netherlands

(2) Marintek A/S
Trondheim, Norway

(3) Swedish Maritime Research Centre
Sweden

(4) National Maritime Institute
England

(5) David Taylor Naval Ship Research and Development Center
Bethesda, Maryland

(6) Hydraulics Laboratory
Division of Mechanical Engineering
National Research Council of Canada
Ottawa, Ontario

(7) Hydraulic Research Station
Wallingford, England

(8) Hydronautics Ship Model Basin
Tracor Hydronautics Inc.
Laurel, Maryland

(9) Offshore Technology Corporation
Escondido, California

(10) Faculty of Engineering and Applied Science
Memorial University of Newfoundland
St. John's, Newfoundland

(11) Institute for Marine Dynamics
National Research Council of Canada
St. John's, Newfoundland

(12) Versuchsanstalt Fur Wasserbav Und Schiffbau
Berlin, West Germany

(13) Danish Ship Research Laboratory
Lyngby, Denmark

(14) British Hovercroft Corp. Ltd.
Experimental and Electronics Labs
England

(15) Department of Shipbuilding and Naval Architecture
University of Strathclyde
Glasgow, Scotland

(16) Ocean Engineering Center
B.C. Research
Vancouver, B.C.

The laboratories and the particulars regarding their facilities are listed in Table 5. Also included is a rating relative to basin size, wave generating capabilities, current generating capabilities, and experience.

The basis for the rating is:

A. Basin Size

The rating is based on a 40 m x 40 m x 5 m tank being a good size for full testing of three-dimensional aspects of iceberg drift. Facilities significantly larger than these were considered excellent and those smaller were given lesser ratings. Flumes were rated no better than poor owing to the limited testing possible. Where laboratories possess both flumes and tanks, the tanks were reported.

B. Wave Generation

The rating is based on multi-directional and multi-spectral wave generation as being good and the capability of compensating for reflected wave as being excellent.

C. Current Generation

The ability to create currents over the full width and depth of the facility either by towing or recirculation was considered good. The capability of both towing or recirculation was considered excellent.

D. Experience

Experience rating is somewhat more qualitative in nature. It is based on specific questions in the questionnaire.

LABORATORY	1. PRINCIPAL DIMENSIONS				2. WAVE GENERATOR								3. CURRENT CAPABILITIES						4 TOWING CARRIAGE		5. APPROXIMATE AVERAGE ANNUAL PERCENT UTILIZATION	6. LABORATORY RATING			
	LENGTH m	WIDTH m	MAXIMUM DEPTHS Shallowest Area m	MAXIMUM DEPTHS Deepest Area m	NONE	WAVEMAKER 1 Piston 2 Paddle 3 Wedge 4 Other	CONTROL 1 Mechanical 2 Electronic 3 Computer	SEA STATE 1 Monochromatic 2 UniSpectral 3 MultiSpectral a UniDirectional b MultiDirectional	APPROXIMATE MAXIMUM WAVE HEIGHT, mm AT PERIODS (SECS) of 0.5	1.0	2.0	3.0	NONE	CURRENTS MAXIMUM STRENGTH FULL BASIN DEPTH mm/s	MAXIMUM STRENGTH 1/2 BASIN mm/s	HORIZONTAL GRADIENT CONTROL Yes	HORIZONTAL GRADIENT CONTROL No	VERTICAL GRADIENT CONTROL Yes	VERTICAL GRADIENT CONTROL No	Yes	No		FACILITY SIZE	WAVE GENERATION	CURRENTS	EXPERIENCE
1. HYDRAULIC RESEARCH LTD. - WALLINGFORD	25	25	2	6		2	3	3a, 3b	40	150	500	250		200	200	X		X			X	75	3	1	2	1
	20	20	1.5	2.5		3	2	3a, 3b	40	150	350	200		200	200	X		X			X	50	3	1	2	1
2. SSPD MARITIME RESEARCH AND CONSULTING	88	39	0	3.5		2	2,3	1, 31, 3b			500	200		1000	1000		X		X	X		100	1	2	1	1
3. OFFSHORE TECHNOLOGY CORPORATION	42	32	1.5	4.0		1	3	3a, 3b			459			220			X		X		X	60	2	2	2	2
4. NATIONAL RESEARCH COUNCIL	50	30	0.5	5.7		1,2	3	3a, 3b	40	160	610	740	X								X	75	2	1	5	3
5. DANISH MARITIME INSTITUTE	240	12	5.2	5.5		2	2	2a	40	480	700	850	X							X		95	4	3	2	2
6. MEMORIAL UNIVERSITY	58	4.5	.8	2.1		2	3	3a		150	610	480	X							X		50	5	3	2	2
7. B.C. RESEARCH	30	26	2.5	2.5		2	3	1					X							X		5	2	4	5	4
8. TRACOR HYDRAULIC INC.	127	7.6	-	4		1	3	3a			610		X							X			4	3	2	2
9. VERSUCHSANSTALT FUER WASSERBAU UND SCHIFFBAU	250	8		4.8		Pneumatic		3a					X							X			4	3	2	2
10. DAVID TAYLOR NSRDC	110	73	6.1	10.7		Pneumatic	2,3	3b				610	X							X			1	2	2	1
11. MARITIME RESEARCH INSTITUTE	60	40	1.2	3.1		2	3	3b				300		600							X	85	2	2	2	1
12. MARINTEK A/S	80	50	0	10		2	2,3	3b		200	600	800		200		X		X			X		1	2	2	1
13. BRITISH MARITIME TECHNOLOGY	46	30	1.5	2.3		2	2	3a, 3b			400			YES	?	?					X		2	2	2	1
14. INSTITUTE FOR MARINE DYNAMICS	75	32	3.5	7.5		2	3	3b	35	250	1100	600	X								X		1	2	5	3
15. BRITISH HOVERCRAFT CORP.																										
16. UNIVERSITY OF STRATHCLYDE																										

RATING : 1 - EXCELLENT
2 - GOOD
3 - AVERAGE
4 - POOR
5 - NON EXISTENT OR NOT TO BE CONSIDERED

TABLE 5 - RESULTS FROM QUESTIONNAIRE

The testing envisaged involves releasing a model iceberg in a given sea state and current field and monitoring its trajectory as it approaches an offshore structure. As discussed earlier, two methods of establishing the current field are recirculating flow and towing. Uniform velocity conditions are difficult to achieve in a tank of reasonable dimensions by recirculation. Towing the structure, creates a uniform current field as viewed from the carriage, however, there is some modelling effect on the waves. For long wave lengths, this modelling effect is minimal.

Whether recirculation or towing, the difficulty is in interpreting test results relative to the very complex and perhaps non-ideal, input test conditions. Sorting the individual effects of waves, currents, added masses, and other parameters is a problem and the possibility of tank effects tainting the results is always a possibility. The best method of sorting out this maze is to utilize a computer model in conjunction with testing. Progressive laboratories have adopted this two-model (physical and computer) approach as a research tool and as a means of reducing testing costs.

The computer model developed in conjunction with this study makes available a tool for data evaluation which has been absent in previous test programs. This tool lends another dimension to testing which promises more success in the complex process of sorting out the relationship between observed model behaviour relative to measured inputs and determining any model scale effects.

The highest rated laboratory from Table 5 is SSPD Maritime Research and Consulting in Sweden. Its major advantage over other laboratories is that it can create currents by recirculation and by towing. The second highest in ranking are the David Taylor Naval Ship Research and Development Center in the USA and Marintek A/S in Norway. The major disadvantage of the second ranking is that the David Taylor Laboratory can only

tow and Marintek can only recirculate to provide currents. A third ranking group includes British Maritime Technology and Hydraulic Research Ltd. in England, and Maritime Research Institute in Holland. The third ranking of these laboratories is mainly due to the size of their facilities.

Owing to the time required in reaching steady state drift under the influence of waves and currents and the difficulty achieving a uniform current field by recirculation, the possibility of undertaking towing tests should be considered in more detail. It is believed that a smaller test tank could be utilized in a towed experiment although the desired sea state is generally only simulated in a small, central area of a small tank. The alternative of recirculation requires a flow development length of approximately ten times the water depth to achieve a uniform velocity distribution.

The choice of model scale is best left up to the discretion of the individual laboratory to optimize the results relative to their facilities. Any of the first three ranked groups possess the facilities and experience to undertake a study. A range of model scales should be suggested, though, to provide an indication of the level of effort.

REFERENCES

REFERENCES

Adee, B.H. and Martin, W. (1974), "Analysis of Floating Breakwater Performance", Proc. Floating Breakwater Conf., Univ. of Rhode Island, pp. 21-40.

Arctec Canada Ltd. and Offshore Technology Corp. (1984), "Ice Mass Velocity Study", Report No. FR-1324C.

Arctic Sciences Ltd. (1983), "Iceberg Modelling Off Canada's East Coast: A Review and Evaluation".

Bai, K.J. and Yeung, R. (1974), "Numerical Solutions of Free Surface Problems", Proc. 10th Symp. Naval Hydrodyn., Cambridge, Mass., pp. 609-647.

Ball, P., Gaskill, H.S. and Lopez, R.J. (1981), "Environmental Data Requirements For Real Time Iceberg Motion Model", Proc. of the 6th International Conference for Port and Ocean Engineering Under Arctic Conditions, pp. 1369-1379.

Black, J.L., Mei, C.C., and Bray, M.C.G. (1971), "Radiation and Scattering of Water Waves by Rigid Bodies", J. of Fluid Mechanics, Vol. 46, pp. 151-164.

Chakrabarti, S.K. (1978), "Wave Forces on Multiple Vertical Cylinders", J. Waterway Port Coastal and Ocean Div., ASCE, Vol. 104, No. WW2, pp. 147-161.

Chakrabarti, S.K. (1984), "Moored Floating Structures and Hydrodynamic Coefficients". Proc. Ocean Structural Dynamics Symposium, Corvallis, pp. 251-266.

Cheema, P.S. and Ahija, H.N. (1978), "Computer Simulation of Iceberg Drift", Proceedings of the Offshore Technology Conference, Houston. pp. 565-571.

Dempster, R.T. (1974), "The Measurement and Modelling of Iceberg Drift", Oceans '74, Halifax, pp. 125-129.

Faltinsen, O.M. (1977), "Numerical solution of transient nonlinear free surface motion outside or inside moving bodies". Proceedings of the 2nd International Conference on Numerical Ship Hydrodynamics, Berkeley, California, pp. 347-357.

Faltinsen, O.M. and Michelsen, F.C., (1974), "Motion of Large Structures in Waves at Zero Froude Number". Proc. Symposium on the Dynamics of Marine Vehicles and Structures in Waves, University College London.

Fenton, J.D. (1978), "Wave Forces on Vertical Bodies of Revolution", JFM, Vol. 85, pp. 241-255.

Garrett, C.J.R. (1971), "Wave Forces on a Circular Dock", JFM, Vol. 46, pp. 129-139.

Garrett, (1984), "Statistical Prediction of Iceberg Drift", Iceberg Research, No. 7, March.

Garrison, C.J. (1978), "Hydrodynamic Loading Of Large Offshore Structures", Three-Dimensional Source Distribution Methods. In Numerical Methods in Offshore Engineering, eds. O.C. Zienkiewicz, R.W. Lewis, and K.G. Stagg, Wiley, Chichester, England, pp. 97-140.

Garrison, C.J. (1984), "Nonlinear Wave Loads on Large Structures" Proceedings of the 3rd International Offshore Mechanics and Arctic Engineering Symposium, New Orleans.

Garrison, C.J. and Chow, P.Y., (1972), "Wave Forces on Submerged Bodies". J. Waterways Harbors and Coastal Eng. Div., ASCE, Vol. 98, No. WW3, pp. 375-392.

Gaskill, H.S. and Rochester, J. (1984), "A New Technique for Iceberg Drift Prediction", Cold Regions Science and Technology, Vol. 8, pp. 223-234.

Graham, J.M.R., (1980), "The Forces on Sharp-edged Cylinders in Oscillatory Flow at Low Keulegun-Carpenter numbers", J. Fluid Mech, vol. 51.97, Part 1, pp. 331-346.

Hogben, N. (1974), "Fluid Loading on Offshore Structures, A State-of-the-Art Appraisal Wave Loads". Maritime Tech. Monograph, No. 1, RINA.

Hogben, N., Miller, B.L., Searle, J.W., and Ward, G. (1977), "Estimation of Fluid Loading on Offshore Structures". Proc. Inst. Civil Eng., Vol. 63, pp. 515-562.

Hogben, N. and Standing, R.G. (1974), "Wave Loads on Large Bodies". Proc. Int. Symp. on the Dynamics of Marine Vehicles and Structures in Waves, Univ. College, London, pp. 258-277.

Hooft, J.P. (1982), "Advanced Dynamics of Marine Structures". J. Wiley and Sons, New York, 345 pp.

Hsiung, C.C. and Aboul-Azm, A.F. (1982), "Iceberg Drift Affected by Wave Action", Ocean Eng., Vol. 9, pp. 433-439.

Isaacson, M. de St. Q. (1978a), "Vertical Cylinders of Arbitrary Section in Waves". J. Waterway Port Coastal and Ocean Div., ASCE, Vol 104, No. WW4, pp. 309-324.

Isaacson, M. de St. Q. (1978b), "Interference Effects Between Large Cylinders in Waves". Proc. Offshore Tech. Conf.,

Houston, Paper No. OTC 3069, Vol. 1, pp. 185-192. Also, J. Petroleum Tech., Vol. 31, No. 4, pp. 505-512.

Isaacson, M. de St. Q. (1979a), "Wave Induced Forces in the Diffraction Regime". In Mechanics of Wave-Induced Forces on Cylinders, ed. T.L. Shaw, Pitman, London, pp. 68-89.

Isaacson, M. de St.Q. (1979b), "Wave Forces on Compound Cylinders." Proc. Civil Engineering in the Oceans IV, ASCE, San Francisco, Vol. 1, pp. 518-530.

Isaacson, M. de St. Q. (1982a), "Response of Compliant Structure to Steep Waves", Proc. Offshore Tech. Conf., Houston, Paper No. OTC 4190.

Isaacson, M. de St.Q. (1982b), "Nonlinear-wave effects on fixed and floating bodies". Journal of Fluid Mechanics, Vol. 120, pp. 267-281. See also corrigendum, Vol. 133, 1983, p. 169.

Isaacson, M. de St. Q. (1982c), "Fixed and Floating Axisymmetric Structures in Waves". J. Waterways, Port, Coastal and Ocean Div., ASCE, Vol. 108, No. WW2, pp. 180-199.

Isaacson, M. de St. Q. (1985), "Iceberg Interactions With Offshore Structures". Proc. of the Conf. Arctic '85, San Francisco.

Isaacson, M. de St.Q. and Fraser, A.F., (1979), "Effect of Moorings on Floating Breakwater Response". Proc. of the Specialty Conference Civil Engineering in the Oceans IV, Vol. I, San Francisco. pp. 471-486.

Kaplan, P., Jiang, C.-W., and Bentson, J., (1983), "Hydrodynamic Analysis of Barge-Platform System in Waves". The Naval Architect, July 1983, RINA.

Kristensen, M., and Squire, V.A., (1983), "Modelling of Antarctic Tabular Icebergs in Ocean Waves, Ann. Glaciology, Vol. 4, pp. 152-157.

Lever, J.H., Reimer, E., and Diemand, D., (1984), "A Model Study of the Wave-Induced Motion of Small Icebergs and Bergy Bits". Proc. 3rd International Offshore Mechanics and Arctic Engineering Symposium, New Orleans.

Lighthill, J. (1979), "Waves and Hydrodynamic Loading". Proc. 2nd Int. Conf. on the Behaviour of Offshore Structures, BOSS '79, London, Vol. I, pp. 1-40.

Loken, E.A., (1981), "Hydrodynamic Interaction Between Several Floating Bodies of Arbitrary Form in Waves". Proc. Int. Symp. on Hydrodynamics in Ocean Eng., Trandheim, Vol. 2, pp. 745-779.

Loken, A.E. and Olsen, O.A. (1976), "Diffraction Theory and Statistical Methods to Predict Wave Induced Motions and Loads". Proc. Offshore Technology Conf., Houston, Paper No. OTC 2502.

MacCamy, R.C. and Fuchs, R.A., (1954), "Wave Forces on Piles: A Diffraction Theory". U.S. Army Corps of Engineers, Beach Erosion Board, Tech. Memo No. 69.

McIver, P. and Evans, O.V., (1984), "Approximation of Wave Forces on Cylinder Arrays". Applied Ocean Research, Vol. 6, No. 2, pp. 101-107.

Maeda, H., (1974), "Hydrodynamical Forces on a Cross Section of a Stationary Structure". Proc. Int. Symp. on the Dynamics of Marine Vehicles and Structures in Waves, Univ. College, London, pp. 80-90.

Matsui, T. and Tamaki, T., (1981), "Hydrodynamic Interaction Between Groups of Vertical Axisymmetrical Bodies Floating in Waves". Proc. Int. Symp. on Hydrodynamics in Ocean Eng., Trondheim, Vol. 2, pp. 817-836.

Mei, C.C. (1978), "Numerical Methods in Water-Wave Diffraction and Radiation". Annual Reviews in Fluid Mechanics, Vol. 10, pp. 393-416.

Mei, C.C. (1983), "The Applied Dynamics of Ocean Surface Waves". Wiley, New York, 740 p.

Mountain, D.G., (1980), "On Predicting Iceberg Drift". Cold Regions Science and Technology, Vol. 1, pp. 273-282.

Newman, J. N. (1977), "Marine Hydrodynamics". M.I.T. Press, Mass.

Ohkusu, M., (1974), "Hydrodynamic Forces on Multiple Cylinders in Waves". Proc. Int. Symp. on the Dynamics of Marine Vehicles and Structures in Waves, Univ. College, London, pp. 107-112.

Orheim, O., Wadham, P., and Kristensen, M., (1982), "Iceberg Response to Sea State". Iceberg Res., Vol. 1, 10-15.

Rahman, M., (1984), "Wave Diffraction by Large Offshore Structures: An Exact Second-order Theory". Applied Ocean Research, Vol. 6, No. 2, pp. 90-100.

Russel, W.E., Riggs, N.P., and Robe, R.Q. (1978), "Local Iceberg Motion - A Comparison of Field and Model Studies". Proceedings of the 4th International Conference on Port and Ocean Engineering under Arctic Conditions, St. John's, Vol. 2, pp. 294-798.

Shirasawa, K., Riggs, N.P. and Huggeridge, D.B., (1984), "The Drift of a Number of Idealized Model", Cold Regions Science and Technology, Vol. 10, pp. 19-30.

Smith, S.D. and Banke, E.G., (1981), "A Numerical Model of Iceberg Drift". Proceedings of the 6th International Conference on Port and Ocean Engineering Under Arctic Conditions, Vol. 2, Quebec, pp. 1001-1011.

Smith, D.S. and Banke, E.G. (1982), "The Influence of Winds, Currents, and Towing Forces on the Drift of Icebergs". Cold Regions Science and Technology, Vol. 6, pp. 241-255.

Sodhi, D.S. and Dempster, R.T., (1975), "Motion of Icebergs Due to Changes in Water Currents", IEEE Ocean '75, pp. 348-350.

Sodhi, D.S. and El-Tahum, M., (1980) "Prediction of an Iceberg Drift Trajectory During a Storm". Annals of Glaciology, Vol. 1, pp. 77-82.

Stansby, P.K. and Slaouti, A., (1984), "On Non-Linear Wave Interaction with Cylindrical Bodies: A Vortex Sheet Approach". Applied Ocean Research, Vol. 6, No. 2, pp. 108-115.

Spring, B.H. and Monkmeyer, P.L., (1974), "Interaction of Plane Waves with Vertical Cylinders". Proc. 14th Coastal Eng. Conf., Copenhagen, Vol. III. pp. 1828-1847.

Squire, V.A., (1981), "Numerical Simulation of Ice Floes in Waves". Tech. Rep. 81-1, 57 pp., Scott Polar Res. Inst., Cambridge.

Van Oortmerssen, G. (1979), "Hydrodynamic Interaction Between Two Structures, Floating in Waves". Proc. 2nd Int. Conf. on the Behaviour of Offshore Structures, BOSS '79, London, Vol. 1, pp. 339-356.

Van Oortmerssen, G., (1981), "Some Hydrodynamic Aspects of Multi-Body System". Proc. Int. Symp. on Hydrodynamics in Ocean Eng., Trondheim, Vol. 2, pp. 725-744.

Vinje, T. and Brevig, P. (1981), "Numerical Calculation of Forces from Breaking Waves". Proceedings of the Int. Symp. on Hydrodynamics in Ocean Eng., Trondheim, Norway, pp. 547-565.

Vinje, T., Xie, M-G. and Brevig, P. (1982), "A Numerical Approach to Nonlinear Ship-Motion". Proceedings of the 14th Symposium on Naval Hydrodynamics, Ann Arbour, Michigan.

Wadhams, P., Kristensen, M. and Orheim, D., (1983), "The Response of Antarctic Icebergs to Ocean Waves". J. Geophysical Res., Vol. 88, No. C10, pp. 6053-6065.

Wang, S. and Wahab, R., (1971), "Heaving Oscillations in a Free Surface". J. Ship Research, Vol. 15, pp. 33-48.

Wehausen, J.V. (1971), "The Motion of Floating Bodies". Ann. Rev. Fluid Mech., Vol. 3, pp. 237-268.

Wichers, J.E.W., (1982), "On the Low-Frequency Surge Motion of Vessels in High Seas". Proc. Offshore Tech. Conf. Houston, Paper No. OTC 4437.

Wichers, J.E.W., and van Sluijs, M.F., (1979), "The Influence of Waves on the Low-Frequency Hydrodynamic Coefficients of Moored Vessels". Proc. Offshore Tech. Conf., Houston, Paper No. OTC 3626.

Yamamoto, T., (1976), "Hydrodynamic Forces on Multiple Circular Cylinders". J. Hydraulics Div., ASCE, Vol. 102, No. HY9, pp. 1193-1210.

Yeung, R.W. (1982), "Numerical Methods in Free-Surface Flows, Annual Reviews in Fluid Mechanics, Vol. 14, pp. 395-442.

Zienkiewicz, O.C., Bettess, P., and Kelly, D.W., (1978), "The Finite Element Method for Determining Fluid Loadings on Rigid Structures". Two and Three-Dimensional Formulations. In Numerical Methods in Offshore Engineering, eds. O.C. Zienkiewicz, P. Lewis, and K.G. Stagg, John Wiley, Chichester, England, pp. 141-183.

APPENDIX: SAMPLE OUTPUT OF THE NUMERICAL MODEL

(3)

```
Listing of 63 at 13:10:32 on JUL  7, 1985 for CCid=MDSQ Page    1

      ICEMOT:    ICE MASS MOTIONS NEAR A LARGE
                 FIXED OFFSHORE STRUCTURE


      PRIMARY OUTPUT FILE

      STRUCTURE:       CIRCULAR CYLINDER EXTENDING TO SEABED
      ICE MASS:        CIRCULAR CYLINDER ABOVE SEABED

      OPTION CONTROL TAGS      IA  IB  IC  ID  IE  IF
                                1   1   1   3   2   1

      WATER DEPTH:             AD  = 100.000

      ICE MASS DIMENSION       DIM = 100.000

      STRUCTURE DIMENSION      DST = 100.000


              H          WP          ALP         UC         BETC
           10.000     15.000       5.000      1.000        0.0

            AMS        AMC(1)      AMC(2)      AMC(3)      AMC(4)      AMC(5)      AMC(6)
        392699.00      885.30      885.30     1250.00         0.0         0.0         0.0

              ZG          ZB          SS          S1          S2         S11         S22
          -22.06      -25.00     7853.98         0.0         0.0  4908738.00  4908738.00

              CD          CA          AR      VDR(3)      VDR(4)      VRD(5)
           1.000       1.000    5000.000       0.050       0.050       0.050

              DT          NT          ND          NA
           2.500         100          10          15

              XG          YG          XS          YS          UI        BETI
        -300.000         0.0         0.0         0.0       2.200         0.0

              NS          NI          N.
              48          37          85

              WP           W          FR          WL          AK
          15.000       0.419       0.067     335.046      0.0188
            DGT2         AKD      DST/WL       DIM/WL
           0.045       1.875       0.298        0.298

                           1           2           3           4           5           6


      MASS MATRIX
```

1	0.393	0.0	0.0	0.0	-0.087	0.0
2	0.0	0.393	0.0	0.087	0.0	0.0
3	0.0	0.0	0.393	0.0	0.0	0.0
4	0.0	0.087	0.0	0.054	0.0	0.0
5	-0.087	0.0	0.0	0.0	0.054	0.0
6	0.0	0.0	0.0	0.0	0.0	0.049

HYDROSTATIC STIFFNESS MATRIX

1	0.0	0.0	0.0	0.0	0.0	0.0
2	0.0	0.0	0.0	0.0	0.0	0.0
3	0.0	0.0	0.785	0.0	0.0	0.0
4	0.0	0.0	0.0	0.038	0.0	0.0
5	0.0	0.0	0.0	0.0	0.038	0.0
6	0.0	0.0	0.0	0.0	0.0	0.0

II	T	UX	UY	UCX	UCY	XG	YG
1	0.0	2.200	0.0	1.000	0.0	-300.000	0.0

	1	2	3	4	5	6

EXCITING FORCES (WRT SWL)

MAGNITUDE:	0.782	0.060	0.248	0.011	0.142	0.000
PHASE:	-34.225	-35.718	19.813	-35.556	145.203	-12.002

EXCITING FORCES (WRT G)

MAGNITUDE:	0.782	0.060	0.248	0.003	0.031	0.000
PHASE:	-34.225	-35.718	19.813	143.624	-31.573	-12.002

	1	2	3	4	5	6

ADDED MASSES (WRT SWL)

1	0.260	0.000	0.003	0.000	-0.055	0.000
2	-0.000	0.258	-0.000	0.055	-0.000	-0.000
3	-0.011	-0.000	0.252	-0.000	0.002	-0.000
4	0.000	0.052	-0.000	0.020	-0.000	-0.000
5	-0.053	-0.000	-0.001	-0.000	0.020	-0.000
6	0.000	-0.000	-0.000	-0.000	-0.000	0.000

DAMPING COEFFICIENTS (WRT SWL)

1	0.237	0.000	-0.004	0.000	-0.045	0.000
2	-0.000	0.216	-0.000	0.041	-0.000	-0.000
3	0.003	0.000	0.041	0.000	-0.001	0.000
4	-0.000	0.039	-0.000	0.007	-0.000	-0.000
5	-0.043	-0.000	0.001	-0.000	0.008	-0.000

```
                6        0.000      -0.000       0.000      -0.000      -0.000       0.000


    VISCOUS DAMPING COEFFICIENTS
                         0.0         0.0         0.053       0.004       0.004       0.0


                         1           2           3           4           5           6

    RESPONSE AMPLITUDE OPERATORS (WRT SWL)

    MAGNITUDE:         0.747       0.060       0.614       0.052       0.580       0.000
    PHASE:           124.152     123.451     171.995     -65.171     117.410     158.200

    RESPONSE AMPLITUDE OPERATORS (WRT G)

    MAGNITUDE:         0.620       0.049       0.614       0.052       0.580       0.000
    PHASE:           125.540     125.454     171.995     -65.171     117.410     158.200


    WAVE DRIFT FORCES
                     0.07237     0.00525

    ZERO FREQUENCY ADDED MASSES

              1        0.225       0.000      -0.000       0.000      -0.047       0.000
              2        0.000       0.225       0.000       0.047      -0.000      -0.000
              3        0.000       0.000       0.726      -0.000      -0.000       0.000
              4        0.000       0.044       0.000       0.016      -0.000      -0.000
              5       -0.044      -0.000       0.000      -0.000       0.016      -0.000
              6        0.000      -0.000       0.000      -0.000      -0.000       0.000


     II       T        UX          UY          UCX         UCY         XG          YG
      2     2.500     2.200       0.001       1.000       0.0      -294.501     0.004

     II       T        UX          UY          UCX         UCY         XG          YG
      3     5.000     2.200       0.002       1.000       0.0      -289.002     0.010

     II       T        UX          UY          UCX         UCY         XG          YG
      4     7.500     2.199       0.003       1.000       0.0      -283.504     0.019

     II       T        UX          UY          UCX         UCY         XG          YG
      5    10.000     2.199       0.004       1.000       0.0      -278.006     0.031

     II       T        UX          UY          UCX         UCY         XG          YG
      6    12.500     2.199       0.005       1.000       0.0      -272.509     0.045

     II       T        UX          UY          UCX         UCY         XG          YG
```

```
      7    15.000     2.199     0.006     1.000     0.0    -267.011     0.061

     II       T        UX        UY        UCX       UCY       XG         YG
      8    17.500     2.199     0.007     1.000     0.0    -261.515     0.080

     II       T        UX        UY        UCX       UCY       XG         YG
      9    20.000     2.198     0.008     1.000     0.0    -256.019     0.101

     II       T        UX        UY        UCX       UCY       XG         YG
     10    22.500     2.198     0.009     1.000     0.0    -250.523     0.124

     II       T        UX        UY        UCX       UCY       XG         YG
     11    25.000     2.198     0.010     1.000     0.0    -245.028     0.150
```

	1	2	3	4	5	6
EXCITING FORCES (WRT SWL)						
MAGNITUDE:	0.657	0.060	0.224	0.011	0.113	0.000
PHASE:	15.876	23.552	56.780	23.867	-165.081	33.231
EXCITING FORCES (WRT G)						
MAGNITUDE:	0.657	0.060	0.224	0.003	0.032	0.000
PHASE:	15.876	23.552	56.780	-157.718	19.271	33.231

	1	2	3	4	5	6
ADDED MASSES (WRT SWL)						
1	0.276	-0.000	-0.006	-0.000	-0.058	0.000
2	-0.000	0.258	0.000	0.055	0.000	-0.000
3	0.010	-0.000	0.249	-0.000	-0.002	0.000
4	-0.000	0.052	0.000	0.020	0.000	-0.000
5	-0.056	0.000	0.001	0.000	0.020	-0.000
6	0.000	-0.000	-0.000	-0.000	-0.000	0.000
DAMPING COEFFICIENTS (WRT SWL)						
1	0.202	0.000	-0.000	0.000	-0.038	0.000
2	0.000	0.217	0.000	0.041	-0.000	-0.000
3	0.008	-0.000	0.037	-0.000	-0.002	0.000
4	0.000	0.039	-0.000	0.008	-0.000	-0.000
5	-0.035	-0.000	-0.000	-0.000	0.007	-0.000
6	0.000	-0.000	0.000	-0.000	-0.000	0.000

VISCOUS DAMPING COEFFICIENTS

```
                    0.0         0.0         0.053       0.004       0.004       0.0


                          1           2           3           4           5           6

 RESPONSE AMPLITUDE OPERATORS (WRT SWL)

 MAGNITUDE:           0.661       0.059       0.534       0.051       0.615       0.000
 PHASE:             177.602    -177.452    -146.160      -6.565     172.978    -154.601

 RESPONSE AMPLITUDE OPERATORS (WRT G)

 MAGNITUDE:           0.526       0.048       0.534       0.051       0.615       0.000
 PHASE:             178.794    -175.320    -146.160      -6.565     172.978    -154.601


 WAVE DRIFT FORCES
                    0.08379     0.00789


    II      T         UX          UY          UCX         UCY         XG          YG
    12    27.500      2.201       0.012       1.000       0.0      -239.521     0.181


    II      T         UX          UY          UCX         UCY         XG          YG
    13    30.000      2.204       0.013       1.000       0.0      -234.008     0.215


    II      T         UX          UY          UCX         UCY         XG          YG
    14    32.500      2.206       0.015       1.000       0.0      -228.490     0.254


    II      T         UX          UY          UCX         UCY         XG          YG
    15    35.000      2.209       0.016       1.000       0.0      -222.964     0.296


    II      T         UX          UY          UCX         UCY         XG          YG
    16    37.500      2.212       0.018       1.000       0.0      -217.431     0.342

 ZERO FREQUENCY ADDED MASSES

          1          0.225      -0.000      -0.001       0.000      -0.047       0.000
          2         -0.000       0.225       0.000       0.047      -0.000      -0.000
          3          0.000       0.000       0.726      -0.000      -0.000       0.000
          4         -0.000       0.044       0.000       0.016      -0.000      -0.000
          5         -0.044      -0.000       0.000      -0.000       0.016      -0.000
          6          0.000      -0.000       0.000      -0.000      -0.000       0.000


    II      T         UX          UY          UCX         UCY         XG          YG
    17    40.000      2.215       0.019       1.000       0.0      -211.891     0.392


    II      T         UX          UY          UCX         UCY         XG          YG
    18    42.500      2.218       0.021       1.000       0.0      -206.342     0.447
```

II	T	UX	UY	UCX	UCY	XG	YG
19	45.000	2.221	0.023	1.000	0.0	-200.786	0.506

II	T	UX	UY	UCX	UCY	XG	YG
20	47.500	2.225	0.024	1.000	0.0	-195.220	0.569

II	T	UX	UY	UCX	UCY	XG	YG
21	50.000	2.228	0.026	1.000	0.0	-189.645	0.637

EXCITING FORCES (WRT SWL)

	1	2	3	4	5	6
MAGNITUDE:	0.613	0.061	0.154	0.011	0.108	0.000
PHASE:	88.227	82.888	130.740	83.036	-89.396	97.158

EXCITING FORCES (WRT G)

	1	2	3	4	5	6
MAGNITUDE:	0.613	0.061	0.154	0.003	0.028	0.000
PHASE:	88.227	82.888	130.740	-97.722	78.953	97.158

ADDED MASSES (WRT SWL)

	1	2	3	4	5	6
1	0.235	0.000	0.002	0.000	-0.051	0.000
2	0.000	0.259	-0.000	0.055	-0.000	-0.000
3	0.007	-0.000	0.246	-0.000	-0.001	-0.000
4	0.000	0.052	-0.000	0.020	-0.000	-0.000
5	-0.047	-0.000	-0.000	-0.000	0.019	-0.000
6	0.000	-0.000	-0.000	-0.000	-0.000	0.000

DAMPING COEFFICIENTS (WRT SWL)

	1	2	3	4	5	6
1	0.200	0.000	0.007	0.000	-0.038	0.000
2	0.000	0.216	-0.000	0.041	-0.000	-0.000
3	-0.014	0.000	0.041	0.000	0.003	0.000
4	0.000	0.039	-0.000	0.007	-0.000	-0.000
5	-0.036	-0.000	-0.001	-0.000	0.007	-0.000
6	0.000	-0.000	0.000	-0.000	-0.000	0.000

VISCOUS DAMPING COEFFICIENTS

0.0	0.0	0.053	0.004	0.004	0.0

	1	2	3	4	5	6

```
349
350     RESPONSE AMPLITUDE OPERATORS (WRT SWL)
351
352     MAGNITUDE:          0.637       0.060       0.414       0.051       0.573       0.000
353     PHASE:           -114.041    -117.962     -70.390      53.145    -129.508     -91.169
354
355     RESPONSE AMPLITUDE OPERATORS (WRT G)
356
357     MAGNITUDE:          0.516       0.049       0.414       0.051       0.573       0.000
358     PHASE:           -110.299    -115.922     -70.390      53.145    -129.508     -91.169
359
360
361     WAVE DRIFT FORCES
362                      0.13204     0.01276
363
364
365       II      T        UX        UY        UCX       UCY       XG        YG
366       22    52.500     2.243     0.029     1.000     0.0     -184.020    0.711
367
368
369       II      T        UX        UY        UCX       UCY       XG        YG
370       23    55.000     2.255     0.031     1.000     0.0     -178.369    0.791
371
372
373       II      T        UX        UY        UCX       UCY       XG        YG
374       24    57.500     2.267     0.033     1.000     0.0     -172.685    0.877
375
376
377       II      T        UX        UY        UCX       UCY       XG        YG
378       25    60.000     2.280     0.036     1.000     0.0     -166.968    0.970
379
380
381       II      T        UX        UY        UCX       UCY       XG        YG
382       26    62.500     2.294     0.038     1.000     0.0     -161.216    1.068
383
384
385       II      T        UX        UY        UCX       UCY       XG        YG
386       27    65.000     2.308     0.041     1.000     0.0     -155.427    1.173
387
388
389       II      T        UX        UY        UCX       UCY       XG        YG
390       28    67.500     2.323     0.043     1.000     0.0     -149.601    1.285
391
392
393       II      T        UX        UY        UCX       UCY       XG        YG
394       29    70.000     2.339     0.046     1.000     0.0     -143.735    1.403
395
396
397       II      T        UX        UY        UCX       UCY       XG        YG
398       30    72.500     2.355     0.049     1.000     0.0     -137.828    1.528
399
400
401       II      T        UX        UY        UCX       UCY       XG        YG
402       31    75.000     2.371     0.051     1.000     0.0     -131.879    1.660
403
404
405                        1         2         3         4         5         6
406
```

```
407
408     EXCITING FORCES (WRT SWL)
409
410     MAGNITUDE:          0.828       0.058       0.265       0.010       0.153       0.000
411     PHASE:            149.504     142.237    -153.896     142.366     -30.938     173.932
412
413     EXCITING FORCES (WRT G)
414
415     MAGNITUDE:          0.828       0.058       0.265       0.003       0.030       0.000
416     PHASE:            149.504     142.237    -153.896     -38.246     151.773     173.932
417
418
419                           1           2           3           4           5           6
420
421
422     ADDED MASSES (WRT SWL)
423
424               1         0.247       0.000       0.011       0.000      -0.053       0.000
425               2         0.000       0.254      -0.000       0.054      -0.000      -0.000
426               3        -0.031       0.000       0.257       0.000       0.006      -0.000
427               4         0.000       0.052      -0.000       0.020       0.000      -0.000
428               5        -0.052      -0.000      -0.002       0.000       0.020      -0.000
429               6         0.000      -0.000       0.000      -0.000      -0.000       0.000
430
431
432     DAMPING COEFFICIENTS (WRT SWL)
433
434               1         0.276      -0.001      -0.009      -0.000      -0.052       0.000
435               2        -0.001       0.214       0.000       0.040       0.000      -0.000
436               3         0.003      -0.000       0.044      -0.000      -0.001       0.000
437               4        -0.000       0.038       0.000       0.007       0.000      -0.000
438               5        -0.051       0.000       0.002       0.000       0.010      -0.000
439               6         0.000      -0.000       0.000      -0.000      -0.000       0.000
440
441
442
443     VISCOUS DAMPING COEFFICIENTS
444                           0.0         0.0         0.053       0.004       0.004       0.0
445
446
447                           1           2           3           4           5           6
448
449
450     RESPONSE AMPLITUDE OPERATORS (WRT SWL)
451
452     MAGNITUDE:          0.773       0.058       0.650       0.052       0.576       0.000
453     PHASE:            -55.205     -57.625      -6.706     114.326     -61.299     -18.955
454
455     RESPONSE AMPLITUDE OPERATORS (WRT G)
456
457     MAGNITUDE:          0.647       0.047       0.650       0.052       0.576       0.000
458     PHASE:            -54.009     -55.665      -6.706     114.326     -61.299     -18.955
459
460
461     WAVE DRIFT FORCES
462                       0.05831     0.00335
463
464
```

```
465     ZERO FREQUENCY ADDED MASSES
466
467              1        0.229      -0.000      -0.003      -0.000      -0.048       0.000
468              2       -0.000       0.228       0.000       0.047       0.000      -0.000
469              3        0.000       0.000       0.727       0.000      -0.000       0.000
470              4       -0.000       0.045       0.000       0.016       0.000      -0.000
471              5       -0.045       0.000       0.001       0.000       0.016      -0.000
472              6        0.000      -0.000       0.000      -0.000      -0.000       0.000
473
474
475
476        II     T         UX         UY         UCX        UCY         XG         YG
477        32    77.500     2.352      0.050      1.000      0.0      -126.024     1.783
478
479
480        II     T         UX         UY         UCX        UCY         XG         YG
481        33    80.000     2.343      0.050      1.000      0.0      -120.177     1.907
482
483
484        II     T         UX         UY         UCX        UCY         XG         YG
485        34    82.500     2.333      0.049      1.000      0.0      -114.357     2.030
486
487
488        II     T         UX         UY         UCX        UCY         XG         YG
489        35    85.000     2.322      0.049      1.000      0.0      -108.567     2.151
490
491
492        II     T         UX         UY         UCX        UCY         XG         YG
493        36    87.500     2.309      0.048      1.000      0.0      -102.809     2.269
494
495     ***** IMPACT ***** EXECUTION TERMINATED
```